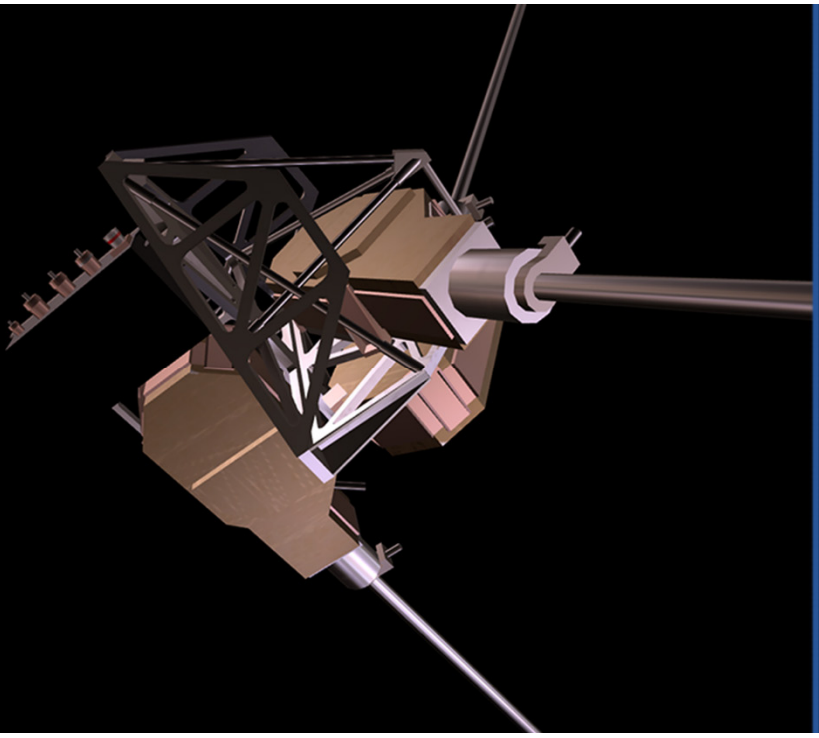

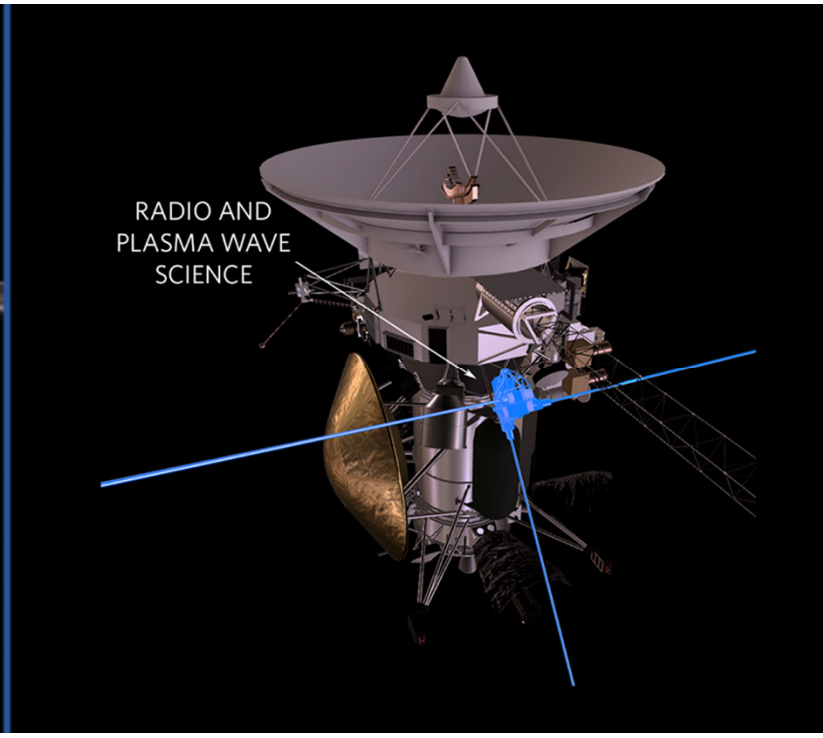

Radio and Plasma Wave Science

The Radio and Plasma Wave Science (RPWS) investigation was designed to study radio emissions, plasma waves, thermal plasma, and dust in the vicinity of Saturn. The **science objectives** included improving our knowledge of the rotational modulation of Saturn's intense radio emission (SKR) and hence Saturn's rotation rate, characterizing plasma waves associated with Saturn's icy satellites and characterizing plasma density in the inner magnetosphere. RPWS was able to detect the dust hitting Cassini throughout the Saturn system and characterize lightning in Saturn's atmosphere.

RPWS was composed of an electric field sensor, a magnetic search coil assembly and a Langmuir probe. The electric field sensor consisted of three deployable antennas. The Langmuir probe, which measured electron density and temperature, was a metallic sphere that measured currents and voltages induced in the probe.

ACKNOWLEDGEMENTS

The following investigators contributed to the Final Mission Report Volume 1: Mission Overview, Science Objectives and Results; Section 3.2: Instruments Science Results – Fields, Particles, and Waves Sensing Instruments – Radio and Plasma Wave Science (RPWS).

RPWS Principal Investigator (PI) and Deputy Principal Investigator (DPI):

Donald A. Gurnett, PI (through October 2015)	*University of Iowa, U.S.*
William S. Kurth, PI (after October 2015); DPI (through October 2015)	

RPWS Investigators:

George B. Hospodarsky, J. Douglas Menietti, Ann M. Persoon	*University of Iowa, U.S.*
Paul Kellogg, Keith Goetz	*University of Minnesota, U.S.*
William M. Farrell, Robert J. MacDowall, Michael D. Desch, Michael L. Kaiser	*Goddard Space Flight Center, U.S.*
Philippe Zarka, Alain Lecacheu, Baptiste Cecconi, Laurent Lamy	*Observatoire de Paris, France*
Philippe Louarn, Christopher C. Harvey	*CESR-CNRS, France*
Patrick Canu, Nicole Cornilleau-Wehrlin, Alain Roux	*CNET/LPP, France*
Patrick Galopeau, Ronan Modolo	*LATMOS/IPSL/UVSQ, France*
Les Woolliscroft, Hugo St. C. Alleyne	*University of Sheffield, United Kingdom*
Helmut O. Rucker, Peter Ladreiter, Georg Fischer	*Austrian Academy of Science, Space Research Institute, Austria*
Rolf Boström, Georg Gustafsson, Jan-Erik Wahlund, Michiko W. Morooka	*Swedish Institute of Space Physics (IRF-U), Sweden*
Arne Pedersen	*University of Oslo, Norway*

RPWS Publication Contributors:

W. S. Kurth, W. M. Farrell, G. Fischer, D. A. Gurnett, G. B. Hospodarsky, L. Lamy, A. M. Persoon, A. H. Sulaiman, J.-E. Wahlund, S.-Y. Ye, P. Zarka

CONTENTS

Figures

Tables

Executive Summary

The Cassini Radio and Plasma Wave Science (RPWS) investigation was successfully carried out over a seven-year cruise and more than thirteen years in orbit at Saturn. As described elsewhere, the instrument performed almost flawlessly; even some occasional processor hangs were understood to the point that we could anticipate modes that might cause them and sequence commands to allow the instrument to recover without ground intervention. While questions were certainly left to answer with future missions (see section entitled Open Questions for Saturn System Science), all of the RPWS science objectives were addressed and advances were made in areas not anticipated at launch, at least partially due to the long mission extensions and agile orbital mechanics involved in the mission and extended mission design.

Top Scientific Findings

The RPWS team debated the top scientific findings of the investigation at length and it is safe to say that while the following is a representative list, it is by no means a consensus in terms of either completeness or order of priority. It does, however, convey the breadth of the investigation, touching on all of Cassini's disciplines including the magnetosphere, satellites, Titan, rings, and Saturn, itself.

- Confirmation of a variable radio period and the discovery of hemispherically differing radio periods.
- First in situ measurements of Saturn's topside ionosphere and evidence of significant interactions with the ring system.
- Comprehensive study of the occurrence of lightning in Saturn's atmosphere and the evolution of a once-per-Saturn-year Great White Spot storm.
- In situ measurements of the Enceladus plumes and their interaction with Saturn's magnetosphere; in situ studies of a dusty plasma.
- Plasma wave phenomena associated with icy satellites, notably Enceladus and Rhea, revealing their electromagnetic connection to Saturn via its magnetic field.
- First in situ characterization of a non-terrestrial cyclotron maser instability-driven radio source (Saturn kilometric radiation).
- In situ measurements of Titan's extensive ionosphere, including the electron density and temperature, evidence for negative ions, and solar cycle dependencies.
- The development of a plasma density model for Saturn's inner magnetosphere.
- Interdisciplinary studies of Saturn's auroras including Saturn kilometric radiation, ultraviolet (UV) and infrared (IR) observations, energetic particles, and the influence of magnetospheric dynamics and solar wind compression events.

- Imaging of SKR source regions and the confirmation that they align with the UV auroras.
- The discovery of Z-mode waves as the source of ~5 kHz narrowband radio emissions first observed by Voyager.
- Anomalously low plasma densities over the unlit side of the B-ring.
- A new low-frequency radio emission phenomenon consisting of drifting tones.
- Finding Titan ahead of Saturn's bow shock and the realization that a complex shock forms ahead of the Titan-Saturn system as opposed to separate shocks.
- The discovery of a seasonally-dependent source of plasma between the A-ring and Enceladus.
- New insights on high Mach number shocks and upstream phenomena through studies of Saturn's bow shock and foreshock region.

The above list demonstrates that RPWS met and exceeded all of its objectives and made significant progress in areas not anticipated prior to arrival at Saturn.

Open Questions for Saturn System Science

Any mission, however extended, always raises questions based on the new knowledge gained. Here we give a brief list of open questions for radio and plasma wave science at Saturn, after Cassini.

- What is the rotation period of Saturn? How do the multiple, variable magnetospheric periods observed in radio, magnetic fields, energetic particles, plasma, aurora, and other phenomena tie to the internally-generated magnetic field at Saturn?
- Given the extraordinarily axi-symmetric magnetic field, why are there such prominent rotational modulations in Saturn's magnetosphere?
- What drives the episodic lightning on Saturn; why is there ~one Great White Spot storm per Saturnian year?
- How does the dust in the Saturnian system interact with Saturn and its atmosphere? How are the rings coupled to the planet other than through gravity?
- What is the predominant form of the electron distribution function at the source of SKR?
- How does the abundant neutral population in Saturn's magnetosphere make it different from fully or mostly ionized magnetospheres?
- What are the various populations of charged dust and molecules that balance charges in dusty media such as in the plumes of Enceladus and in Saturn's topside equatorial ionosphere?

> … all of the RPWS science objectives were addressed and advances were made in areas not anticipated at launch … .

The key open questions are listed above and in the section entitled Open Questions for Saturn System Science. One of the objectives of Cassini was to understand the rotational modulation of Saturn kilometric radiation in the presence of an axi-symmetric magnetic field. Rather than understanding this, the question became more complex. The rotational modulation of SKR was confirmed to be variable and there are often different periods associated with the northern and southern hemispheres. Furthermore, such multiple, variable periods are seen in many aspects of the magnetosphere including the magnetic field, energetic particles, and even the auroral oval. While models exist that reproduce many of these observations, the fundamental origin of this asymmetric behavior in a symmetric system is not understood.

Another aspect of the Saturnian system which is ripe with follow-on questions is the complex processes involving the magnetized plasma in Saturn's magnetosphere in the presence of a large neutral population and pervaded with charged dust grains with sizes ranging from microns to nanometers.

The Cassini mission provided the first opportunities to observe a cyclotron maser instability (CMI) source (of Saturn kilometric radiation) in situ at a location other than at Earth. While these opportunities allowed for the confirmation of a CMI mechanism, only two such source crossings occurred when the Cassini Plasma Science (CAPS) instrument was functioning. Hence, the multiple additional source crossings in the Ring Grazing and Grand Finale orbits did not have the advantage of the CAPS measurements, meaning we do not have more than a couple samples of the electron distribution function responsible for driving the CMI at Saturn. The theory for CMI allows one to infer the resonant energy of electrons and even something about the form of free energy in the source, but having the plasma measurements for additional sources would be beneficial.

RPWS Instrument Summary

The RPWS instrument is a radio and plasma wave spectrometer with the capability of determining the density and temperature of plasmas. The instrument utilizes seven sensors including three monopole electric field antennas with the ability to use two of them as a dipole antenna, a triaxial search coil magnetometer, and a Langmuir probe. Electric fields in the frequency range of 2 Hz to 16 MHz and magnetic fields in the range of 2 Hz to 12 kHz can be measured by the RPWS. The Langmuir probe can determine plasma densities and temperatures in the range of 10 to 10^5 cm^{-3} and below 8 eV through the analysis of voltage-current sweeps. By using the spacecraft potential as a proxy for the electron density, much lower densities, down to 10^{-5} cm^{-3} can be inferred. The instrument is fully described by Gurnett et al. [2004].

The RPWS utilizes a number of receivers to analyze signals from the various sensors. These include a high frequency receiver (HFR) covering electric fields from 3.5 kHz to 16 MHz with the capability of making full polarization and direction-finding measurements in certain modes. The HFR also includes a sounder which can actively stimulate characteristic frequencies of the plasma that enable an alternate approach to determining the plasma density. The medium frequency receiver (MFR) provides electric and magnetic spectral information in the range of 24 Hz to 12 kHz. The low frequency receiver (LFR) provides spectral information for both electric and magnetic fields in the frequency range of ~1 Hz to 26 Hz. The five-channel waveform receiver (WFR) simultaneously captures waveforms from up to five sensors selected from two electric antennas, three magnetic antennas, and the Langmuir probe. Finally, the wideband receiver (WBR) can collect waveform measurements from a selected sensor in a bandwidth of 60 Hz to 10.5 kHz or 0.8 to 75 kHz. The WBR can also provide a 25-kHz band downconverted from selected frequency bands in the HFR.

A typical temporal resolution for survey measurements (covering the full instrument spectrum) is one spectrum per 8 to 16 seconds. The spectral resolution for survey data are Δf/f of 7 to 13%. The HFR has selectable spectral resolutions of 5 to 20% below 318 kHz and n × 25 kHz at higher frequencies. The typical operation of the Langmuir probe provides a full voltage sweep every 24 seconds and can collect currents at fixed bias at rates as high as 20 Hz. Because of the possibility of interference with other instruments, the sounder is only operated briefly every 10 minutes, or so. The WFR and WBR provide the highest resolution observations because actual waveforms are telemetered to the ground for processing optimized to the wave feature under study. However, because of the tremendous data rate generated by these receivers, only relatively short waveform acquisitions can be afforded. These are typically targeted near satellite flybys or regions of interest in the magnetosphere.

Key Objectives for RPWS Instrument

The key RPWS science objectives listed below are taken from Gurnett et al. [2004] and are discussed in the section entitled Science Results. While they were written with the prime mission in mind, the same objectives flow easily into the mission extensions.

Radio emissions

- Improve our knowledge of the rotational modulation of Saturn's radio sources, and hence of Saturn's rotation rate.
- Determine the location of the SKR source as a function of frequency, and investigate the mechanisms involved in generating the radiation.
- Obtain a quantitative evaluation of the anomalies in Saturn's magnetic field by performing direction-finding measurements of the SKR source.

- Establish if gaseous ejections from the moons Rhea, Dione, and Tethys are responsible for the low frequency narrow-band radio emissions.
- Determine if SKR is controlled by Dione's orbital position.
- Establish the nature of the solar wind-magnetosphere interaction by using SKR as a remote indicator of magnetospheric processes.
- Investigate the relationship between SKR and the occurrence of spokes and other time-dependent phenomena in the rings.
- Study the fine structure in the SKR spectrum, and compare with the fine structure of terrestrial and Jovian radio emissions in order to understand the origin of this fine structure.

Plasma waves

- Establish the spectrum and types of plasma waves associated with gaseous emissions from Titan, the rings, and the icy satellites.
- Determine the role of plasma waves in the interaction of Saturn's magnetospheric plasma (and the solar wind) with the ionosphere of Titan.
- Establish the spectrum and types of plasma waves that exist in the radiation belt of Saturn.
- Determine the wave-particle interactions responsible for the loss of radiation belt particles.
- Establish the spectrum and types of waves that exist in the magnetotail and polar regions of Saturn's magnetosphere.
- Determine if waves driven by field-aligned currents along the auroral field lines play a significant role in the auroral charged particle acceleration.
- Determine the electron density in the magnetosphere of Saturn, near the icy moons, and in the ionosphere of Titan.

Lightning

- Establish the long-term morphology and temporal variability of lightning in the atmosphere of Saturn.
- Determine the spatial and temporal variation of the electron density in Saturn's ionosphere from the low frequency cutoff and absorption of lightning signals.
- Carry out a definitive search for lightning in Titan's atmosphere during the numerous close flybys of Titan.
- Perform high-resolution studies of the waveform and spectrum of lightning in the atmosphere of Saturn, and compare with terrestrial lightning.

Thermal plasma

- Determine the spatial and temporal distribution of the electron density and temperature in Titan's ionosphere.
- Characterize the escape of thermal plasma from Titan's ionosphere in the downstream wake region.
- Constrain and, when possible, measure the electron density and temperature in other regions of Saturn's magnetosphere.

Dust

- Determine the spatial distribution of micron-sized dust particles throughout the Saturnian system.
- Measure the mass distribution of the impacting particles from pulse height analyses of the impact waveforms.
- Determine the possible role of charged dust particles as a source of field-aligned Currents.

RPWS Science Assessment

Tables RPWS-1–RPWS-5 contain assessments of RPWS science based on the objectives in the original Announcement of Opportunity (AO) and the Cassini Traceability Matrix (TM) developed for the Equinox and Solstice missions. Each RPWS science objective is paired with an AO and TM science objective. RPWS objectives span all disciplines addressed by the Cassini mission, to some extent. These include Titan, Icy Satellites, Rings, Saturn, and the Magnetosphere.

Table RPWS-1. RPWS Saturn Science Assessment: AO and TM Objectives are paired with RPWS Science objectives. Objectives are accomplished in terms of acquiring relevant data to address.

Fully/Mostly Accomplished: **Partially Accomplished:**

RPWS Saturn Science Objectives	AO and TM Science Objectives	RPWS Saturn Science Assessment	Comments, if yellow (partially fulfilled)
Saturn Interior Structure and Rotation			
--- Rotation of the Deep Atmosphere	SP3, SN1a		Still unknown
Saturn Ionosphere-Magnetosphere Interaction			
--- Saturn I-M interaction, Auroras	SP4, SC2a		
Saturn Lightning Sources and Morphology			
--- Saturn Lightning	SP6, SN2a, SC1b		
--- Great Storm	SN1b		
Aurorae, Chemistry, and Upper Atmosphere	SC2a		Analysis ongoing

Table RPWS-2. RPWS Rings Science Assessment: AO and TM Objectives are paired with RPWS Science objectives. Objectives are accomplished in terms of acquiring relevant data to address.

Fully/Mostly Accomplished: **Partially Accomplished:**

RPWS Rings Science Objectives	AO and TM Science Objectives	RPWS Rings Science Assessment	Comments, if yellow (partially fulfilled)
Ring Structure and Dynamics			
--- Structure of the dusty rings	RP1, RN1c		
--- Dust in vicinity of F-ring	RC1b, RC2a		
Ring Particle Composition and Size			
--- Size distribution of dust	RP2, RC1a		
Ring-Satellite Interaction			
--- Interaction of Enceladus and E-ring	RP3		
Dust and Meteoroid Distribution			
--- Micron-sized dust within and inside D-ring	RP4		Analysis ongoing
Ring Magnetosphere-Ionosphere Interactions	RP5		Analysis ongoing

Table RPWS-3. RPWS MAPS Science Assessment: AO and TM Objectives are paired with RPWS Science objectives. Objectives are accomplished in terms of acquiring relevant data to address.

Fully/Mostly Accomplished: **Partially Accomplished:**

RPWS MAPS Science Objectives	AO and TM Science Objectives	RPWS MAPS Science Assessment	Comments, if yellow (partially fulfilled)
Saturn Magnetic Field Configuration and SKR			
--- Modulation of SKR	MP1, MN1c		Still do not understand variations
--- Seasonal and Solar Cycle Variations	MC1b		
Magnetosphere Charge Particles	MP2		
--- Enceladus as a source of plasma			
--- Rings as a source of plasma			
Magnetosphere Wave-Particle Interactions	MP3		
--- Upstream waves and waves at shock and magnetopause			
--- Wave-particle interactions in middle magnetosphere			
--- Correlations of SKR and tail reconnection			
Magnetosphere and Solar Interactions with Titan	MP4		
Plasma Interactions with Titan's Atmosphere and Ionosphere	MP5		
Enceladus Plume Variability	MC1a		
Titan's Ionosphere	MC2a		
Magnetotail	MN1a		
Saturn's Ionosphere and Radiation Belts	MN1b		
Ionosphere and Ring Coupling	MN2a		

Table RPWS-4. RPWS Icy Satellite Science Assessment: AO and TM Objectives are paired with RPWS Science objectives. Objectives are accomplished in terms of acquiring relevant data to address.

Fully/Mostly Accomplished: Partially Accomplished:

RPWS Icy Satellite Science Objectives	AO and TM Science Objectives	RPWS Icy Satellite Science Assessment	Comments, if yellow (partially fulfilled)
Icy Satellite Magnetosphere and Ring Interactions			
--- Enceladus plume-magnetosphere interaction	IP5, IC1a, IN1a		
--- Evidence for Dione activity	IN1c		
--- Rhea ring material	IN2a		
--- Tethys contribution to E-ring, magnetosphere	IN2b		
--- Appearance of Hyperion	IN2e		

Table RPWS-5. RPWS Titan Science Assessment: AO and TM Objectives are paired with RPWS Science objectives. Objectives are accomplished in terms of acquiring relevant data to address.

Fully/Mostly Accomplished: Partially Accomplished:

RPWS Titan Science Objectives	AO and TM Science Objectives	RPWS Titan Science Assessment	Comments, if yellow (partially fulfilled)
Titan Meteorology			
--- Search for lightning	TP3		
Titan Upper Atmosphere	TP5		
--- Seasonal variations of Titan's ionosphere	TC1a, TC1b		
Titan-Magnetosphere Interaction	TC2a		
--- Induced magnetic field/magnetosphere interaction	TN1b		

RPWS Saturn System Science Results

Titan Science

The RPWS contributions to Titan science are foremost to map the structure, dynamics and long-term variability of its ionosphere and its induced magnetosphere, both interacting continuously with Saturn's magnetosphere and the solar extreme ultraviolet (EUV) radiation, and occasionally also directly with the enhanced solar wind during more active solar conditions when the magnetopause is pushed back toward Saturn past the orbit of Titan. The RPWS contributions, mostly from the Langmuir probe sensor, were recently reviewed in the Cambridge University Press book Titan, primarily in Chapters 12 and 13 [Galand et al. 2013; Wahlund et al. 2013]. Many more RPWS science results have been produced since then. A total of more than 70 publications with RPWS participation in peer-reviewed journals have resulted regarding Titan science up to 2018. Here we dwell only on the main key results.

The first in situ measurements of Titan's ionosphere and space environment were made by Cassini/RPWS during the Titan A flyby in October 26, 2004 [Wahlund et al. 2005a], and the Langmuir probe sensor has been successfully monitoring the cold plasma, charged aerosol and electron temperature during every Titan flyby since then—a total of 127 flybys. A slight degradation of the Langmuir probe sensitivity was induced by the Saturn radiation belt passes in late 2008, but had no effect on the subsequent science output. The RPWS/Langmuir probe therefore provided good science data from Titan for the full period October 2004 to September 2017 (almost 13 years of data).

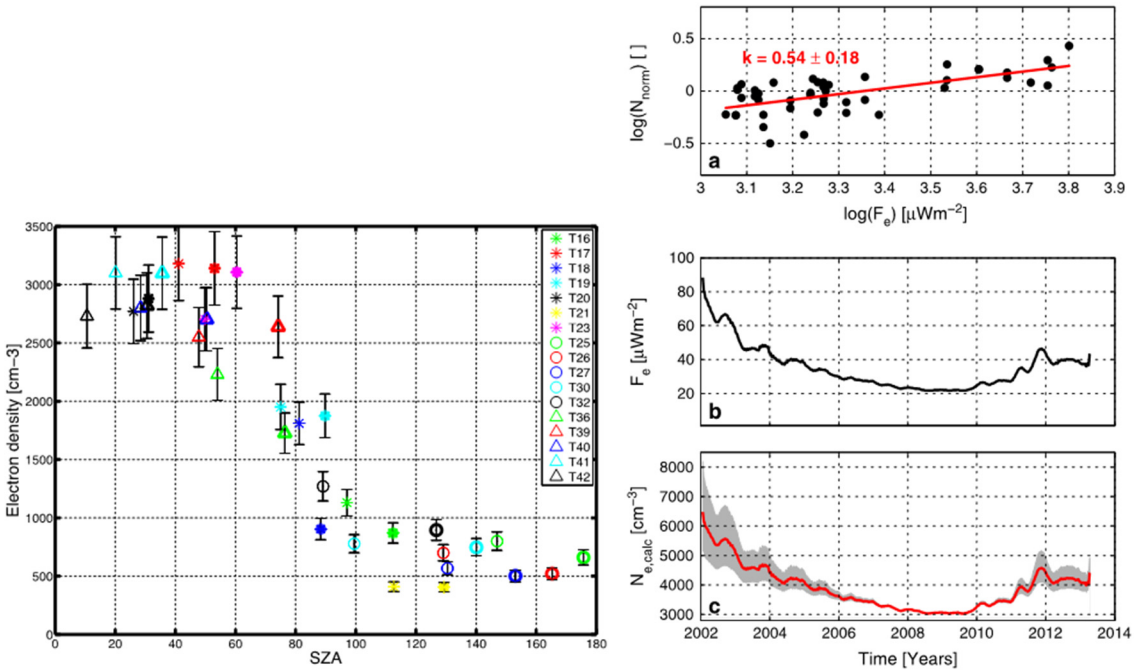

Figure RPWS-1. ***Left*****: Ionospheric peak electron number density versus solar zenith angle [Ågren et al. 2009].** ***Right*****: The variation of the peak electron number density solar EUV flux [Edberg et al. 2013b].**

The main structure of Titan's ionosphere emerged after a few flybys [Ågren et al. 2007, 2009; Robertson et al. 2009] and it became clear that solar EUV radiation dominated the ionization of Titan's upper atmosphere, and varied with the long-term EUV output from the Sun [Edberg et al. 2013b; Shebanits et al. 2017]. Energetic particle precipitation from the magnetosphere is important on the nightside of Titan, but only occasionally makes a significant difference on the dayside [Edberg et al. 2013a]. A most surprising find was the importance of the ionosphere for the production of complex organic chemistry and aerosol particles (dust) below about 1100 km altitude [Coates et al. 2007, 2011; Wahlund et al. 2009b; Vuitton et al. 2009; Ågren et al. 2012; Lavvas et al. 2013; Shebanits et al. 2013, 2016], where the Langmuir probe provided a measure of the detailed amounts of organic ions and charged aerosol particles. The mechanism starts with EUV producing an N_2^+ ion that then reacts primarily with methane, with subsequently more complex C-H-N chemistry and aerosol formation [Lavvas et al. 2013].

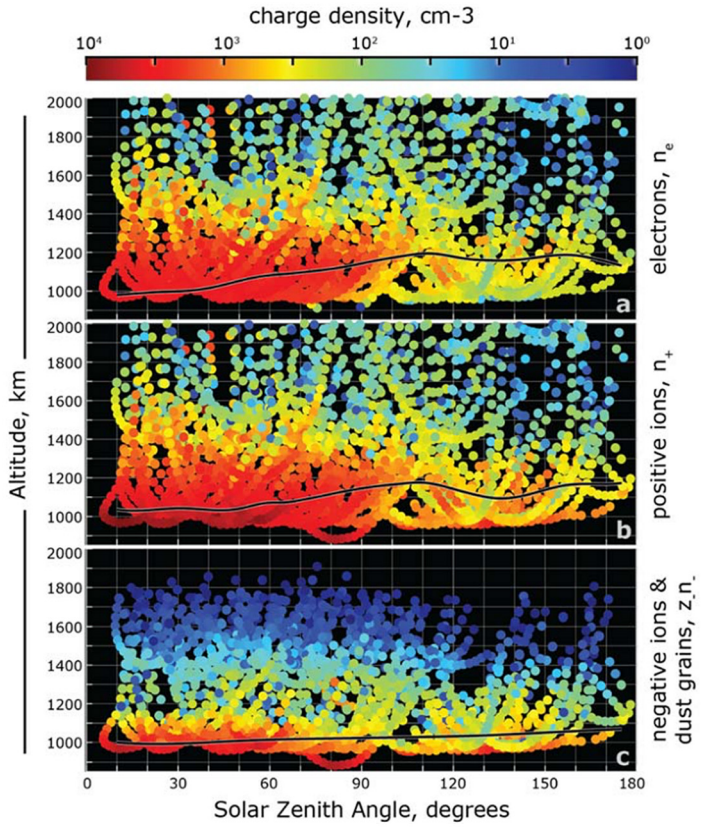

Figure RPWS-2. The ionosphere of Titan. The number densities of electrons (T*op panel*), positively charged ions (*Middle panel*), and negatively charged ions and aerosol particles (*Bottom panel*). Adapted from Shebanits et al. [2013].

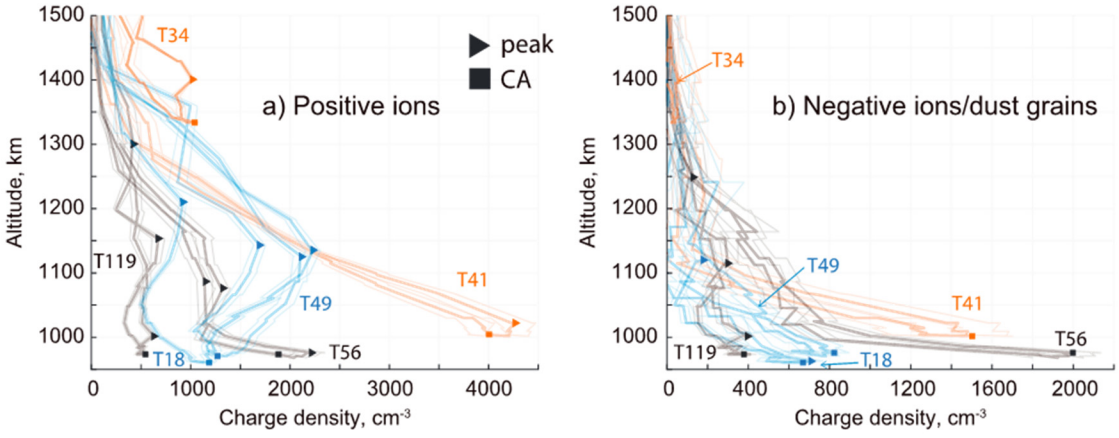

Figure RPWS-3. Examples from six flybys of Titan of altitude profiles of the positive ion and negative ion/aerosol number densities as derived from the RPWS Langmuir probe measurements [Shebanits et al. 2017]. Note the dominance of charged aerosol particles below 1100 km. Dayside flybys are colored in orange, terminator in blue, and nightside in black; the triangles mark the peaks and the squares mark the closest approach (CA) maxima.

Titan's interaction with the magnetosphere of Saturn results in the formation of an induced magnetosphere around Titan. The RPWS sensors have mapped the interaction region [Modolo et al. 2007a, 2007b], proved the existence of cold ionospheric flows from Titan—for example, Edberg et al. [2010, 2011], as well as more energetic ion pickup [Modolo et al. 2007b], and studied how these processes change when Titan enters the magnetosheath [Bertucci et al. 2008; Garnier et al. 2009]. Titan's ionosphere also acts as a conductive medium where electric currents generated in the induced magnetosphere close [Rosenqvist et al. 2009; Ågren et al. 2011]. The escape rate through the cold plasma was determined to be a few kg/s (10^{25} ions/s), which is considered small compared to the exosphere escape rates.

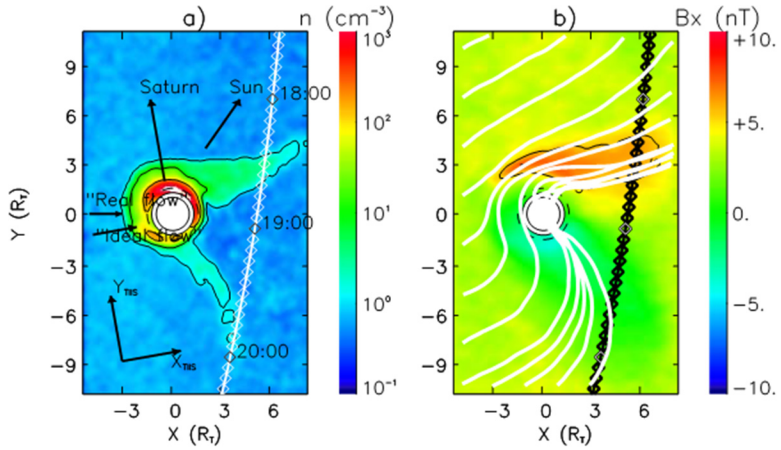

Figure RPWS-4. The induced magnetosphere of Titan as measured and modelled during the T9 flyby through the tail [Modolo et al. 2007b].

Icy Satellite Science

RPWS at Enceladus

Plasma waves

Cassini made 22 close flybys of the icy moon Enceladus which enabled the RPWS to study plasma waves in the moon's near-environment, auroral processes associated with these waves, and the interaction between the magnetospheric plasma and the dust originating in Enceladus' plume. Gurnett et al. [2011a] reported observations of whistler mode auroral hiss emissions produced by magnetic field-aligned electron beams. A ray path analysis of the funnel emission shows the hiss source region within a few moon radii of the Enceladus surface. Figure RPWS-5 is adapted from Figure 2 in Gurnett et al. [2011a] and shows the auroral hiss funnel from the E8 flyby in the top panel and the nearly field-aligned electron beams from the CAPS electron spectrometer (ELS) instrument in the second panel. The magnetometer observations of the field-aligned currents which accelerate the electron beams are shown in the bottom panel. The ramp-like signature of the southward current is associated with a shear-mode Alfven wave excited by the moon-plasma

interaction. Parallel electric fields often associated with the Alfven wave are believed to be accelerated by these waves along magnetic field lines that map to the Enceladus footprint in Saturn's aurora [Gurnett and Pryor 2012].

Leisner et al. [2013] observed northward and southward auroral hiss funnels on both flanks of Enceladus. They found that these funnels are consistently observed on all low-inclination flybys through the Enceladus flux tube, suggesting that the electron beams associated with these auroral hiss funnels are a steady state feature of the Enceladus interaction with the plasma. Sulaiman et al. [2018a] observed an auroral hiss funnel on the ionospheric end of the flux tube connecting the planet to Enceladus.

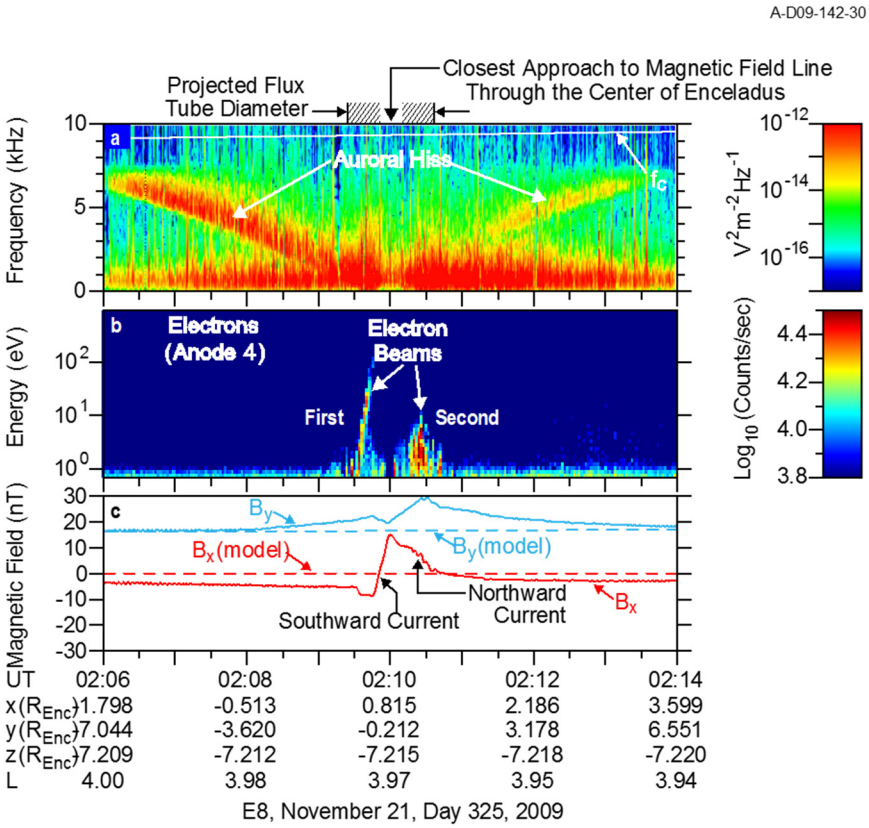

Figure RPWS-5. Evidence of an electrodymanic interaction between Enceladus and Saturn's magnetosphere in the form of auroral hiss generated by electron beams.

PLASMA-DUST INTERACTIONS

The measurement of dust grains in the vicinity of Enceladus and the interaction of these grains with the ambient plasma became a focus of RPWS research. Farrell et al. [2009] presented high-time resolution spectral evidence from the E3 flyby of small water-ice grain impacts on the electric antennas in the vicinity of Enceladus and a sudden, large drop in the electron density in the same region, a density depletion that they attribute to the absorption of electrons by submillimeter-sized

icy particles. Morooka et al. [2011] presented Langmuir probe observations to provide evidence for the presence of dusty plasma in the Enceladus plume region. The data show large increases in the ion and electron densities just south of the equatorial plane in the plume region for four Enceladus flybys in 2008, but there is a two order of magnitude difference in these plasma densities with $n_e/n_i < 0.01$. This plasma signature is attributed to electron absorption by dust grains in the plume, which subsequently become negatively charged. The ion and electron density increases in the plume region just south of the equatorial plane are shown in the top panel of Figure RPWS-6, which is adapted from Figure 5 in Morooka et al. [2011]. No plasma wake signature is observed in this data. The middle panel of Figure RPWS-6 shows the strong drop in the n_e/n_i density ratio in this same region where the presence of dust grains had been previously determined [Farrell et al. 2009]. The bottom panel in Figure RPWS-6 shows almost Keplerian ion speeds measured by the Langmuir probe which are well below the plasma corotation speed, reaching a minimum below Keplerian speeds in the plume region. The interaction between the cold plasma and the negatively charged small dust grains is believed to cause this slowing of the plasma that moves with Enceladus, explaining the lack of a plasma wake behind the moon.

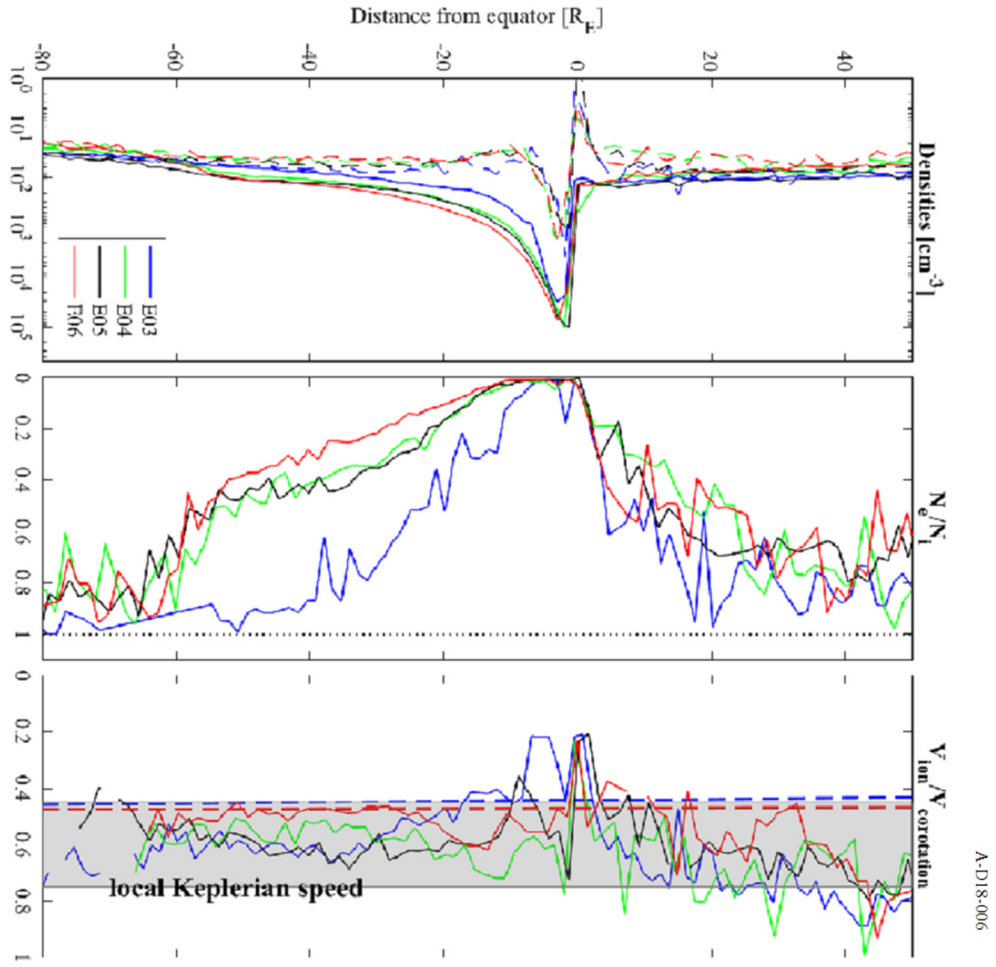

Figure RSWS-6. The variation of electron densities (*Top*), ratio of electron to ion densities (*Middle*) and the ratio of the ion velocity relative to corotation in the vicitnity of Enceladus.

The presence of dust grains inferred by the ion-electron density difference led to a number of research results. Ye et al. [2014a] discovered that, after a dust grain impacted the RPWS electric antennas, a dust ringing effect was observed by the RPWS Wideband Receiver, characterized as periodic plasma oscillations. The frequency of these oscillations was shown to be consistent with the local electron plasma frequency, providing a measurement of the electron density. Densities derived from this method in the Enceladus plume region were found to be consistent with electron densities derived by the Langmuir probe for four consecutive Enceladus flybys in 2008. Shafiq et al. [2011] presented Langmuir probe observations of the E3 flyby to derive estimates of the dusty plasma parameters and found that the dust density would vary depending on the grain size. The submicron-sized dust grains dominate in the plume region with densities of 10^2 cm^{-3}. The micrometer-sized and larger sized grains are estimated to have densities of only 6.3×10^{-5} cm^{-3}.

OTHER RESEARCH

Omidi et al. [2012] used an electromagnetic hybrid simulation to explore the impact of charge exchange between the plasma and the neutral gas and the electron absorption by dust particles on the deceleration of the corotating plasma near Enceladus. They found that the charge exchange between the corotating ions and the neutral gas in the plume played a dominant role in the deceleration of the plasma.

Farrell et al. [2012] found that, in Enceladus' northern hemisphere within ~5 R_E, there is a quasi-time stationary plasma feature, a clear electron density dropout in the RPWS data coincident with a sharp deceleration in the plasma flow. They infer the presence of dust in the northern hemisphere by this plasma feature. They further suggest that the submicron dust population in the northern hemisphere is secondary ejecta, small fast dust grains resulting from surface impacts by larger micron-sized dust grains which originated in, among other possible sources, the moon's plume.

Engelhardt et al. [2015] presented evidence for the existence of a dust trail downstream of Enceladus and extending north of the moon up to 4 R_E. The trail region is characterized by a strong electron density depletion coincident with a nearly constant ion density profile, suggesting that some fraction of the electrons have been absorbed by the dust grains that have been observed in this region.

Farrell et al. [2017a] used a particle-in-cell electrostatic simulation to examine the cold, low-energy ions produced in the Enceladus plume and the development of plasma sheaths about the negatively-charged, submicron dust grains that can act to trap these newly created ions which subsequently exit the plume region at the subcorotational speed of the dust grains. The authors further suggest that only about 3% of the ion population, with energies exceeding the sheath trapping potential, contribute to the ion pickup current and the associated magnetic field perturbations. The Langmuir probe measures both of these ion populations.

Rhea interaction

The moon Rhea orbits at a distance of 8.74 R_S (1 R_S = 60,268 km) from Saturn and is its largest icy satellite, with a radius of 764 km. Since Rhea has essentially no internal geological activity [Pitman et al. 2008] and only a very tenuous exosphere consisting of oxygen and carbon dioxide [Teolis et al. 2010] the moon was expected to be essentially a passive absorber, with little interaction with Saturn's corotating magnetosphere which streams by at a nominal corotational velocity of 85.4 km/s. Nonetheless, Cassini plasma measurements [Wilson et al. 2010] show that the plasma ions in the vicinity of the moon are slowed down by about 30% relative to rigid corotation due to their interaction with the moon. Measurements of the fluxes of energetic (several hundred keV) electrons [Roussos et al. 2012] shows that these electron fluxes have a broad depletion extending out to as much as 5 to 7 times the radius of Rhea. This extended depletion region has been interpreted by Roussos et al. [2012] as possibly being caused by dust or ring particles orbiting Rhea within the Hill sphere which is estimated to have a radius of about 7.7 times the radius of the moon. At lower energies, below about 100 keV, the electron fluxes show sharper depletion boundaries consistent with the geometric wake generated by absorption at the surface of the moon. Curiously, electron density measurements of the cold plasma by the Langmuir probe and by RPWS measurements of the upper hybrid resonance frequency show only a small decrease in the plasma density in the wake region, suggesting that the moon might be a significant source of cold plasma. Measurements of the electric and magnetic fields of plasma waves by the RPWS [Santolik et al. 2011] show that intense plasma waves are generated in the magnetic flux tube connected to the surface of the moon. Three types of plasma waves were observed: (i) bursty electrostatic waves near the electron plasma frequency, (ii) intense whistler-mode waves below one half the electron cyclotron frequency, and (iii) broadband electrostatic waves at frequencies well below the ion plasma frequency. The waves near the electron plasma frequency are believed to be driven by low energy (35 eV) electron beams accelerated in the vicinity of Rhea, and the whistler mode emissions are thought to be generated by the loss-cone anisotropy introduced in the low energy (230 eV) electron distribution by absorption at the surface of the moon. Pitch angle scattering by these waves may be able to explain some of the structure in the flux of energetic electrons reported in the vicinity of the moon.

Dust and Dusty Ring Science

One of RPWS's scientific goals is to detect the micron-sized dust particles that concentrate near the ring plane of Saturn [Gurnett et al. 2004]. In addition to gravity, these particles are also subject to solar radiation pressure and electromagnetic forces, making their orbit dynamics drastically different from the meter-sized main ring particles [Horányi 1996]. The dynamic orbit evolution and plasma sputtering make the lifetime of these particles less than a few thousand years [Burns et al. 2001], which requires these diffuse rings to be replenished continuously. During the Cassini mission, cryovolcanic activity near the south pole of Enceladus was discovered to be the source of E-ring material [Spahn et al. 2006b; Porco et al. 2006]. Other diffuse rings are formed mainly through collisions (meteoroid-moonlet impacts or collisions among the small bodies) and diffusion of collisional debris by non-gravitational forces [Hedman et al. 2007; Williams and Murray 2011].

The longevity of the Cassini mission and good coverage of space by the orbits allowed ample opportunities to explore the dusty rings of Saturn and the plume of Enceladus, providing important in situ measurements of dust density profiles and size distributions in these regions.

During Cassini's Saturn orbit insertion (SOI), RPWS WBR detected micron-sized dust particles at ~500 to 2000 impacts per second around the ring plane crossings [Gurnett et al. 2005]. Due to the high gain antenna (HGA) to ram pointing (protecting the spacecraft from dust hazards), the designated dust instrument Cosmic Dust Analyzer (CDA) [Srama et al. 2004] was not operating during SOI, so RPWS provided the only in situ measurement of dust particles then in this crucial region [Wang et al. 2006]. Based on the power spectrum measured by the monopole antenna, Wang et al. [2006] estimated the root mean square size of the particles detected to be around 2.6 micron. The particles detected near the ring plane were shown to have a power law distribution with power index −2.

In the first few years of the mission, Cassini made a number of inclined and equatorial crossings of the E-ring, particularly near the orbit of Enceladus.

In the first few years of the mission, Cassini made a number of inclined and equatorial crossings of the E-ring, particularly near the orbit of Enceladus. The ice particles detected by RPWS in this region were estimated to be a few microns [Kurth et al. 2006b]. The peak impact rates measured around the orbit of Enceladus were around 50 per second, corresponding to densities of order of 5×10^{-4} m^{-3}. The vertical dust flux profiles could be described by Gaussian function with a scale height of about 2800 km. It was also noted that density peaks could have a vertical offset of a few hundred km. Radial density profiles derived from the equatorial orbit measurements showed a peak near the Enceladus orbit and power law decreases inside and outside the Enceladus orbit, consistent with the previous optical measurements of the ring profile.

Ye et al. [2016a] analyzed the ring plane crossing data (within 6 R_S) collected by RPWS between SOI and equinox (85 crossings). Since the WBR can record the voltage waveform of each individual impact, they were able to derive the dust size distribution based on the sizes of the voltage jumps. It was found that the E-ring particle size distribution can be characterized by a power law function with a power law index around −4. Figure RPWS-7 shows the trajectories of Cassini during 53 high inclination ring plane crossings before equinox. The color code indicates dust density estimated for particles with radius larger than 1 micron. The density profiles derived based on the impact rates showed that dusty ring near the G-ring has a narrow profile (~240 km FWHM). In contrast, E-ring is much thicker. The thickness of E-ring has a minimum ~4000 km FWHM at Enceladus' orbit, and increases with the distance away from Enceladus' orbit. Ye et al. [2016a] constructed an E-ring density model based on fitting the vertical density profiles with Lorentzian functions and radial profiles with power law functions. Near Enceladus' orbit, the vertical dust density profiles showed slight dips around the ring plane, likely due to the gravitational scattering of the particles by the moon. The E-ring peak location was shown to be shifted to the north outside Enceladus' orbit and to the south inside Enceladus' orbit, consistent with optical measurements [Hedman et al. 2012]. The E-ring warp is due to the locking of the pericenters and apocenters of

the dust orbits out of the ring plane by the vertical component of the solar radiation pressure [Hamilton 1993]. So, it was predicted that the E-ring warp would change with time due to the seasonal change of solar radiation pressure normal direction relative to the ring plane.

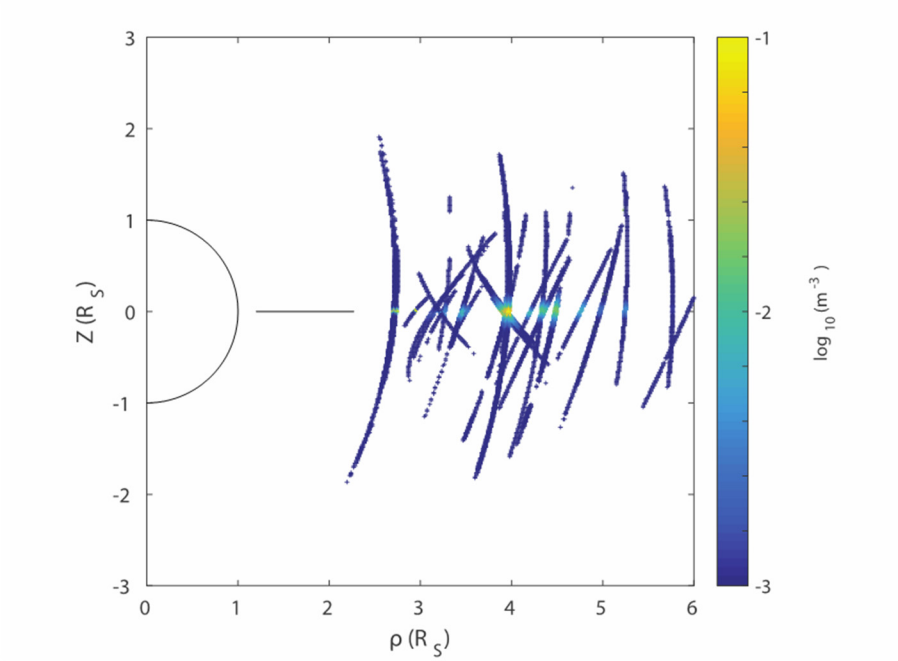

Figure RPWS-7. Trajectories of Cassini during 53 high inclination crossings between SOI and equinox in polar coordinates. The color code shows base ten logarithm of estimated dust density (>1 micron), so that yellow represents 0.1/m^3 and blue represents 0.001/m^3.

Cassini shifted to high inclination orbits and crossed the E-ring multiple times in 2016, providing opportunities to compare the vertical dust density profiles to those measured before equinox. The density profiles showed that the E-ring warp indeed reversed after equinox, with the dust density peak shifting to the south of the ring plane outside Enceladus' orbit and to the north inside Enceladus' orbit. These results confirm the seasonal control of the E-ring warp and role of solar radiation pressure in the dynamics of micron-sized dust particles in the E-ring.

Another asymmetry in the E-ring is the day-night asymmetry, as revealed by both remote sensing [Hedman et al. 2012] and in situ measurements (CDA and RPWS). The E-ring appears to be more compressed and bright on the noon side and more stretched out and faint on the night side. This local time asymmetry is likely related to two factors. One is the dependence of the orbital precession rate on the particles properties like size and charge-to-mass ratio and the other one is the recently discovered noon-to-midnight electric field which is of particular importance in driving the E-ring dynamic evolution.

The plume of water vapor and icy particles ejected from the south pole of Enceladus is perhaps the most exciting discovery of the Cassini mission [Dougherty et al. 2006; Porco et al. 2006]. The ejected material constitutes the major contents of the E-ring and Enceladus torus and

after ionization they become a major source of plasma in the magnetosphere of Saturn. Several instruments onboard Cassini are sensitive to the ice particles in the plume. On the small end of the size spectrum, nanoparticles are directly detected by the CAPS, where nanograins appear as energetic charged particles in the ELS and ion mass spectrometer (IMS) [Jones et al. 2009; Hill et al. 2012; Dong et al. 2015]. In a dusty plasma, electrons are attached to these nanograins, leading to a large difference between the electron and ion densities measured by the RPWS Langmuir probe in and around the plume [Wahlund et al. 2009a; Yaroshenko et al. 2009; Shafiq et al. 2011; Morooka et al. 2011; Engelhardt et al. 2015]. On the large end of the size spectrum, both CDA and RPWS are sensitive to micron-sized dusts [Srama et al. 2006; Kempf et al. 2008; Farrell et al. 2009, 2010; Omidi et al. 2012]. During the plume crossing when both CDA and RPWS were operating, the dust density profiles measured by the two instruments are consistent within the estimated uncertainty range for RPWS [Ye et al. 2014b]. Recently, it has been found that the Magnetospheric Imaging Instrument (MIMI) / Low-Energy Magnetospheric Measurement System (LEMMS) instrument is also sensitive to dust impacts in the plume of Enceladus, and the dust peak matches well with the dust density profile measured by RPWS [Krupp et al. 2017].

The plasma charge balance in the vicinity of Enceladus has been shown by the Langmuir probe measurements to be modified by the presence of dust particles. During the crossings of the Enceladus plume, Cassini RPWS observed sharp frequency decreases of the upper hybrid resonance in the vicinity of the moon, indicating electron density dropouts most likely due to absorption by the dust particles [Farrell et al. 2009]. Inside the plume, however, the dust impact signals are so intense that the upper hybrid resonance is hard to identify. Ye et al. [2014a] presented an independent method of determining the electron density inside the dusty plume of Enceladus, using the plasma oscillations induced by dust impacts and detected by the WBR. The frequencies of these oscillations were shown to be consistent with the local plasma frequency, thus providing a measurement of the electron density. It was proposed that the electrons from the impact plasma constitute a fast beam relative to the background plasma, which will excite Langmuir waves through the bump-on-tail instability.

During the Ring Grazing orbits between December 2016 and April 2017, Cassini crossed through the Janus/Epimetheus ring 20 times. The WBR was scheduled to collect waveform data during the ring plane crossings, from which dust density profiles and size distributions have been derived [Ye et al. 2018a]. Figure RPWS-8 shows the statistics of dust impacts observed during the ring plane crossing on day of year (DOY) 361, 2016. *Panel a* shows the impact counts as a function of voltage and time. *Panel b* shows the gain of the receiver, which is set based on waveform amplitudes to maximize the use of the analog-to-digital converter (A/D) dynamic range while minimizing clipping (exceeding the range of the A/D converter) [Gurnett et al. 2004]. *Panel c* shows the dust density (1 micron size threshold) calculated from the impact rates, assuming an effective impact area of 1 m^2. The red line in *panel c* represents a horizontal cut of *Panel a* situated at 0.034 Volts, the voltage that corresponds to 1 micron dust size. The count rate profile for 1 micron particles has a width (~600 km) similar to the CDA high-rate detector (HRD) density profile. *Panel d* shows the size distribution slope estimated within a 10-second moving window (blue diamonds). The scatter of the blue diamonds indicates the uncertainty of the estimated size distribution slope, increased when the number of impacts detected within the moving window decreases.

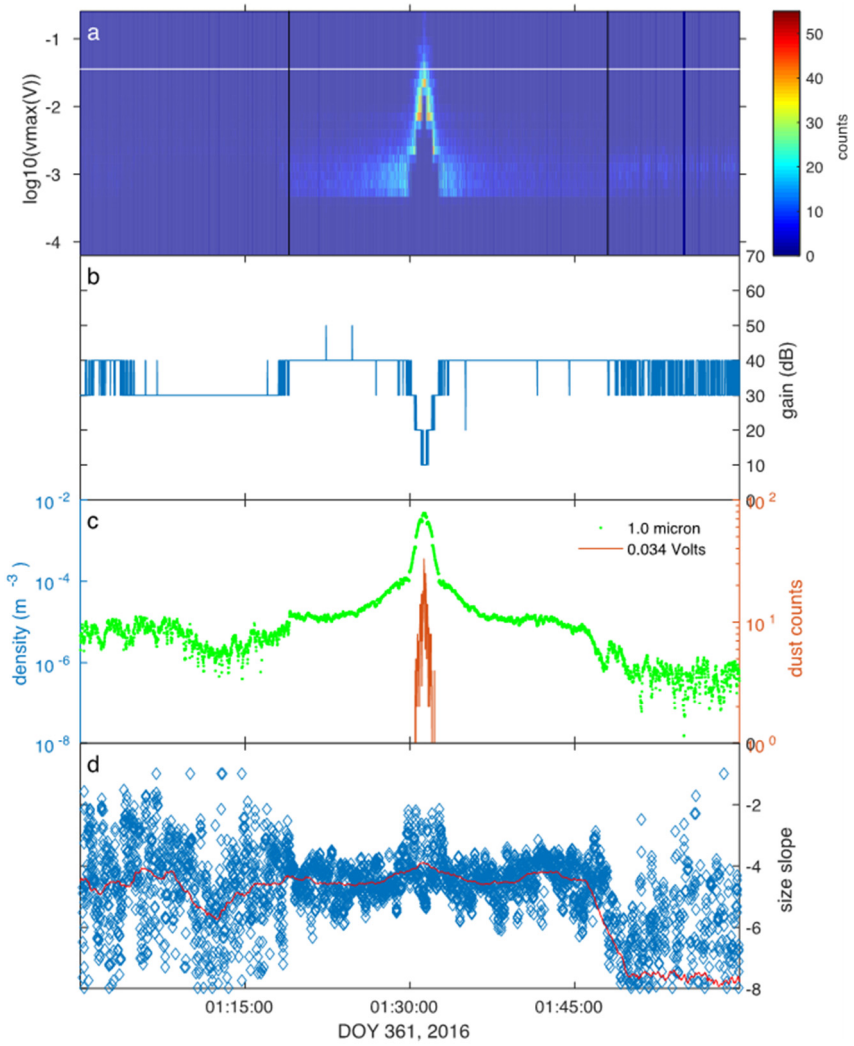

Figure RPWS-8. Dust analysis for the ring plane crossing on DOY 361, 2016. *Panel a*: Impact counts as a function of voltage and time. Black vertical lines mark the times of mode changes, between which the monopole antenna was used. *Panel b*: Gain of the receiver. *Panel c*: Dust density (1 micron size threshold) calculated from the impact rates. The red line shows the horizontal cut of *Panel a* situated at 0.046 Volts (marked with white horizontal line in *Panel a*). *Panel d*: Differential size (radius) distribution slope estimated within a 10-second moving window (blue diamonds, red line shows smoothed value with a 120-second moving window).

For example, when the antenna mode was switched to dipole, fewer impacts were detected, causing higher uncertainty level of the size slope. The red line indicates smoothed values of the individual size slopes (blue diamonds) using a 120-second moving window. This smoothed size slope is also used to scale the density values to the fixed size threshold shown in *Panel c*.

The RPWS dust density profiles were fitted with Lorentzian functions and compared to that measured by the CDA HRD (Figure RPWS-9). There is one order of magnitude difference between the two results, which is within the uncertainty limit estimated for the RPWS measurement.

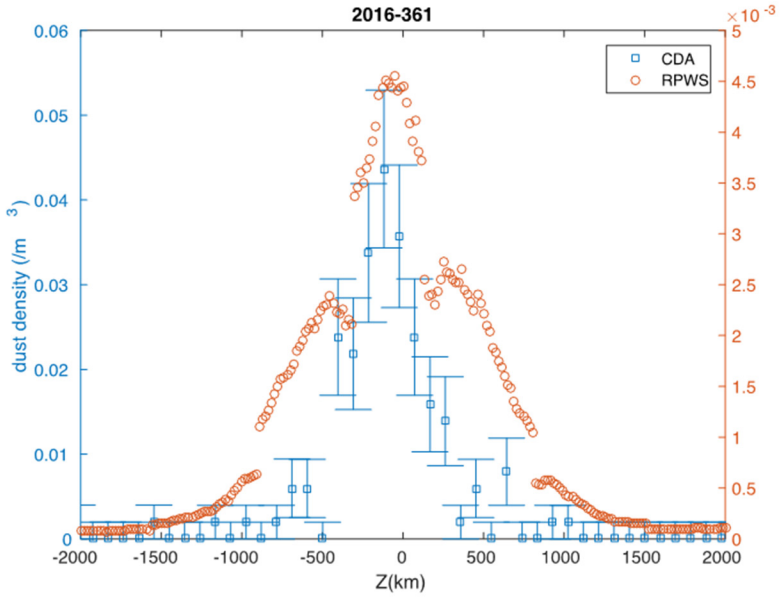

Figure RPWS-9. Comparison of vertical dust density profiles measured by RPWS and CDA HRD during the ring plane crossing on DOY 361, 2016.

The HRD profile also has a slightly narrower peak width. The dust densities inferred from the Langmuir probe sweep data (assuming a differential size distribution slope −4.5) agree with the WBR results [Morooka et al. 2018]. The peak locations of the RPWS dust density profiles shift north and south but are within 100 km of the ring plane (CDA HRD density profiles show a systematic southward shift of 130 km). These peak offsets are within the maximum offsets of the moons Janus and Epimetheus due to their slight orbit inclinations.

On April 26, 2017, Cassini dived into the gap between Saturn's main ring system and its atmosphere starting the 22 Grand Finale orbits. RPWS observed few micron dust impacts during the first five and last ten proximal orbits, not enough for characterizing the size distribution [Ye et al. 2018b]. The lack of micron dust in this region is probably due to the plasma drag in the ionosphere, where the cold density plasma corotate with the planet at a speed lower than the Keplerian speed of the dust particles. So, the micron dusts would lose speed and fall into the planet. During the higher altitude D-ring crossings (rev 276–282), RPWS detected more dust impacts with the density estimated to be about two orders of magnitude lower than F-ring orbits. The monopole antenna measurements near the D-ring indicated that spacecraft was charged positively (the impact signals were mostly positive, whereas at larger radial distances the impacts detected by monopole were mostly negative). The Langmuir probe also measured positive spacecraft potentials and electron bite-outs around the ring plane. The positive potential might be due to kinetic ion impacts, similar to what Langmuir probe (LP) observed in the deep ionosphere. Close inspection of the waveforms indicates a possible dependence of the impact signal decay time on ionosphere plasma density, which showed large variations from orbit to orbit.

RPWS was also able to detect nanoparticles originated from the inner solar system (0.2 AU) [Schippers et al. 2014, 2015] and Jupiter's moons [Meyer-Vernet et al. 2009], based on the bursty noise spectrum measured on the monopole antenna of RPWS. During the cruise phase of Cassini, the RPWS instrument was turned on with setup suitable for dust detection at three different heliocentric distances: 1, 1.6, and 2.9 AU. Signature of nanoparticle impacts were detected during all three operating periods, suggesting ubiquitous presence of these particles in the solar wind. The observed flux distribution is consistent with nanodust produced in the inner heliosphere, picked up by the solar wind, and carried to the outer heliosphere [Mann et al. 2007; Mann and Czechowski 2012]. Meyer-Vernet et al. [2009] analyzed RPWS observations during the Jovian flyby and estimated the flux of streaming nanoparticles ejected by the Jovian moon Io based on the bursty wave spectrum, which is consistent with the flux measured by the onboard dust analyzer CDA and Galileo dust instrument.

Magnetosphere-Ring Interaction Science

The Cassini mission brought about a profound new view the interaction of the amazing Saturnian main ring system with the magnetospheric space environment. During the Voyager era, it was presumed that meteors continually bombarded the rings. The spokes were thought to represent a stunning visual manifestation of these intense impacts. The associated impact-ionized vapor plume then delivered ring water and oxygen ions along connecting magnetic field lines to the ionosphere. These water ions were thought to chemically disrupt the ionosphere hydrogen cycle and deplete the ionosphere locally of electrons. It was also thought that these ring-generated ions possibly modify the color of the cloud tops. In this view, the rings were considered a source of quasi-energetic plasma delivering heavy ions to the exobase above the cloud-tops. Figure RPWS-10

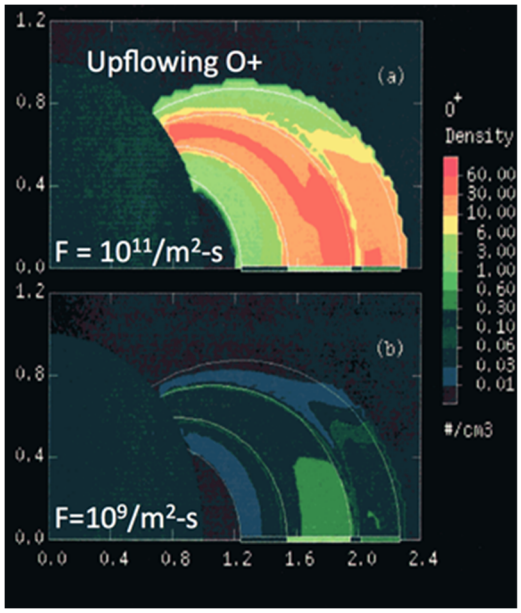

Figure RPWS-10. Impact-driven Ring Plasma Model [Wilson and Waite 1989].

shows the predicted impact-generated plasma flux from the rings, with peak densities over the dense portion of the central B-ring [Wilson and Waite 1989]. Voyager, unfortunately, did not actually fly over the rings and thus confirmation of this impact-driven ring plasma source could only be inferred.

At both the very beginning (SOI) and very end of the Cassini mission, the spacecraft flew directly across magnetic field lines that connect back down to the main rings, and thus obtained unique direct measurements of the plasma environment across the main A-ring, B-ring, and C-ring.

Saturn orbit insertion

Gurnett et al. [2005] presented a new view of the plasma environment over the main rings from the SOI overflight of the shadowed face of the rings. Figure RPWS-11 shows the corresponding plasma density as derived from the narrow-banded upper hybrid waves, electron plasma oscillations, and high frequency edge of the auroral hiss. All of these plasma wave features allow a high resolution direct derivation of the local electron density (see Gurnett et al. [2005] for a more detailed description of that derivation). In the profile, the various plasma wave sources are identified.

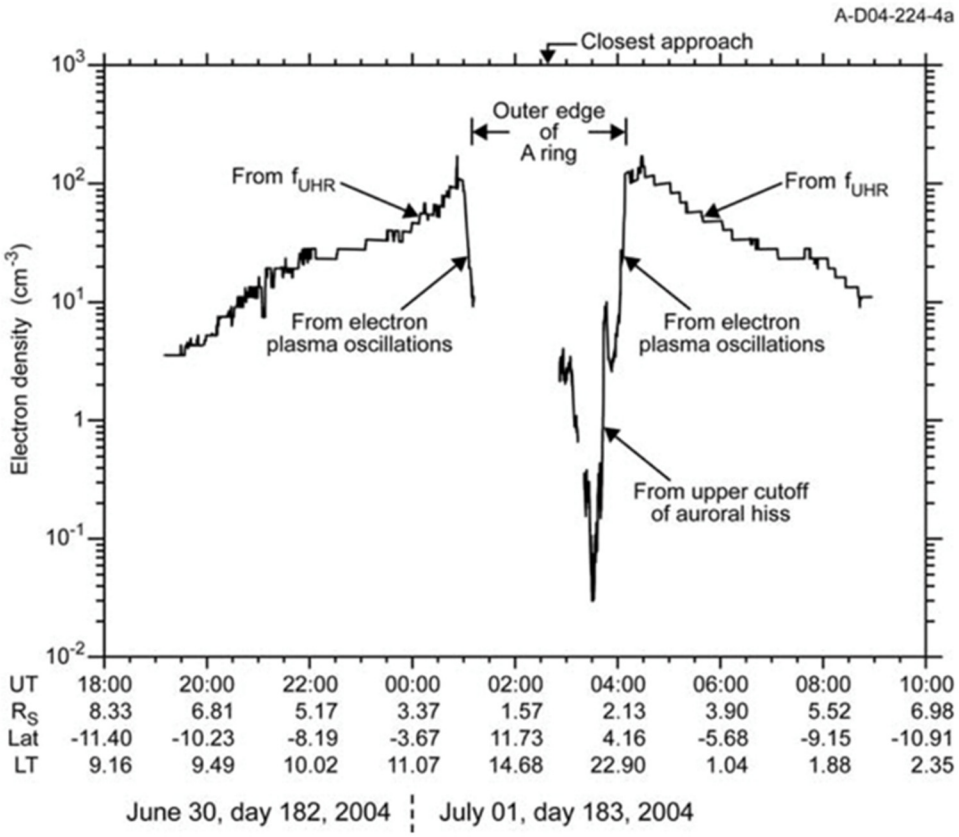

Figure RPWS-11. The electron density over the main rings as derived by the plasma waves detected by RPWS (see Gurnett et al. [2005] for more details).

There are two stunning features to this profile:

1. That immediately adjacent to the dense A-ring, there is an electron density maximum at over 100 electrons/cm^3, with the high density region (>10/cm^3) extending out to beyond L = 5. It would later be found [Persoon et al. 2009, 2015] that this high density region is a plasma torus created by ionization and pickup of new ions born in the Enceladus plume and a seasonal contribution from photo-ionized neutrals originating from the rings themselves. Thus, at equinox, the maximum in plasma density in this torus shifts radially outward to 4 R_S, but at solstice, the Sun-facing rings become a neutral and plasma source shifting the torus plasma maximum closer to the A-ring (see Figure 6 and 7 of Persoon et al. [2015]). The peak density in the torus is about 10% of the Io torus at Jupiter and represents a dominant controlling element in the inner magnetosphere of Saturn [Gurnett et al. 2007].

2. That the region over the main rings is devoid of plasma, with an electron density drop of near 10000 from the outer edge of the A-ring to values of 0.04 electrons/cm^3 at 1.76 R_S over the central portion of the B-ring [Xin et al. 2006; Farrell et al. 2017b]. This void region has been identified as a ring plasma cavity (RPC) with its lowest density near the synchronous location. The profile of electron density over the main rings varied inversely with ring optical depth, with the lowest plasma densities observed over the central dense B-ring and a local maxima sense when passing over field lines connected to the Cassini Division. (In Figure RPWS-11, this Cassini Division plasma maxima is seen near 03:45 spacecraft event time (SCET) with the local peak near 10/cm^3.)

This electron density profile was unexpected and almost diametrically opposite to what would have been predicted from an impact-driven ring plasma system, where the maximum in plasma density is expected in the central B-ring (like in Figure RPWS-10).

Evidence for photolytic-driven rings

RPWS SOI observations confirm the model of Tseng et al. [2013] that the ring-ionosphere-magnetosphere interaction is driven by photolytic processes, not impact processes [Farrell et al. 2017b]. Specifically, the sun-facing side of the main rings are a source of photo-dissociated neutrals that then get ionized to form a relatively low energy exo-ionosphere. This exo-ionosphere cannot directly access the shadowed/unlit side of the rings: the ring particles represent obstacles to their transport. Thus, the plasma density on the unlit side is modulated by ring density, being lowest where the ring obstruction is the highest—in the central B-ring. Local maxima are expected where the local ring particle density is low, like across the Cassini Division. There is little evidence of impact-generated plasma like that predicted during the Voyager era.

New main ring-magnetosphere current system

Xin et al. [2006] reported a strong auroral hiss signal detected at the deepest depletion of the electrons within the RPC near 1.76 R_S. The whistler-mode auroral hiss emission is a classic signature of the presence of energetic-field-aligned electron beams, in this case flowing outward from the rings along field lines connecting to the ionosphere. They reported that the RPC environment had a stunning similarity to plasma cavities found in polar auroral regions, usually associated with field-aligned currents that drive the aurora. The observation suggested that there is a current system driven by the rings-magnetosphere interaction, with the electron beams and currents near the synchronous point at 1.76 R_S possibly being part of the current closure system.

Figure RPWS-12 illustrates the concept of this new ring current system presented in Xin et al. [2006]. While the plasma on field lines over the rings would be corotating, the particles and associated photo-dissociated gas of the rings would be moving in Keplerian motion, creating drag on the plasma. This drag creates an associated change in plasma speed, ΔV. Beyond the synchronous point, the plasma is slowed by the Keplerian-moving particles and gas, creating an outward radially-directed E-field in order to maintain the new subcorotation speed $E' = \Delta V \times B$. This new E-field drives an outward current, J, which acts to then form a magnetohydrodynamic $J \times B$ force to balance the plasma-ring drag force. Inward of the synchronous point, the corotating plasma is accelerated by the ring drag force, creating an inward radial E-field and current that forms a $J \times B$ force to offset the acceleration. At the edges of the rings, these cross-ring currents become field-aligned parallel current that close down to the ionosphere along connecting magnetic field lines at the outer edge of the A-ring near L = 2.25 and inner edge of the D-ring near L ~ 1.11. The rings thus behave as an electrical generator in the plasma, driving currents from the ring surfaces along magnetic field lines down to the ionosphere.

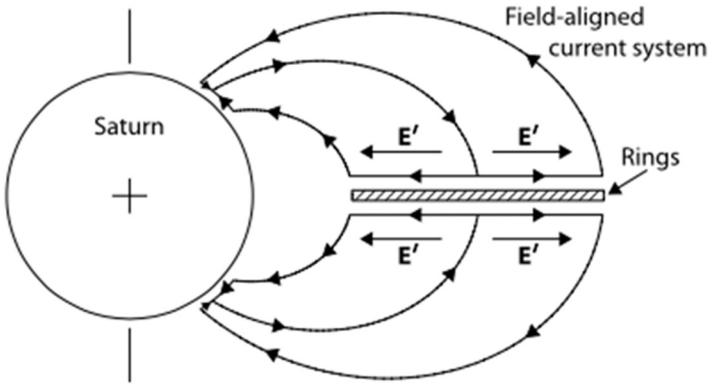

Figure RPWS-12. The proposed large-scale current system that would be induced in Saturn's magnetosphere by the interaction of the rings (including any associated gas) with the corotating magnetospheric plasma. Figure from Xin et al. [2006].

Subsequent RPWS observations confirm the presence of the various elements of this current system:

1. After SOI, Gurnett reported that bursts of auroral hiss emission were observed during SOI at the outer edge of the A-ring by RPWS. These events were initially reported to possibly be from impacts on the rings. However, the burst localization limited to only the very outer edge of the A-ring suggests the non-unique possibility that these auroral hiss emissions are associated with bursty field-aligned electron beams that make up the outer edge of the Xin et al. current system at L ~ 2.2.

2. Farrell et al. [2005b, 2008] reported on z-mode radiation emitted from active plasma hot spots along the outer edge of the A-ring where the rings and corotating magnetospheric plasma disk interact. Newly-born corotating ions created by photo-ionization of neutrals from the Enceladus torus or sunlit side of the rings would be the source of this ring-plasma interaction. Farrell et al. [2005b] and Menietti et al. [2016b] proposed wave generation mechanisms to explain the z-mode emitted from active regions.

3. Kopf et al. [2011] reported on the fine structure of Saturnian Kilometric Radiation from active auroral regions. They found there was a population of events having fine structure emission frequency vs time emission drifts consistent with emission at low latitudes from the L = 2.2 field line. The observation suggests the L = 2.2 field line at the outer edge of the A-ring is active, with parallel currents creating SKR at the field line footprint above the cloud-tops.

4. As discussed in this section, auroral hiss indicative of electron beams and inward flowing currents were detected near the synchronous point at 1.76 R_S [Xin et al. 2006]. This observation was the inspiration for the model of the main ring-magnetosphere current system.

Some added key evidence for this current system is still being derived from the ongoing analysis of the proximal orbit sequence that occurred in 2017.

Proximal orbit analysis and added evidence for the main ring-magnetosphere current system

While detailed analysis of the proximal orbits is still ongoing, Wahlund et al. [2018] reported on a very strong Saturnian ionosphere-D-ring electrical connection, which would represent the current closure of the Xin et al. [2006] model at the inner radial edge of the main rings. Using the RPWS Langmuir probe, they found that Cassini passed through a cold, dense electron region during proximal perigee, which has been interpreted to be entry into the Saturnian ionosphere. Figure RPWS-13 shows an example proximal electron density profile from orbit 271. The peak densities are in excess of $10^3/cm^3$, consistent with passing through the ionosphere. However, as evident in this and other passes, the ionospheric densities had relative maxima and/or unusual fluctuations

on field lines connected to the D-ring (near ±10° latitude). This effect was reported by Wahlund et al. [2018] to be associated with the Keplerian D-ring charged particles driving currents on field lines connected to the corotating ionosphere plasma.

At higher altitude proximal perigee passes, like orbit 277, Cassini passed through the inner edge of the D-ring (also immersed in the outer edge of the ionosphere). In these cases, the electron density had a distinct bite-out or decrease near the equator which is believed to be due to the presence of D-ring particulates that have absorbed the local ionospheric plasma. The RPWS instrument also detected micron-sized dust grain impacts revealing the presence of these D-ring particulates. The complex dusty plasma interactions remain a subject of considerable study even after the end of the mission.

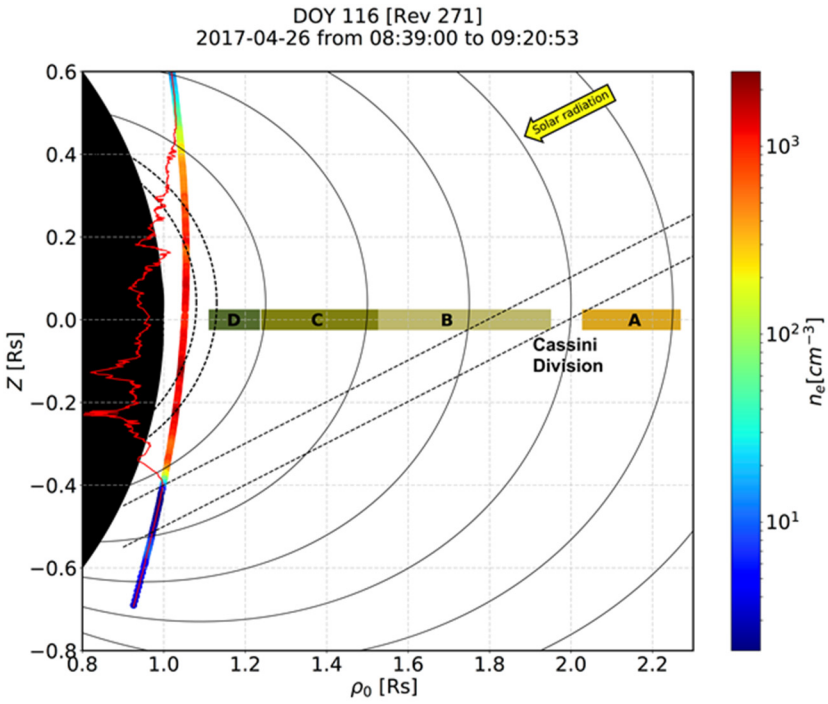

Figure RPWS-13. The Cassini spacecraft trajectory during April 26, 2017, crossed through the gap between the planet Saturn (solid black) and its rings (denoted D, C, B, Cassini Division, A) from north to south. The color code signifies the electron number density as measured by RPWS, which is also shown as a red line (in linear scale, density increases toward the left) where detailed structures can be detected. Four dominant electron density enhancements are connected via Saturn's magnetic field to, or inside, the inner edge of the D-ring (dashed lines). The solar elevation angle was 26.7° during the event, and the shadows of the B- and A-rings result in decreased ionization in the south. From Wahlund et al. [2018].

With repeated sampling of magnetic field lines connected to the main rings during the proximal orbit, Sulaiman et al. [2018b] reported the first observations of VLF saucers originating from Saturn's ionosphere, similar to what was observed at the Earth by the Fast experiment [Ergun et al. 2003]. Furthermore, Sulaiman et al. [2019] found evidence to strongly support the single observation that Xin et al. [2006] reported, hinting a ring-ionosphere current system. This concluded

the existence of a persistent, large-scale, and ordered electrodynamic connection between Saturn and its main rings.

The spokes in the context of the ring-plasma cavity and ring current environmental systems

The enigmatic spokes found near the center of the B-ring (near the synchronous location) were the source of numerous observation and theoretical works during the Voyager era. Their amazing observation captured the imagination since they represented a dynamic, impulsive, modern process occurring on the ring surfaces. Unfortunately, Voyager did not pass over the rings so the space environment associated with the spokes remained unknown until Cassini.

The review by Goertz [1989] described the spokes as being a result of a meteoric impact onto the rings that releases high volumes of charged dust, neutrals, ions, and electrons from the ring surface. Immediately after impact, the plume charged species undergo pickup, with electrons getting picked up immediately, then ions and then the more massive dust. This spatial spread in charged species created by local pickup thus was hypothesized to form an azimuthally-directed transient E-field. The various species then were predicted undergo an ExB drift to migrate radially forming spokes from the central B-ring.

However, during SOI and the proximal orbits, Cassini transited field lines that connect to the spoke locations (although spoke activity was not reported during these times). Farrell et al. [2006] reported that the Voyager spoke occurrences are spatially co-aligned with the ring-plasma cavity observed during SOI. Figure RPWS-14 overlays the SOI observations of the RPC with the Voyager-detected spoke occurrences [Grün et al. 1992]. The stunning spatial coincidence suggests that the spokes might then be some visual manifestation of the larger electrical current system containing the electron beam, auroral hiss, and plasma cavity detected during the Cassini SOI passage.

Any new dusty-plasma plume forming in the central B-ring is thus injected into the low density RPC environment with a radially-directed E-field (see Figure RPWS-12) along the ring surface [Xin et al. 2006]. The radial E-field may then provide the acceleration the spoke's charged dust in the radial direction. This new acceleration process would replace the more complex requirement of having to form a transient azimuthal E-field to create the subsequent radial transport.

HST observations [McGhee et al. 2005] indicated that the spokes on the sun-lit faces of the rings—those visible to Hubble Space Telescope (HST)—tended to disappear when the ring tilt angles exceeded ~15°, under increasing solar UV radiation conditions. Farrell et al. [2006] noted that at these angles the local photo-electron emission from the ring surfaces would exceed the electron densities in the plasma cavity—thus destroying the RPC environment and changing the local surface potential polarity from negative to positive. They suggested this photo-electron effect from solar exposure might explain the reported loss of the spokes at relatively large tilt angles observed by HST.

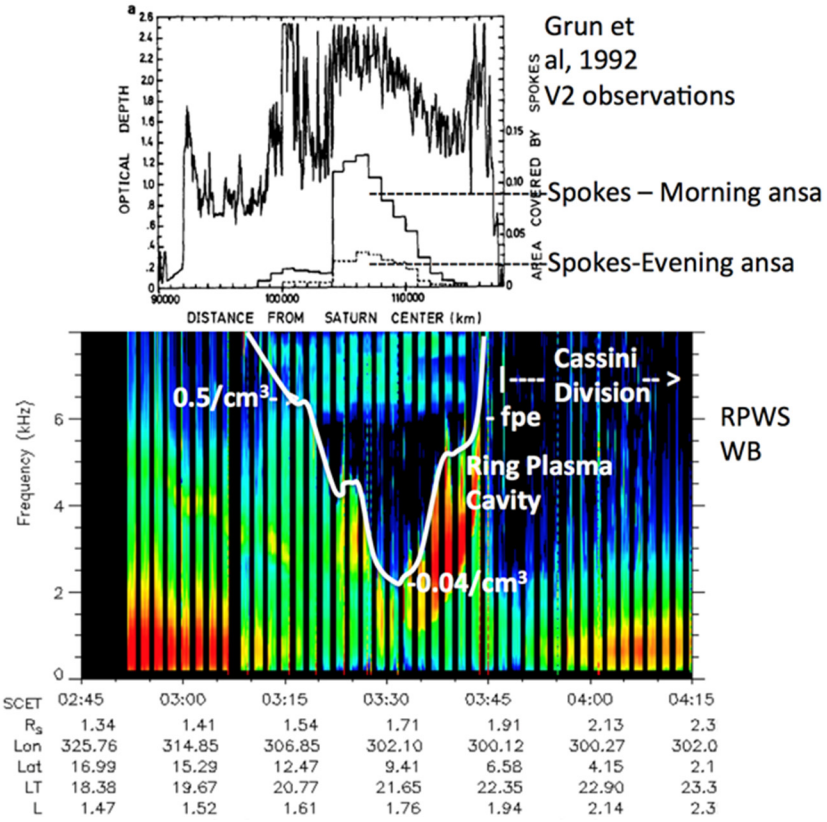

Figure RPWS-14. The ring plasma cavity detected during SOI as evident by the deep minimum in electron plasma frequency (indicated with the white line) in the RPWS wideband spectrogram. *Top panel*: location of the Voyager-observed spokes occurrence from Grun et al. [1992] with the two plots co-aligned by L-shell value. Presented by W. M. Farrell, M. D. Desch, M. L. Kaiser, W. S. Kurth, and D. A. Gurnett at the Joint Juno-Cassini workshop 2015.

Radio Emissions and Periodicities

Saturn's radio emissions started to be observed by Cassini/RPWS over the 10–1000 kHz range (see section entitled Kilometric Radiation) from distances of a few astronomical units. From late 2002 to early 2003, they were embedded in Jovian radio emissions and solar radio bursts. Their signal-to-noise ratio increasing with decreasing distance to Saturn, they became the dominant emission for the mid-2003 to mid-2004 year preceding Saturn's orbit insertion. These emissions divided into three main components, which have been analyzed separately or comparatively, as described below, to address most of the scientific objectives described in previous sections. Figure RPWS-15 shows examples of Saturn Kilometric Radiation (SKR), 5- and 20-kHz narrowband (NB) emissions and Saturn Drifting Bursts (SDBs) along with Saturn Electrostatic Discharges (SEDs) at the higher frequencies.

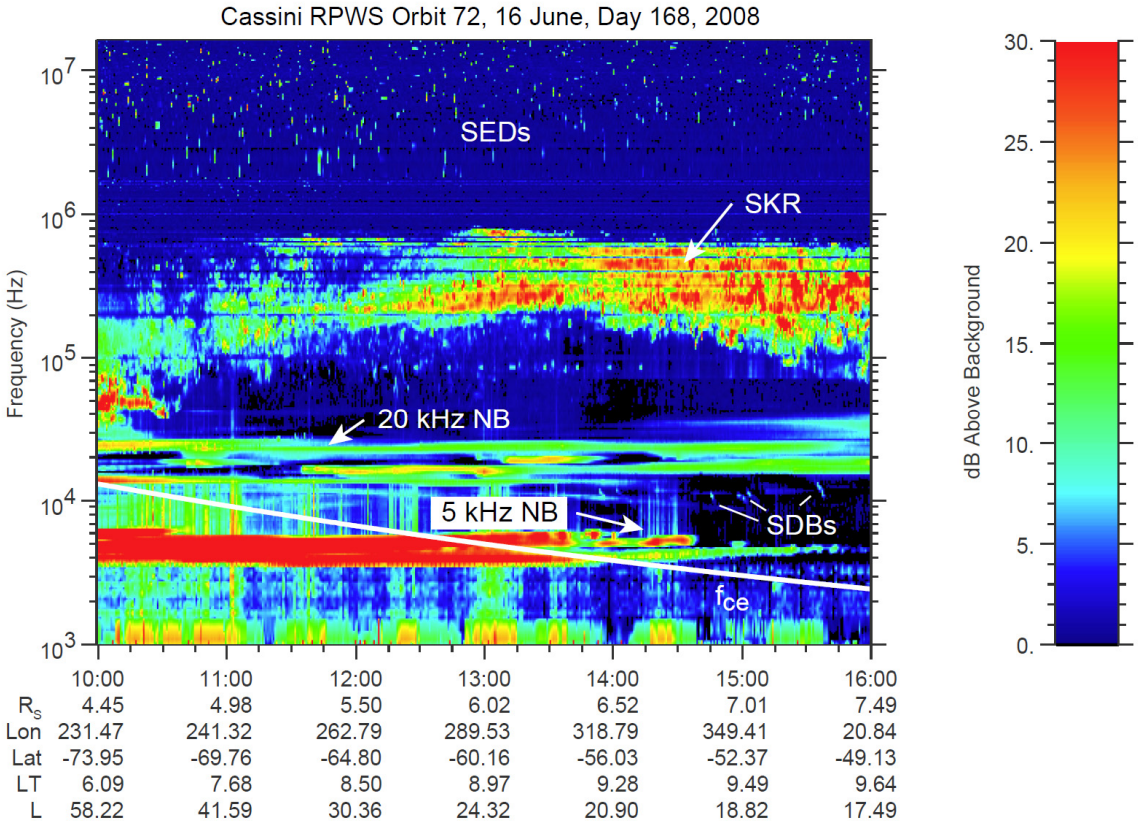

Figure RPWS-15. An illustration of the the major Saturnian radio emissions. From highest frequencies: SEDs, Saturn electrostatic discharges from lightning; SKR, Saturn Kilometric Radiation, 20- and 5-kHz NB, emissions, and SDBs, Saturn drifting bursts.

Kilometric radiation

Saturn's Kilometric Radiation is the most intense radio emission component, produced in the auroral regions. Several reviews of SKR properties have accompanied the Cassini mission [Kurth et al. 2009; Badman et al. 2014], the most recent one summarizing our current knowledge before Cassini Grand Finale [Lamy 2017] (see in particular Figure 1 of Lamy [2017] which plots all RPWS observations of SKR over the course of the Cassini mission).

REMOTE PROPERTIES

- The SKR spectrum was studied statistically with RPWS observations from a wide variety of Cassini's positions. It extends from a few kHz to 1 MHz and appears to be most intense when observed from the dawn-side at mid-latitude [Lamy et al. 2008a; Kimura et al. 2013]. Southern SKR was predominant up to 2010 to mid-2011 (slightly after the equinox of 2009), while the northern SKR was predominant after,

consistent with a seasonal control of field-aligned currents driving auroral emissions by solar illumination of Saturn's ionosphere.

- The SKR sources were routinely located by RPWS/HFR direction-finding (goniopolarimetric analysis, which additionally provided the apparent wave beaming angle. The radio sources were observed to be hosted by magnetic field lines at all longitudes whose footprints map to the circumpolar auroral oval [Farrell et al. 2005a; Cecconi et al. 2006; Lamy et al. 2009]. The emission is strongly anisotropic, with a beaming angle decreasing with frequency, which produces arc-shaped emissions in the t-f plane [Lamy et al. 2008b; Cecconi et al. 2009; Lamy et al. 2013].
- SKR is a right-handed (RH) fully elliptically polarized emission. It is seen predominantly in the R-X (and marginally in the L-O) mode, with RH/LH (LH/RH) polarization witnessing emissions coming from the northern/southern (southern/northern) hemispheres, respectively. SKR was remotely found to display quasi-purely circular polarization at latitudes below 30° and strongly linearly polarized above [Cecconi and Zarka 2005a; Masters et al. 2009].
- SKR displays several types of dynamics. At timescales of a few minutes, SKR displays fine structures drifting in frequency and reminiscent of auroral kilometric radiation (AKR) fine structures observed at Earth. Multiple origins accounting for the slow drifts of a few kHz/min are debated [Kurth et al. 2005b]. At timescales of hours, active flux tubes hosting anisotropic radio sources produce isolated arcs in the time-frequency plane, whose characteristics relate to the wave beaming angle and the position/motion of the source with respect to the observer. At timescales of 11 h, the emission is strongly rotationally modulated (see section entitled Radio Periodicities). At longer timescales, SKR strongly brightens episodically, indicating auroral storms driven or not by the solar wind and thus probing large-scale magnetospheric dynamics [Kurth et al. 2005a, 2016; Clarke et al. 2005; Crary et al. 2005; Jackman et al. 2005, 2009, 2010; Badman et al. 2008a, 2016; Nichols et al. 2009; Lamy et al. 2013; Reed et al. 2018].

In situ characteristics:

SKR sources were crossed twice at 10–20 kHz before the Cassini Grand finale. Their detailed study revealed that SKR is fully consistent with the Cyclotron Maser Instability (CMI) developed for AKR at Earth. It is radiated perpendicular to the magnetic field-lines from shell-like electron distribution functions of 6–9 keV [Lamy et al. 2010a; Mutel et al. 2010; Bunce et al. 2010; Schippers et al. 2011; Kurth et al. 2011; Menietti et al. 2011a, 2011b]. SKR polarization turned to be strongly linearly polarized at the source, as expected for perpendicular emission, and was found to be circularized along its propagation through the surrounding environment in agreement with expectations from the magneto-ionic theory in a cold, weakly inhomogeneous, plasma [Lamy et al. 2011a]. A statistical survey of the ring-grazing orbits revealed three additional passes of the spacecraft within low frequency dawnside northern SKR sources. The amplified waves were again

found to be strongly linearly polarized, radiated quasi-perpendicularly from the field lines through the CMI from 6-12 keV unstable electrons. Additionally, the SKR source region was interestingly seen to be only partially colocated with the UV auroral oval as the local plasma density was surprisingly variable and sometimes high enough to quench the CMI [Lamy et al. 2018a]. Cassini proximal orbits will provide further insights to the statistical characterization of SKR high frequency sources.

Narrowbanded emissions

At the lower edge of SKR spectrum, narrowbanded (NB) emissions have been observed between 3 and 70 kHz, and divide in two main components around 5 kHz and 20–40 kHz. Their observation by RPWS has been reviewed by [Ye et al. 2011].

The 5 kHz emissions, early labelled n-SMR for NB myriametric emissions in analogy with narrowband kilometer (nKOM) at Jupiter, were observed to rise in association with sudden SKR intensifications and related to ejection events from the plasma disk [Louarn et al. 2007]. The 5 kHz component was found to be intense and weakly circular polarized while the 20–40 kHz component, proposed to be referred to as n-SKR, appeared to be weaker and highly circularly polarization, both being better observed from high latitudes [Lamy et al. 2008a].

The source locus, dynamics, and wave growth of NB emissions were investigated in depth through a series of statistical and case studies [Menietti et al. 2009, 2010b, 2016b; Ye et al. 2009, 2010a; Wang et al. 2010; Gu et al. 2013]. Both components were found to propagate in the L-O ordinary mode. The 20–40 kHz component was proposed to be generated by mode conversion of electrostatic upper hybrid waves on the boundary of the plasma torus. The 5 kHz component is produced on the Z-mode from the lower density region near the inner edge of the Enceladus torus and possibly from the auroral regions as well by a generation mechanism not unambiguously identified yet.

Saturn Drifting Bursts

Another type of low frequency radio emissions called Saturn Drifting Bursts (SDBs) was detected with RPWS below 50 kHz [Taubenschuss et al. 2011]. These bursty emissions are highly circularly polarized, propagating in R-X and L-O modes and display emission at the fundamental and first harmonic frequencies. They last for a few minutes and occur intermittently as slowly drifting events in the time-frequency spectrogram. Possible generation mechanism include CMI and linear or nonlinear mode conversion.

Radio periodicities

RPWS brought crucial observations to the study of the rotational modulation of Saturn's magnetosphere through measurements of periods of SKR and NB emissions (see reviews in Gurnett [2011]; Lamy et al. [2011a]; Lamy [2017]; Carbary and Mitchell [2013]; Szego et al. [2015]).

The first SKR periodicity measured by RPWS witnessed a value differing by 1% to the SKR period identified from Voyager/Planetary Radio Astronomy (PRA) observations 25 years earlier [Gurnett et al. 2005]. Such a large variation implies that the SKR period does not probe the internal rotation rate. The measured SKR period was then found to display weak variations associated with those of solar wind speed [Cecconi and Zarka 2005b; Zarka et al. 2007].

The major discovery brought by RPWS was then the identification of two SKR periods [Kurth et al. 2008] corresponding to the two kronian hemispheres, differing by ~1%. These periods were found to both vary with time in anti-correlation over yearly timescales and crossed closely after equinox, a trend which was interpreted as a seasonal driving of solar illumination [Gurnett et al. 2009a, 2010b, 2011b; Lamy 2011]. These dual periods were later noticed in NB emissions and auroral hiss as well [Gurnett et al. 2010a; Ye et al. 2010b; Ye et al. 2017] and more generally observed in numerous magnetospheric observables including magnetic oscillations, energetic neutral atom (ENA) emissions, aurorae [Mitchell et al. 2009c; Carbary et al. 2010, 2011; Nichols et al. 2010; Andrews et al. 2010, 2011; Provan et al. 2011; Badman et al. 2012a, 2012b]. It is now accepted that these dual rotational modulations all originate from two rotating hemispheric systems of field-aligned currents, whose origin may be atmospheric vortices [Jia et al. 2012].

The post-equinox period displayed a confused situation with poorly determined radio and magnetospheric periods. Over 2010–2012, they remained close to each other at locked phases, suggesting retro-interaction between both currents systems [Garnier et al. 2014], while sudden jumps of periods were tentatively attributed to Saturn's great whit spot activity [Fischer et al. 2014b] or to variable solar wind conditions [Provan et al. 2015]. Both periods eventually merged between mid-2013 and mid-2014 before crossing and diverging from each other after mid-2014 up to September 2017 [Provan et al. 2016; Ye et al. 2016b, 2017; Lamy 2017]. Figure RPWS-16 summarizes the variation of northern and southern SKR periods found by Ye et al. [2018c].

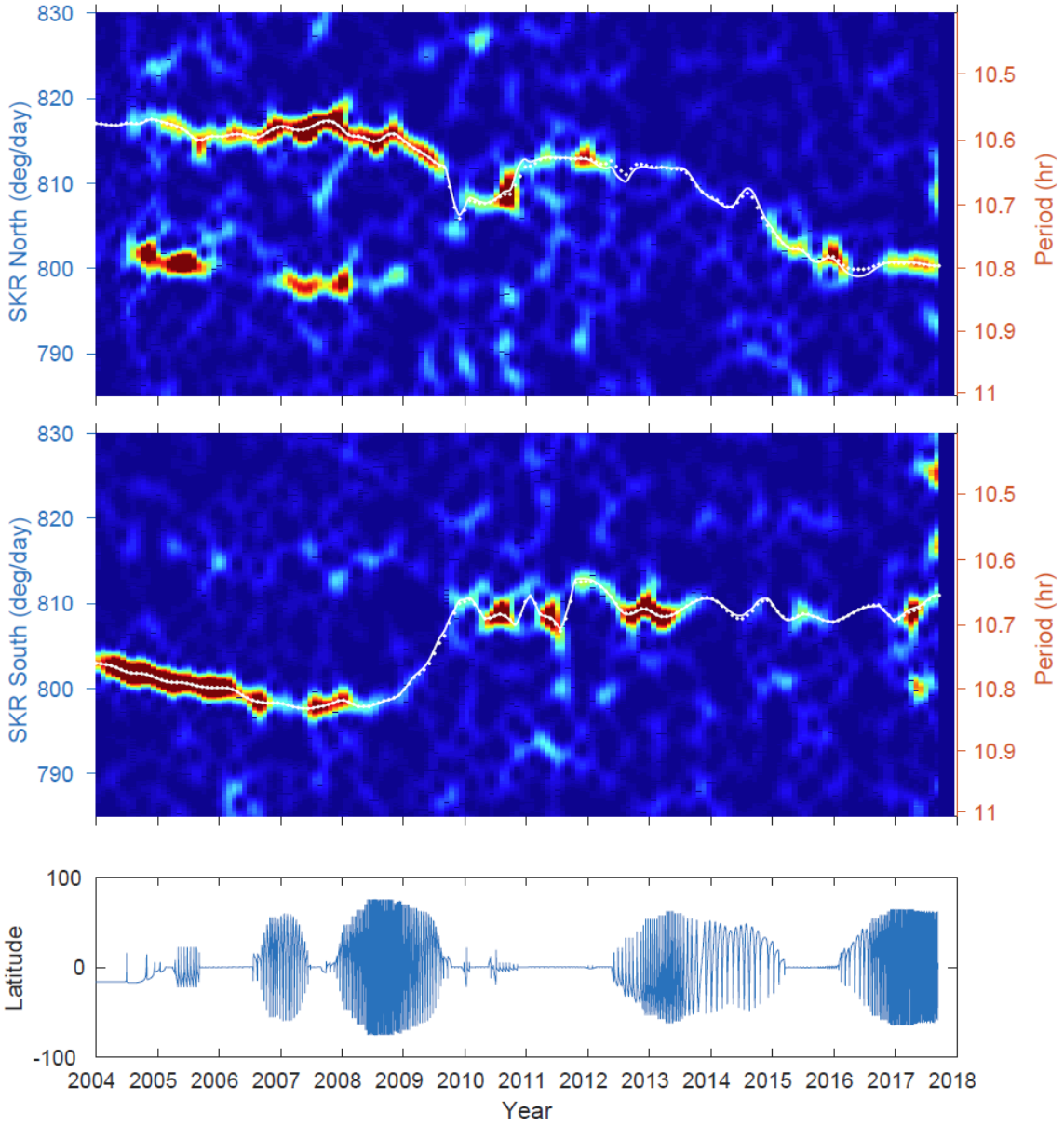

Figure RPWS-16. Rotational modulation spectrograms for SKR. *Top panel*: northern, *Middle panel*: southern hemispheres. The spectrograms show normalized modulation power (calculated using the least-squares spectral analysis) as a function of rotation rate and time. The white dotted lines show the automatically traced rotation rates (zeroth order) of north/south SKR. The white solid lines are corrected SKR rotational modulation rates (based on the zeroth-order rates and corrected by the phase drifts traced in Figure 1 of Ye et al. [2018c]). *Bottom panel*: is the latitude of Cassini.

Magnetosphere and Solar Wind Interactions Science

The Cassini RPWS instrument has helped investigate many different effects due to the interaction of the solar wind and the Saturnian magnetosphere, … .

The Cassini RPWS instrument has helped investigate many different effects due to the interaction of the solar wind and the Saturnian magnetosphere, how the standoff distance of the bow shock to the variations in the SKR intensity and frequency range, the presence of upstream Langmuir waves in the solar wind, and the detection of lion-roar like emissions in the magnetosheath. The following sections briefly discuss these observations and the various studies that RPWS has contributed to.

Solar wind influence on the Saturnian magnetosphere and aurora

The exact nature and importance of the solar wind influence on the Saturnian magnetosphere has long been debated. At Earth, the solar wind is the primary source of plasma in the magnetosphere and solar wind dynamics drive changes in the magnetosphere, including magnetic storms that lead to magnetic reconnection, plasma transport, and aurora. At Jupiter, the rapid rotation, large spatial scales, and internal source of plasma from the moon of Io, cause the magnetospheric dynamics to be primarily driven by centrifugal stresses rather than solar wind dynamics. The solar wind influence on the Saturnian magnetosphere has generally been considered to have both internal and solar-wind-driven processes. For example, the Voyager results suggested that the SKR pulsed at a period close to the planetary rotation period, but also that the emitted intensity was correlated with the solar wind dynamic pressure. This possible solar wind influence on the magnetospheric dynamics was an active area of research throughout the Cassini mission.

The approach to Saturn and the many orbits in which Cassini was located in the solar wind during apogee allowed in situ measurements of the solar wind while remote sensing measurements of the Saturn system were obtained. The remote sensing included Saturnian auroral imaging from the Hubble telescope and Cassini, plus observations by RPWS of the auroral radio emissions. During the approach to Saturn in early 2004, the Hubble Space Telescope took a number of ultraviolet images of the Saturn aurora and the comparison of these images to the Cassini observations were reported in a series of papers [Clarke et al. 2005; Crary et al. 2005; Kurth et al. 2005a]. During these observations, Saturn's auroras respond strongly to solar wind conditions, with the main controlling factor being solar wind dynamic pressure and electric field, with the orientation of the interplanetary magnetic field playing a much more limited role [Crary et al. 2005]. Clarke et al. [2005] reported that Saturn's auroral emissions varied slowly, with some features appearing to be related to corotation, and others are fixed to the solar wind direction. The auroral oval shifts quickly in latitude and is often not centered on the magnetic pole. In response to a large increase in solar wind dynamic pressure Saturn's aurora brightened dramatically, the brightest auroral emissions moved to higher latitudes, and the dawn side polar regions were filled with more intense emissions. The SKR emissions were also found to increase in intensity and drop in frequency

during the dynamic pressure increase and this intensity was correlated with the intensity of the aurora as shown in Figure RPWS-17 [Kurth et al. 2005a].

The relationship between solar wind dynamics, SKR, other magnetospheric properties, and the variation in the aurora continued in a number of different studies. During the SOI period, Jackman et al. [2005] suggested a major compression of Saturn's magnetosphere took place. Bunce et al. [2005] examined the in situ affects measured by Cassini that the corotating interaction region (CIR)-related compression had on Saturn's magnetospheric dynamics. For example, at ~02:00 UT on day 184, a burst of SKR emission is observed which disrupts the existing pattern of planetary modulated emission seen both upstream of the magnetosphere and during the inbound pass [Jackman et al. 2005; Kurth et al. 2005a]. Simultaneously, inside the magnetosphere, Cassini experienced a region of depressed and variable magnetic field. In addition, ion and electron observations show that this occurs as the spacecraft is engulfed by a hot, tenuous plasma population. They proposed that this behavior is indicative of a major episode of tail reconnection, triggered by the impact of the compression region on Saturn's magnetosphere.

The MIMI Ion and Neutral Camera (INCA) on the Cassini spacecraft also detected abrupt increases in energetic neutral atom flux coming from the general direction of Saturn's magnetotail that are well correlated with the enhancements in the Saturn kilometric radiation. Given the similarities between these events and substorm activity on Earth, including their dependence on interplanetary conditions, Mitchell et al. [2005] concluded that Earth-like substorms occur within Saturn's magnetosphere.

Taubenschuss et al. [2006b] examined the external control of SKR by the solar wind in the frame of the Linear Prediction Theory (LPT). Four basic solar wind quantities (solar wind bulk velocity, the solar wind ram pressure, the magnetic field strength of the interplanetary magnetic field (IMF) and the y-component of the IMF) were found to exert a clear influence on the SKR intensity profile. All four inputs exhibit nearly the same level of efficiency for the linear prediction indicating that all four inputs are possible drivers for triggering SKR, but all showed different lag times, ranging from ~13 hours for the ram pressure to ~52 h for the bulk velocity.

In contrasts to these earlier observations of direct correlations between solar wind magnetospheric dynamics, Gérard et al. [2006] reported results from a coordinated Hubble Space Telescope-Cassini campaign that took place between October 26 and November 2, 2005. During this period, Saturn's magnetosphere was in an expanded state and the solar wind was quiet, as indicated by the location of the magnetopause, in situ particle measurements, weak auroral SKR emission, and the generally low brightness of the aurora. The aurora exhibited considerable longitudinal structure and time variations over intervals of a few hours, in spite of the absence of observable external triggers and generally low intensity. In particular, enhancements of the dawn-morning oval were seen while no apparent indication of solar wind activity was observed. These features rotated at a speed corresponding to about 65% of the planet's angular velocity. Also, an ENA acceleration event occurred in the magnetotail on October 26 without any measured signature of solar wind activation. These observations suggest an intrinsically dynamical magnetosphere where injection of hot plasma occasionally takes place in the night or dawn sector during quiet

magnetospheric conditions, possibly connected with either the Dungey or the Vasyliunas convection cycle.

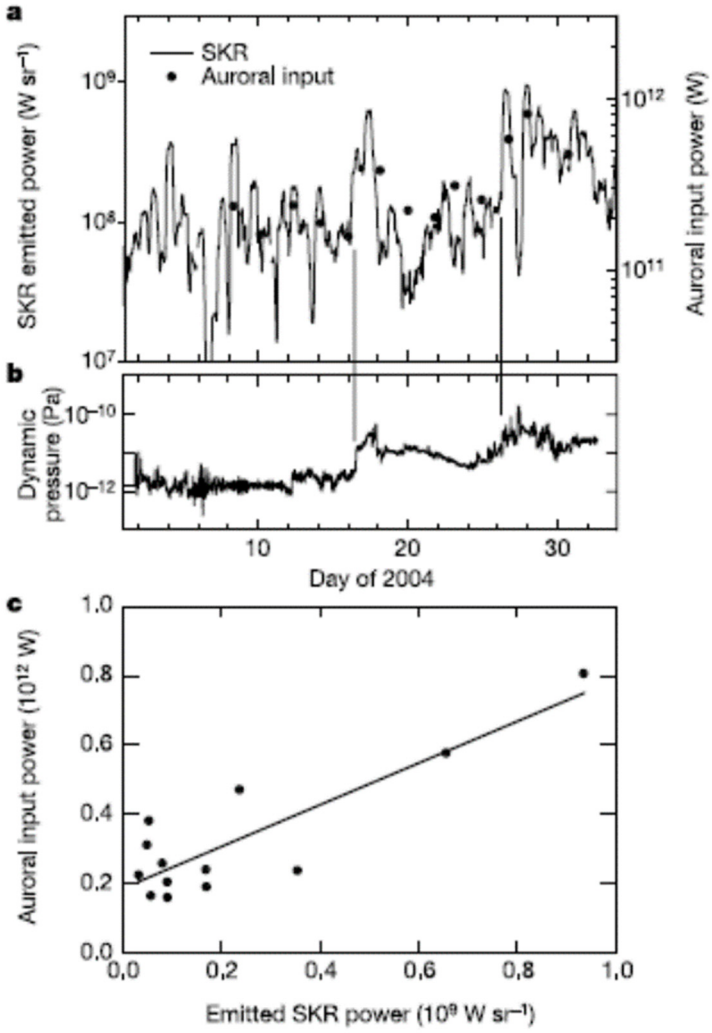

Figure RPWS-17. Correlations between auroral input power and emitted SKR power. *Panel a*: shows the time-averaged power emitted as SKR over plotted with the estimated auroral input power based on the ultraviolet aurora integrated intensity. *Panel b*: shows the solar wind dynamic pressure determined from Cassini measurements of the solar wind density and speed, and propagated to Saturn with a simple radial magnetohydrodynamic model. *Panel c*: compares the auroral input power and emitted radio power. Based on Figure 1 of Kurth et al. [2005a].

Louarn et al. [2007] reported on radio signatures observed at Saturn which are strikingly similar to the Jovian energetic events observed by Galileo. These radio signals consist of a sudden intensification of the SKR followed by the detection of a periodic narrowband radiation at about 5 kHz which most likely originates with plasma evacuation from Saturn's plasma disk. These radio signatures suggest that although Saturn's auroral activity is largely triggered by the solar wind,

energetic processes developing in the plasma disk are also involved, possibly associated with plasma transports and consequent releases of rotational energy.

In a study with a slightly different emphasis, Zarka et al. [2007] examined the possible role of the solar wind on the SKR radio period. As discussed in detail in the section entitled Radio Periodicities, as Cassini approached Saturn, the SKR period was measured to vary on the order of ~1% [Gurnett et al. 2005], and measurements over the first few years of the mission found that it actually exhibits two different periods [Kurth et al. 2008], and that each auroral polar region has its own dominate period that also varied with time [Gurnett et al. 2009a]. Zarka et al. [2007] found that the SKR period varied systematically by about ±1% with a characteristic timescale of 20–30 days, and that these fluctuations were correlated with solar wind speed at Saturn, suggesting that SKR is controlled in part, by conditions external to the planet's magnetosphere. No correlation was found with the solar wind density, dynamic pressure or magnetic field; suggesting that the solar wind speed therefore has a special role in this variation.

Rucker et al. [2008] reexamined the relationship between the SKR intensity and solar wind dynamics (both measured by Cassini and measured by Ulysses at ~5 AU and propagated to Saturn) for the year 2004. This study also found that the SKR intensity is positively correlated with solar wind pressure, and suggested that it may be possible to use the measured SKR properties as a monitor for the solar wind conditions.

Badman et al. [2008a] looked for variation of the SKR power observed by Cassini following arrival of thirteen solar wind compression event and investigated the phasing of the intensified or reduced emission peaks during the compression event, and the relative phasing and intensity of the emission peaks before and after the compression compared to the predictions of the drifting SKR period [Kurth et al. 2007]. They found that even though the behavior of the SKR following the compressions was somewhat variable, they confirmed that there was an overall positive correlation between the change in solar wind dynamic pressure and the change in emitted SKR power, and that the timings of the initial SKR intensifications following the compressions could be independent of the long-term phasing of the SKR bursts, but during the disturbed interval the SKR continues to pulse close to the expected times. Distinct extra bursts of SKR emission were also detected both before and during the compressions. The intensity of the detected emissions during the disturbed intervals was variable, sometimes remaining intense for several days, sometimes reducing, and in rare cases it disappeared. This variability showed that the SKR emissions cannot be simply used as a diagnostic of the prevalent solar wind conditions (e.g., when Cassini is inside Saturn's magnetosphere), without careful consideration of other influencing factors.

Clarke et al. [2009] built on the Cassini approach observations by using more aurora imaging data from a large campaign of observations in 2007 and 2008 of Saturn using the Hubble Space Telescope, in association with measurements from Cassini and determining solar wind conditions both by propagating measurements from 1 AU and by using Cassini observations when it was in the solar wind. The data found a one to one correspondence between the arrival of solar wind shocks at Saturn and increases in Saturn's auroral power and SKR emission, plus a decrease in the auroral oval radius. At the times of two reverse shocks, the SKR emission appeared to increase,

and possibly also the UV emission although the statistics were poor. These data are consistent with a causal relationship between solar wind disturbances and auroral and SKR emission increases as suggested in the earlier studies.

Mitchell et al. [2009c] adds to the above Clarke et al. [2009] results by examining the MIMI ENA results in conjunction with the auroral images and SKR observations. In the ENA observations, recurrent ring current oxygen intensity enhancements are usually detected that begin near midnight and increase in intensity and area as they rotate through the dawn meridian toward noon, and there is a close temporal association between recurrent ring current enhancements and recurrent SKR enhancements. For the single example of this recurring phenomenon for which continuous UV auroral imaging was available, bright corotating auroral emissions distributed in latitude from about 70 to 80 degrees tracked the ring current ion enhancement as it moved in local time from post-midnight to late morning. It was suggested that these recurrent events are caused by recurrent reconfiguration of the thin night-side current sheet in the 15–20 R_S region, probably associated with Vasyliunas-cycle reconnection and plasmoid release in the tail initiated relatively close to Saturn. The energy in such events presumably derives from Saturn's rotation, in combination with the mass loading of the cold plasma produced from Enceladus' extended gas cloud. However, a strong correlation was also found to exist between a solar wind pressure pulse resulting in magnetospheric compression and a ring current event, a sudden SKR power increase, and dawn-side auroral brightening. This correlation suggest a link between the asymmetric ring current enhancements and a rotating field aligned current system that drives both SKR enhancements and auroral displays. Such a relationship is implied for both the recurrent events with the Saturn rotation period and the solar wind pressure induced events.

The exploration of the nightside magnetosphere is reported in a series of papers by Jackman and coauthors. Jackman et al. [2009] revealed evidence of plasmoid-like magnetic structures and other phenomena indicative of the Saturnian equivalent of terrestrial substorms. In general, there was a good correlation between the timing of reconnection events and enhancements in the auroral SKR emission. Eight of nine reconnection events studied occur at SKR phases where the SKR power would be expected to be rising with time. Thus, while the recurrence rate of substorm-like events at Saturn is likely much longer than the planetary rotation timescale, the events are favored to occur at a particular phase of the rotation. Three examples were found in which the SKR spectrum extended to lower frequencies than usual. These low frequency extension SKR events were labeled low frequency extension (LFE) and were interpreted as an expansion of the auroral particle acceleration region to higher altitudes (lower radio frequency) along magnetic field lines as a direct consequence of an increase in the magnetosphere-ionosphere current density driven by substorm-like events. Saturnian substorms are likely a much more prevalent phenomenon than this small number of observations suggests, but the statistics in this study were hampered by viewing geometries, primary the small amount of time that Cassini spent in the deep magnetotail near the nominal current sheet location. Many examples of LFEs are observed by

In general, there was a good correlation between the timing of reconnection events and enhancements in the auroral SKR emission.

Cassini from a wide set of vantage points, but the spacecraft is only in the right position to observe the corresponding magnetic signature (if any) a fraction of the time.

Jackman et al. [2010] explored the dynamic response of Saturn's magnetotail to an episode of solar wind compression that took place while Cassini was sampling Saturn's nightside equatorial magnetosphere in 2006. Following an initial increase in solar wind dynamic pressure, the magnetosphere was compressed and became more streamlined, with an elevated lobe field strength as external pressure compressed the tail. Then, assuming a favorable IMF direction (for at least part of the interval, as seems entirely plausible), dayside reconnection may have been ongoing, leading to an increase in the amount of open flux inside the magnetosphere, flaring of the magnetotail, and continued elevated lobe field strength. Because of the longer time scales involved at Saturn for loading of the tail with open flux, it can take several days for the tail to be inflated to a point where reconnection is likely to occur, and this study suggested that the time scale observed in this case was of order ~6–7 days. No strong evidence for magnetotail reconnection events during this loading phase were detected, however, toward the end of this period a sharp decrease in lobe field strength and what appears to be significant current sheet deflection toward the equator from its previously hinged position was observed. Several days later the current sheet was displaced southward from its previously hinged position, and magnetic signatures consistent with the passage of a plasmoid were observed. These field signatures are closely correlated with intense radio emission, evidenced by LFEs of radio emission, corresponding to radio sources detected at higher altitudes. All of the above features are believed to be a common consequence of the impact of a solar wind compression on Saturn's magnetosphere.

Jackman et al. [2015] presented a rare observation of strong planetward flow following a reconnection episode in Saturn's tail from August 2006, when the Cassini spacecraft was sampling the region near 32 R_S and 22 h LT. Cassini observed a strong northward-to-southward turning of the magnetic field, which is interpreted as the signature of dipolarization of the field as seen by the spacecraft planetward of the reconnection X line. This event was accompanied by very rapid (up to ~1500 km s^{-1}) thermal plasma flow toward the planet. At energies above 28 keV, energetic hydrogen and oxygen ion flow bursts were observed to stream planetward from a reconnection site downtail of the spacecraft. Meanwhile, a strong field-aligned beam of energetic hydrogen was also observed to stream tailward, likely from an ionospheric source. SKR radio emissions enhancements similar to ones previously associated with plasmoid formation and release were detected slightly more than an hour after the observation of the dipolarization. The reconnection episode as inferred from the planetward directional flow duration lasts on the order of ~1.5 h, a significant fraction of a planetary rotation. The continuing presence of energetic O+ ions throughout the event demonstrates that this must be a case of long-lasting Vasyliunas-type reconnection occurring beyond 32 R_S in the premidnight region, perhaps indicating quasi-steady reconnection of the type. Because of the persistent presence of O+, we find little evidence for lobe involvement in the reconnection.

Kimura et al. [2013] investigated the very long-term (six years of measurements) variations of northern and southern SKR spectra, separated by polarization. This study confirms the prominent

role of solar wind pressure over one solar cycle, and additionally identified a seasonal dependence of the SKR activity, with a maximum in summer.

Kurth et al. [2016] reports on the SKR measurements obtained during a Saturn auroral campaign carried out in the spring of 2013 which used multiple Earth-based observations, remote-sensing observations from Cassini, and in situ-observations from Cassini. Saturn kilometric radiation was remotely monitored nearly continuously providing a measure of the auroral activity and a means of understanding the temporal relationships between the sometimes widely spaced remote sensing observations of the auroral activity. While beaming characteristics of the radio emissions are known to prevent single spacecraft observations of this emission from being a perfect auroral activity indicator, a good correlation between the radio emission intensity and the level of UV auroral activity was observed, when both measurements are available, similar to what the previous studies had shown. Given the known influence of solar wind dynamics on both SKR intensity and auroral activity as discussed above, the SKR integrated power is also a proxy for solar wind activity. This study found that there is a good correlation between the 10-h averages of SKR power flux and the power estimated input to the aurora on the basis of the UV brightness, justifying the SKR as a simple proxy for auroral activity through the campaign. The SKR emissions also give evidence for a recurrent pattern of solar wind interaction with Saturn's magnetosphere, suggesting a two-sector structure and associated corotating interaction regions influencing the level of auroral activity on Saturn. However, there are other SKR intensifications that may be due to internal processes.

Bunce et al. [2014] presented an unusual case in January 2009, where Ultraviolet Imaging Spectrograph (UVIS) observes the entire northern UV auroral oval during a 2 h interval while Cassini traverses the magnetic flux tubes connecting to the auroral regions near 21 LT, sampling the related magnetic field, particle, and radio and plasma wave signatures. The motion of the auroral oval evident from the UVIS images was found to be consistent with the appropriate phase of the magnetosphere oscillations in the northern hemisphere, whereas previous interpretations have assumed a static current system. Concurrent observations of the auroral hiss (typically generated in regions of downward directed field-aligned current) support this revised interpretation of an oscillating current system.

Thomsen et al. [2015b] presented observations that suggest that under some conditions the solar wind governs the character of the plasma sheet in the outer magnetosphere. Observations from September 2006, near local midnight at a radial distance of 37 R_S, showed a planetward flowing ion population for ~5 hours, which was accompanied by enhanced SKR emissions. This ion beam was interpreted as the outflow from a long-lasting episode of Dungey-type reconnection, i.e., reconnection of previously open flux containing magnetosheath material. The beam occurred in the middle of a several-day interval of enhanced SKR activity and lobe magnetic field strength, likely caused by the arrival of a solar wind compression region with significantly higher than average dynamic pressure (magneto-hydrodynamic (MHD) propagation models of the solar wind from 1 AU observations to Saturn during this period suggest the presence of higher density solar wind). There was also a change in the composition of the plasma-sheet plasma, from water-group-dominated material clearly of inner-magnetosphere origin to material dominated by light-ion composition,

consistent with captured magnetosheath plasma. This event suggests that under the influence of prolonged high solar wind dynamic pressure, the tail plasma sheet, which normally consists of inner-magnetospheric plasma, is eroded away by ongoing reconnection that then involves open lobe field lines. This process removes open magnetic flux from the lobes and creates a more Earth-like, Dungey-style outer plasma sheet dominantly of solar wind origin. This behavior is potentially a recurrent phenomenon driven by repeating high-pressure streams (corotating interaction regions) in the solar wind.

During a coordinated auroral observing campaign on April 21–22, 2013, instruments onboard Cassini and the Hubble Space Telescope observed Saturn's northern and southern aurora while Cassini traversed Saturn's high latitude auroral field lines [Badman et al. 2016]. Signatures of upward and downward field-aligned currents were detected in the nightside magnetosphere, with the location of the upward current corresponded to the bright ultraviolet auroral arc seen in the auroral images, and the downward current region located poleward of the upward current in an aurorally dark region. In the area poleward of the auroral oval, magnetic field and plasma fluctuations were identified with periods of ~20 and ~60 min. During April 21, 2013 the northern and southern auroral ovals were observed to rock in latitude in phase with the respective northern and southern planetary period oscillations. A solar wind compression impacted Saturn's magnetosphere at the start of April 22, 2013, identified by the intensification and extension to lower frequencies of the SKR. At this time, a bulge appeared along the pre-dawn auroral oval, which appeared to have moved sunward when this region was next observed. The midnight sector aurora remained a narrow arc at this time. Subsequently, the post-midnight aurora broadened in latitude and contracted towards the pole. The motion in this sector was in the opposite direction to that expected from the planetary period oscillation. There was also an intensification of the auroral field-aligned currents. These observations are interpreted as the response to tail reconnection events instigated by solar wind compression, initially involving Vasyliunas-type reconnection of closed mass-loaded magnetotail field lines, and then proceeding onto open lobe field lines, causing the contraction of the polar cap region on the post-midnight sector.

Felici et al. [2016] presented a case study of data from Saturn's magnetotail, when Cassini was located at ~22-hour Local Time at 36 R_S from Saturn that suggests for the first time that a low-energy ionospheric outflow event has been detected at planets other than Earth. During several entries into the magnetotail lobe, tailward flowing cold electrons and a cold ion beam were observed directly adjacent to the plasma sheet and extending deeper into the lobe. The electrons and ions appear to be dispersed, dropping to lower energies with time. The composition of both the plasma sheet and lobe ions show very low fluxes (sometimes zero within measurement error) of water group ions. The magnetic field has a swept-forward configuration which is atypical for this region, and the total magnetic field strength is larger than expected at this distance from the planet. Ultraviolet auroral observations show a dawn brightening, SKR is enhanced and extends down to lower frequencies, and upstream heliospheric models suggest that the magnetosphere is being compressed by a region of high solar wind ram pressure. This event is interpreted as the observation of ionospheric outflow in Saturn's magnetotail, with the active atmospheric regions most likely the main auroral oval.

The majority of the previously discussed studies involved periods where Saturn's magnetosphere encountered a high density solar wind. The study by Kinrade et al. [2017] discusses observations during a period that Saturn's magnetosphere was in a rarified solar wind region. During this period on June 14, 2014 (day 165), the Hubble Space Telescope observed an unusual auroral morphology, where for 2 h, the Saturn's far ultraviolet (FUV) aurora faded almost entirely, with the exception of a distinct emission spot at high latitude. The spot remained fixed in local time between 10 and 15 LT and moved poleward to a minimum colatitude of ~4°. Interestingly, the spot constituted the entirety of the northern auroral emission, with no emissions present at any other local time—including Saturn's characteristic dawn arc, the complete absence of which is rarely observed. Solar wind parameters from propagation models, together with a Cassini magnetopause bow shock crossing, indicate that Saturn's magnetosphere was in an expanded magnetosphere configuration during the interval, suggesting it was likely embedded in a rarefaction region. The spot was possibly sustained by reconnection either poleward of the cusp or at low latitudes under a strong component of interplanetary magnetic field transverse to the solar wind flow. The subsequent poleward motion could then arise from either reconfiguration of successive open field lines across the polar cap or convection of newly opened field lines. The spot's fixed LT position may be attributed to the negative IMF BY conditions incident at the time, combined with increased subcorotation of open flux toward higher latitudes. The emission intensity was also possibly enhanced by a sector of upward planetary period oscillation (PPO) current rotating through the region. These observations show conclusively that the mechanisms producing noon auroral spots and the main oval auroras (i.e., the dawn arc) are distinct, since in this case the cusp spot occurred without the arc. These observations also suggest that reconnection can occur in an expanded magnetosphere, in agreement with the cusp observations of Arridge et al. [2016a, 2016b], who found evidence of reconnection under a range of upstream solar wind conditions.

Solar wind parameters from propagation models, …, indicate that Saturn's magnetosphere was in an expanded magnetosphere configuration during the interval, suggesting it was likely embedded in a rarefaction region.

A recent study by Roussos et al. [2018] uses a novel technique to overcome the lack of an upstream solar wind monitor at Saturn. Cassini MIMI/LEMMS observations of solar energetic particle (SEP) and galactic cosmic ray (GCR) transients, that are both linked to energetic processes in the heliosphere such us interplanetary coronal mass ejections (ICMEs) and CIRs, are used to trace enhanced solar wind conditions at Saturn's distance. A survey of the MIMI/LEMMS dataset between 2004 and 2016 resulted in the identification of 46 SEP events. Most events last more than two weeks and have their lowest occurrence rate around the extended solar minimum between 2008 and 2010, suggesting that they are associated to ICMEs rather than CIRs, which are the main source of activity during the declining phase and the minimum of the solar cycle. Also, 17 time periods (> 50 days each) are identified where GCRs show a clear solar periodicity (~13 or 26 days). The 13-day period that derives from two CIRs per solar rotation dominates over the 26-day period in only one of the 17 cases catalogued. This interval belongs to the second half of 2008 when

expansions of Saturn's electron radiation belts were previously reported to show a similar periodicity. That observation not only links the variability of Saturn's electron belts to solar wind processes, but also indicates that the source of the observed periodicity in GCRs may be local. In this case GCR measurements can be used to provide the phase of CIRs at Saturn. The survey results also suggest that magnetospheric convection induced by solar wind disturbances associated with SEPs is a necessary driver for the formation of transient radiation belts that were observed throughout Saturn's magnetosphere on several occasions during 2005 and on day 105 of 2012. Also, an enhanced solar wind perturbation period that is connected to an SEP on day 332 of 2013 was the definite source of a strong magnetospheric compression (enhanced SKR and LFEs were also detected at this time) which led to open flux loading in the magnetotail. This event lists can a guide to better constrain or identify the arrival times of interplanetary shocks or solar wind compressions for single case studies or statistical investigations on how Saturn and its moons (particularly Titan) respond to extreme solar wind conditions or on the transport of SEPs and GCRs in the heliosphere.

OTHER AURORAL OBSERVATIONS

X-ray aurorae are detected at Jupiter, but no detection has been made at Saturn. Saturnian X-ray aurorae may be expected to be powered by charge exchange between energetic ions and the planet's atmospheric neutrals. If the ions are of solar origin, the emission should be brightest during episodes of enhanced solar wind activity. Using propagating SW parameters measured near the Earth to Saturn to estimate the timing of solar wind enhancements to reach Saturn, a number of Chandra observations were obtained in April–May 2011. Cassini in situ measurements confirm that two of the observations were carried out at the time when a significant SW disturbance reached Saturn. Variability was observed between the two Chandra datasets, but no evidence for X-ray brightening in the auroral regions were detected during this period, suggesting that the strength of any charge exchange auroral X-ray emission on Saturn was below Chandra's detectability threshold [Branduardi-Raymont et al. 2013].

Upstream Langmuir waves

Langmuir waves are often detected by Cassini in the foreshock region upstream of the Saturnian bow shock [Hospodarsky et al. 2006]. In planetary foreshocks, electrostatic Langmuir waves at frequencies close to the local plasma frequency (f_{pe}) are generated by electrons reflected from the bow shock via the beam-plasma instability. The fact that the Langmuir waves are generated near f_{pe} allows an estimate of the solar wind electron plasma density (n_e) to be determined from the frequency of the waves when they are present. This ability to estimate the density was used in a study by Bertucci et al. [2007a] to compared low frequency (<<1 Hz) waves detected by the Magnetometer instrument to similar variations observed in ne as determined from the Langmuir wave frequency. Langmuir wave derived solar wind density measurements have also been used in a number of studies investigating the bow shock shape and stand-off distance. These studies are discussed in the section entitled Bow Shock Shape and Location.

Using the RPWS Wideband Receiver measurements, Píša et al. [2015, 2016] examined the characteristics of the Langmuir waves detected upstream of Saturn. Typical Langmuir wave amplitudes observed by the RPWS at Saturn are in a range of 0.01 to 1 mV/m, with the largest amplitudes detected ~10 mV/m. The estimated energy density for the largest measured amplitudes at Saturn does not exceed the threshold for strong turbulence processes, suggesting that weak turbulence saturation processes are more important in the Langmuir wave saturation inside Saturn's foreshock. The maximum wave intensity is observed around the upstream foreshock boundary with a slight shift behind the tangent magnetic field line toward the downstream position and with a decrease in intensity along the solar wind direction deeper in the foreshock. The wave amplitude also decreases with distance along the tangent field line, but decreases more slowly compared to the dependence on the depth. This dependence shows an amplitude decrease of almost one order of magnitude over the distance of 100 R_S.

The typical Langmuir wave spectrum at Saturn exhibits a single intense peak (62% of all selected waveforms). However, spectra with a superposition of two (25%) or more (13%) intense peaks are also observed [Píša et al. 2016]. Using magnetic field observations and a model of the bow shock, plasma wave activity across Saturn's foreshock has been mapped. The single peak spectra are observed across the entire foreshock, while more complicated spectra are more likely measured deeper inside the foreshock and closer to the bow shock. A gap in wave occurrence and intensity at the tangent point delimits two foreshock regions similar to those observed at Venus and Earth. In the case of Saturn's foreshock, this gap is caused by the larger radius of curvature of the shock.

Lion Roar emissions

Píša et al. [2018] presented an observation of intense electromagnetic emissions in Saturn's magnetosheath as detected by the Cassini spacecraft in the dawn sector (magnetic local time ~06:45) over a time period of 11 hours. The waves were narrow-banded in frequency with a peak frequency of about 0.16 f_{ce}, where f_{ce} is the local electron gyrofrequency. Using plane wave propagation analysis, the waves were found to be right hand circularly polarized in the spacecraft frame and propagate at small wave normal angles (<10°) with respect to the ambient magnetic field. Electromagnetic waves with similar properties known as “lion roars” have been reported by numerous missions in the terrestrial magnetosheath. These Cassini observations are the first evidence of such emission outside the terrestrial environment.

Electromagnetic waves with similar properties known as “lion roars” have been reported by numerous missions in the terrestrial magnetosheath.

Bow shock shape and location

Studying the global shape, location, and dynamics of the bow shock offers important insights into the physics governing its formation and the magnetospheres response to solar wind dynamics. A

number of authors [Achilleos et al. 2006; Masters et al. 2008; Went et al. 2011] have used the Cassini data to develop models of the average shape of Saturn's bow shock as well as the response of this surface to changes in the dynamic pressure of the upstream solar wind. RPWS data has contributed to these studies by detecting the occurrence of bow shock crossings and by providing upstream solar wind densities from the frequency of the Langmuir waves near these crossings. The solar wind density has been used both as an in situ verification of solar wind propagation models [Hansen et al. 2005; Zieger and Hansen 2008] and to estimate the solar wind dynamic pressure.

A number of studies have investigated the properties of the bow shocks themselves at Saturn [Masters et al. 2013a, 2013b, 2017; Sulaiman et al. 2015; Sundberg et al. 2017], and the particles and regions associated with the bow shock, including hot flow anomalies [Masters et al. 2009], superthermal electrons [Masters et al. 2016], and upstream whistler mode waves [Sulaiman et al. 2017a]. The T96 Titan encounter (see the section entitled Titan Science for more details) occurred during a period of high solar wind pressure that caused Saturn's bow shock to be pushed inside Titan's orbit, exposing the moon and its ionosphere to the solar wind. Omidi et al. [2017] using electromagnetic hybrid (kinetic ions and fluid electrons) simulations and Cassini observations, showed a formation of a single deformed bow shock for the Titan-Saturn system.

Saturn Science—Lightning

The first indication of lightning in Saturn’s atmosphere was obtained in November 1980 by the radio instrument on-board Voyager 1. Strong impulsive signals in the frequency range of a few MHz were detected and termed Saturn electrostatic discharges (SEDs) [Warwick et al. 1981]. The Voyager SEDs were thought to stem from an atmospheric source in the equatorial region of Saturn, and a source in Saturn’s B-ring was excluded by Kaiser et al. [1983] with an argument of visibility. However, no storm clouds in the equatorial region could be identified in the Voyager images. The Cassini mission has greatly enhanced our knowledge about Saturn lightning, and combined radio and imaging observations have clearly established the atmospheric origin of the SEDs. This is discussed in the first subsection below, and the subsequent subsections will describe the occurrence of SED storms in the Cassini era, the fascinating great white spot (GWS) event of 2010/2011, the physical parameters of the SEDs, the usage of the SEDs as a tool to investigate Saturn’s ionosphere, and the scarcity of lightning whistler observations. Finally, we will mention that the new discoveries by Cassini will enable limited future ground-based observations of Saturn’s thunderstorm and lightning even without a spacecraft in Saturn’s orbit.

New discoveries by Cassini will enable limited future ground-based observations of Saturn’s thunderstorm and lightning even without a spacecraft in Saturn’s orbit.

Radio and imaging observations of Saturn lightning storms

The first link between SEDs and cloud features in Saturn's atmosphere was found in 2004: Cassini Imaging Science Subsystem (ISS) imaged the so-called dragon storm, and the RPWS instrument detected SEDs at the same time [Porco et al. 2005; Fischer et al. 2006a]. These combined observations revealed consistent longitudes and longitudinal drift rates of the cloud feature and the SED source. Later, the white storm clouds were also found to be brighter when the SED rates were high [Dyudina et al. 2007; Fischer et al. 2007a]. Finally, Saturn lightning flashes were first detected optically on the nightside of Saturn around equinox, when the reflected light from the rings towards the planet (ring-shine) was minimized. The Cassini cameras spotted flash-illuminated cloud tops with a diameter of about 200 km, suggesting that the lightning comes from 125–250 km below [Dyudina et al. 2010], and most likely from the water-cloud layer. At Earth, the charging of water cloud particles in thunderstorms is most effective in a temperature range of −10° C to −25° C. At Saturn this temperature range is located at a level of 8–10 bars, about 200 km below the cloud tops, i.e., consistent with the altitude range found by Dyudina et al. [2010]. Another indication that the Saturn lightning source is in the water cloud layer comes from Cassini Visual and Infrared Mapping Spectrometer (VIMS) near-infrared spectra of the Great White Spot. They revealed spectroscopic evidence for ammonia and water ices [Sromovsky et al. 2013] brought up to higher altitudes by strong vertical convection. So it is thought that the same particle charging mechanisms are at work on Saturn and Earth. As most of the sunlight is absorbed above 2 bars, Saturn's weather and thunderstorms at deep pressure levels should be powered by the planet's internal energy [Desch et al. 2006]. It drives the vertical convection which brings up the water cloud to the visible atmospheric level where it is observed as a bright eruption by Cassini ISS and VIMS. Dyudina et al. [2010] also measured the optical flash energy to be about 10^9 J, which suggests that Saturn lightning is superbolt-like with total energies of about 10^{12} J [Fischer et al. 2011a], and not a fast and weak discharge as hypothesized by Farrell et al. [2007].

The left side of Figure RPWS-18 shows an image made by Cassini ISS of a Saturn lightning storm with two outbreaks, separated by about 25° in longitude [Fischer et al. 2018]. They are both located at the same planetocentric latitude of 35°South, a region nicknamed storm alley since many SED storms occurred there. They can be easily seen as the bright white features with a size of about 2000 km. Saturn's thunderstorms could also be imaged with the backyard telescopes of amateur astronomers as the right side of Figure RPWS-18 shows. The observations of amateur astronomers turned out to be very useful: they provided information on the location and the morphological evolution of the thunderstorms when the Cassini cameras were not looking [Fischer et al. 2011d; Mousis et al. 2014]. On the other hand, the Cassini optical instruments were able to study Saturn's thunderstorms in a very high spatial resolution [e.g., Dyudina et al. 2007; Sayanagi et al. 2013] revealing their exact sizes and dynamics. In the Cassini images, one can also see dark ovals that spew out of the stormy regions over the course of weeks [Dyudina et al. 2007] (see also Figure RPWS-18). These dark ovals show no SED activity since they are still visible for several weeks after the end of an SED storm. Baines et al. [2009] believe that their dark color originates from carbon soot particles that could have been produced by the dissociation of methane in the high-temperature lightning channels.

Figure RPWS-18. Two outbreaks of a Saturn lightning storm during the year 2008. The left image was obtained by Cassini ISS on June 18, 2008; and the right image was made by the amateur astronomer Christopher Go on May 1, 2008 (cloud features marked with white arrows).

Occurrence of SED storms

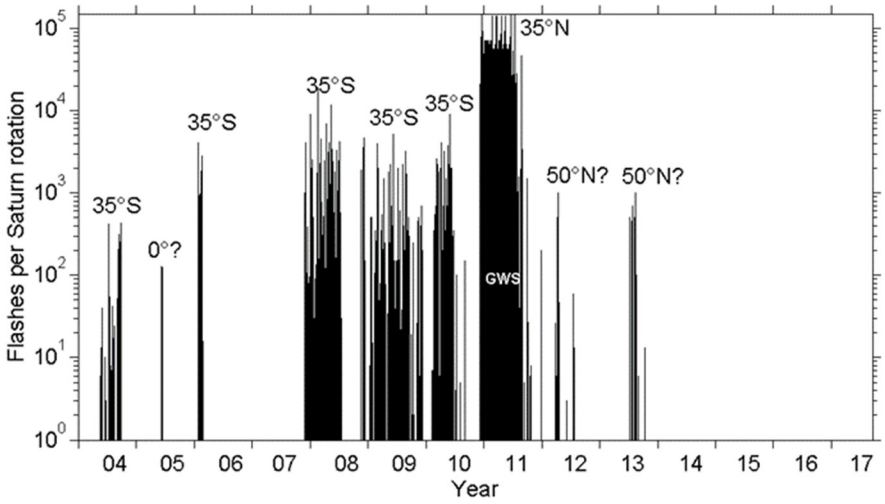

Figure RPWS-19. Number of flashes/SEDs per Saturn rotation detected by Cassini RPWS as a function of time (years from 2004 until 2017). The text in the figure denotes the planetocentric latitudes of the thunderstorms, and GWS marks the SEDs from the Great White Spot.

Figure RPWS-19 shows the number of SEDs per Saturn rotation as a function of time (year from 2004 until 2017) throughout Cassini's orbital tour around Saturn. Some bursty SED-like emissions recorded in July 2003 at a distance of 1.08 AU from Saturn [Gurnett et al. 2005] turned out to be Jovian decametric arcs [Fischer et al. 2006c]. The first SEDs were detected by Cassini RPWS in May 2004, and the last SEDs were seen in October 2013.

Figure RPWS-19 shows that Saturn lightning storms can last from a few days up to several months, and there was one storm that almost lasted throughout the year 2009. There are also long

time intervals with no SED activity, especially from February 2006 until November 2007 and during the last four years of the mission. The absence of SEDs after October 2013 could be explained by a kind of convective inhibition state of the atmosphere after the GWS of 2010/2011 [Li and Ingersoll 2015]. The flash rate during the GWS was about 1–2 orders of magnitude higher than during the other regular 2000 km-sized SED storms. For the GWS the flash rate was about 10 SEDs per second [Fischer et al. 2011c], whereas the regular storms typically have flash rates of a few SEDs per minute [Fischer et al. 2008]. Saturn's thunderstorms only raged at specific latitudes, preferentially at the so-called storm alleys around 35° South (regular storms) and 35° North (GWS). At those latitudes there are broad minima in wind speed with small westward velocities with respect to the Voyager Space Launch System (SLS). Only a few smaller storms were potentially located at different latitudes (equator or 50° N). Since Cassini RPWS could not exactly determine the locations of the thunderstorms on Saturn, a good collaboration with the Cassini imaging team and ground-based amateur astronomers was essential as pointed out in the previous subsection. Most SEDs occurred ±2 years around equinox (August 2009), and the SED storms switched from the southern hemisphere to the northern hemisphere one year after equinox, suggesting a seasonal influence [Fischer et al. 2011c].

The Great White Spot

There are two different classes of thunderstorms on Saturn [Aplin and Fischer 2017], (i) regular 2000 km-sized storms, and (ii) the rare and giant GWS that usually occur only once per Saturn year (29.5 Earth years). The previous GWS on Saturn broke out in 1990 and was located in the northern equatorial region [Sanchez-Lavega et al. 1991].

The 2010/2011 GWS was located around a planetocentric latitude of 35° N, and it reached a latitudinal extension of about 10,000 km about three weeks after it started in early December 2010 (first SEDs detected on December 5). The storm developed an elongated eastward tail with additional storm cells that wrapped around the whole planet (a distance of 300,000 km) by February 2011 [Fischer et al. 2011c]. In Figure RPWS-20, one can see an image of the GWS from March 2011. The main lightning activity took place in the so-called head of the storm (westernmost bright white clouds on the left side in the top panel of Figure RPWS-20), which drifted westward with a velocity of −27 m/s (westward motion w.r.t. Voyager SLS). The head spawned the largest anticyclonic vortex ever seen on Saturn that drifted with −8 m/s [Sayanagi et al. 2013]. The different drift velocities led to a collision between the head and the anticyclonic vortex in mid-June 2011, which caused a significant drop in SED activity. After the collision, the SED activity became intermittent and SEDs finally disappeared at the end of August 2011.

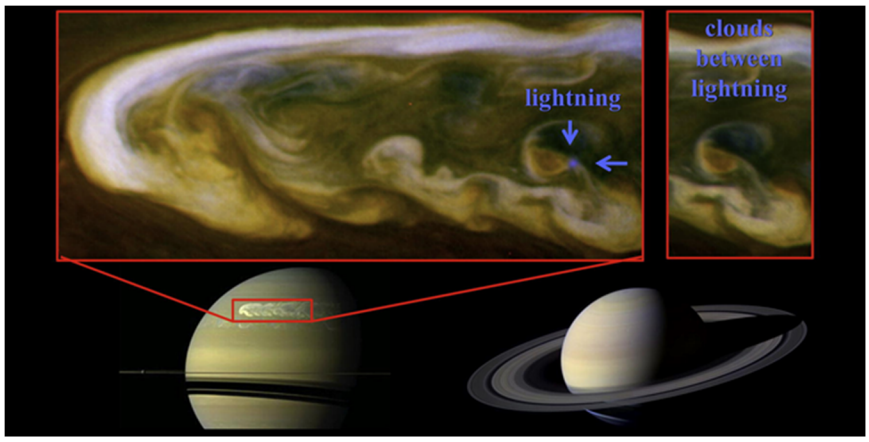

Figure RPWS-20. The upper part of this figure shows two Cassini images taken on March 6, 2011. The *left panel* shows a blue spot attributed to a lightning flash which is absent in the *right panel* image taken half an hour later. The lower part of this figure displays two Saturn images to show the large extent of the Great White Spot. Figure from Dyudina et al. [2013].

Dyudina et al. [2013] could also identify visible flashes in blue wavelengths on Saturn's dayside, which is also shown in Figure RPWS-20. The optical flashes appeared in the cyclonic gaps between anticyclonic vortices where the atmosphere looked clear down to the level of deep clouds. Dyudina et al. [2013] also estimated the optical power of the flashes to be about 10^{10} W, and the total convective power of the GWS to be of the order of 10^{17} W. Since this power is similar to Saturn's global power radiated to space, storms like the GWS should be important factors in the thermal balance of Saturn's atmosphere. Fischer et al. [2014b] suggested that the powerful storm was an intense source of gravity waves that may have caused a global change in Saturn's thermospheric winds via energy and momentum deposition. These changes might have also influenced the periodicity of SKR, which should be driven by the upper atmosphere. The GWS also caused a large stratospheric vortex with temperatures of 80 K above the normal level and an enhanced abundance of stratospheric acetylene [Fletcher et al. 2012].

Physical parameters of SEDs in comparison to Earth lightning

The radio emissions of Saturn lightning are stronger by a factor of 10^4 than the radio emissions from terrestrial lightning in the frequency range of a few MHz. Zarka et al. [2006] and Fischer et al. [2006b] found spectral radio powers of the order of 10 to 100 W/Hz, confirming previous Voyager measurements by Zarka and Pedersen [1983]. RPWS detected the first SEDs from beyond 300 Saturn radii [Fischer et al. 2006a] in May 2004. This corresponds to a staggering distance of about 3000 Earth radii compared to only 14 Earth radii, within which RPWS detected terrestrial lightning during its Earth flyby [Gurnett et al. 2001]. Similarly, the total energy of one superbolt SED is about 10^{12} J, a factor of 10^4 larger than the typical total energy of a terrestrial flash with 10^8 J. The large SED energy could be related to the fact that the breakdown voltage increases with pressure, and the SED source should be located at a pressure level of 8–10 bars. Higher breakdown fields would allow more charges to accumulate before it comes to a powerful breakdown [Fischer et al. 2008].

Similar to terrestrial intracloud lightning, an SED consists of many subpulses, and the total duration of one SED can be as long as a few hundred milliseconds. Most SEDs are somewhat shorter, and the average SED duration is around 60–70 ms [Zarka et al. 2006]. The SED duration can be well described by a distribution with an exponential decrease in SED numbers with increasing burst duration. Such distributions are characterized by a so-called e-folding time, and for SEDs this e-folding time is in the range from 35–50 ms [Fischer et al. 2007a]. The RPWS instrument had a millisecond mode with which the signal amplitude could be measured at a fixed frequency with a high temporal resolution of 1 ms. However, it turned out that this time is still too long to resolve the substructures of an SED. High temporal resolution observations were provided by ground-based SED observations (see the section entitled Ground-based Saturn lightning observations for the future), and Mylostna et al. [2013] found substructures with a duration of the order of 100 microseconds. The temporal structure of a burst should be related to its frequency spectrum. The frequency spectrum of terrestrial lightning shows a roll-off with $1/f^2$ or even steeper above 1 MHz. Zarka et al. [2006] and Fischer et al. [2006b] found a distinctly different spectrum for SEDs which is almost flat or with a slight roll-off of $1/f^{0.5}$ from 4–16 MHz. The reason for such a flat spectral behavior of SEDs is unknown.

Lightning as a tool to investigate Saturn's ionosphere

SEDs usually occur in episodes of a few hours when the thunderstorm is on the side of Saturn facing Cassini, whereas the SEDs are absent when the storm is on the backside of the planet. However, some SEDs can propagate from beyond the visible horizon due to ducted ionospheric propagation, and we call this the over-the-horizon effect [Zarka et al. 2006].

Figure RPWS-21 shows an SED episode that lasts for about six hours. The SEDs are the short vertical bursts, which appear as narrow-banded signals due to the frequency sweeping receiver, although they are intrinsically broadband. Assuming straightline SED propagation, the peak electron plasma frequency of Saturn's ionosphere can be easily determined from the low frequency cutoff denoted by the white line [Fischer et al. 2011b]. Therefore, it is necessary to know the exact location of the storm cloud, and it is indicated in Figure RPWS-21 when the storm cloud was appearing at the horizon, passing the central meridian (CM), and disappearing again. Fischer et al. [2011b] found peak electron densities of 10^4 cm^{-3} at midnight and 10^5 cm^{-3} at noon for the storms at the kronocentric latitude of 35° S. This diurnal variation of about 1 order of magnitude is still too large to be explained by ionospheric models [Moore et al. 2012]. The SED measurements are still the only technique to obtain the electron densities of Saturn's ionosphere at all local times, since radio occultation only works for local times at dawn and dusk. Figure RPWS-19 shows the different SED behavior when the storm cloud is close to the horizon: SEDs get weaker when the cloud comes near the day-side horizon due to the oblique angle of propagation leading to absorption in Saturn's ionosphere. On the other hand, SEDs were detected about one hour before the cloud reached the visible night-side horizon, and the over-the-horizon SEDs are denoted in the figure. This effect not only exists when Cassini is on the morning side, but also with Cassini on the evening side with an SED storm that disappears towards the night-side [Fischer et al. 2018]. The typical over-the-horizon effect extends 30° to 45° beyond the night-side horizon and has been modelled by ray tracing [Gautier et al. 2011].

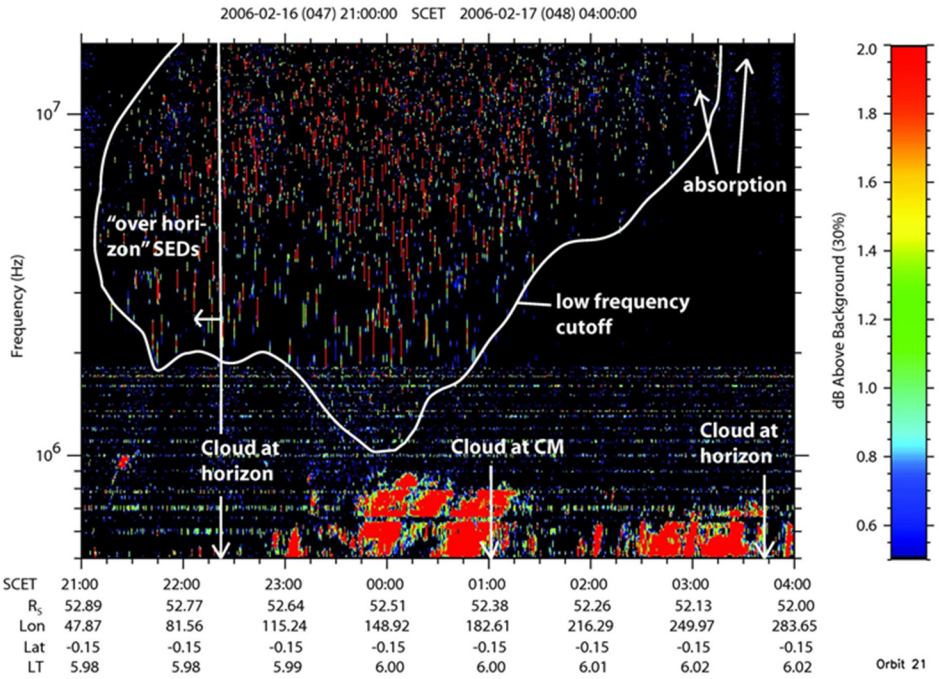

Figure RPWS-21. Dynamic spectrum (color-coded radio wave intensity as function of time and frequency) of an SED episode as measured by RPWS on February 16–17, 2006. The white line denotes the low frequency cutoff and other features are described in the text. The bottom numbers show the Spacecraft Event Time (SCET), the distance of Cassini to Saturn's center in Saturn radii, and the longitude, latitude, and local time of Cassini. Figure from Fischer et al. [2008].

The wave polarization of SEDs has been measured below 2 MHz (in the so-called quasi-static frequency range), and it is thought that it is fixed in Saturn's ionosphere. Fischer et al. [2007c] found SEDs to be highly polarized (80%) with just one sense of rotation, which was right-handed with respect to the wave propagation direction for SEDs originating from the southern hemisphere. They explained this by the dominance of the ordinary mode and the absorption of the extraordinary mode in the ionosphere. Consequently, SEDs from the northern hemisphere were found to be left-hand circularly polarized [Fischer et al. 2011c], since the magnetic field and the wave propagation vector point to the same direction in the northern hemisphere, whereas they are opposite to each other in the southern hemisphere.

Saturn lightning whistlers

Lightning is known to emit whistler waves at very low frequencies which propagate along magnetic field lines from the source to the observer. For Saturn the detection of only one lightning whistler has been reported in the literature. Akalin et al. [2006] detected one whistler signal in the frequency range of 200–400 Hz that lasted for 2 seconds. It was detected by the RPWS wideband receiver on October 28, 2004, on a magnetic field line with an L-shell value of 6.5. They concluded that the whistler originated from the northern hemisphere from a latitude of 67°, but no corresponding SED activity was seen. The scarcity of whistler observations by Cassini can be explained by Cassini's trajectory, since the stormy regions at latitudes around 35° N and S are connected to low magnetic

L-shells which were traversed by Cassini only during orbit insertion and the proximal orbits of 2017. However, an intense search for lightning whistlers led to the detection of only three tentative events during the proximal orbits. This is probably due to the absence of lightning storms in 2017 as shown in Figure RPWS-17.

Ground-based Saturn lightning observations for the future

We already mentioned that SEDs are typically 10,000 times stronger than terrestrial lightning in the frequency range of a few MHz. This has led to their first detection with an Earth-based radio telescope, which was achieved by the giant UTR-2 facility (effective area of 150,000 m²) in the Ukraine [Zakharenko et al. 2012; Konovalenko et al. 2013]. At Earth, the SEDs have a radio flux of a few hundred Jansky (1 Jy = 10^{-26} W/m²/Hz), and the sensitivity of UTR-2 is a few Jansky. The new discoveries about Saturn's thunderstorm by Cassini will enable some limited future observations of Saturn's lightning and thunderstorms even without a spacecraft in Saturn's orbit. During the times of Saturn apparition we should be able to identify thunderstorms in Saturn's atmosphere with a high confidence from the images of the ground-based amateurs, since we now know what they should look like. Saturn can be well-observed from Earth for roughly 6–9 months per year, and a confirmation of a storm's SED activity is now possible with large Earth-based radio telescopes. It is interesting to know when the next SED storm will take place after the long inactivity of more than four years at the end of the Cassini mission.

Search for Titan lightning

The existence of lightning on Saturn's enigmatic moon Titan has been suggested soon after the Voyager 1 flyby in 1980, although no corresponding radio emissions were detected by Voyager [Desch and Kaiser 1990]. The potential effects of lightning on Titan's atmospheric chemistry have been widely investigated up to the production of organic compounds that could be essential precursors for the evolution of life [Plankensteiner et al. 2007]. Furthermore, the Cassini cameras observed convective cloud activity in Titan's atmosphere. However, no radio bursts that would clearly indicate the existence of Titan lightning were found by RPWS during the numerous flybys [Fischer et al. 2007b; Fischer and Gurnett 2011]. Hence, Titan lightning is a very rare event if it exists at all.

Saturn Science—Ionosphere

The ionosphere of Saturn is still a work in progress, and the first in situ measurements by RPWS of the cold ionosphere properties have just been reported [Wahlund et al. 2018]. Several other manuscripts have been submitted, and they all show a very strong interaction between the D-ring and the ionosphere of Saturn, causing the ionosphere to become extremely variable with more than two orders of magnitude and trigger a dust-ionosphere layer near the equator.

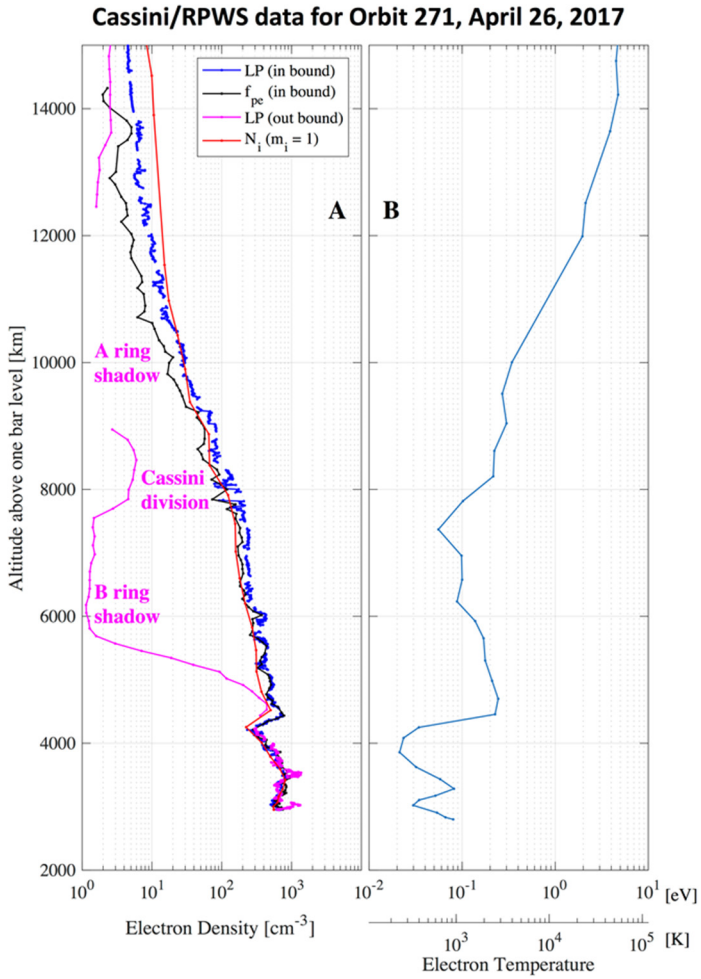

Figure RPWS-20. Cassini/RPWS altitude profiles of the ionosphere number density (*Panel A*) and inbound electron temperature (*Panel B*) during the crossing on April 26, 2017. Two independent methods for estimating the inbound electron density (blue and black) gave almost identical results, confirming their validity. The Langmuir probe ion density (N_i, assuming H^+) also produces values in agreement with the estimated electron densities, confirming that hydrogen ions dominated during this first flyby. The lower LP electron densities over the outbound sector (magenta) indicate that much of the A- and B-rings are opaque to ionizing extreme ultraviolet radiation.

Sulaiman et al. [2017c] reported the first observations of lower hybrid resonance waves in Saturn's ionosphere. They are believed to be generated through the interaction of whistler-mode waves and density gradients present in the ionosphere.

Plasma Waves

The almost 300 orbits by Cassini have allowed the RPWS to study a variety of plasma and radio waves in the magnetosphere of Saturn. See Gurnett et al. [2005]; Mauk et al. [2009]; Kurth et al. [2009]; Hospodarsky et al. [2012, 2016] for overviews of the Saturn magnetosphere and some of the wave observations.

In the inner magnetosphere (<10 R_S), whistler mode chorus [Hospodarsky et al. 2008; Menietti et al. 2013a, 2013b, 2014a, 2014b], quasi-periodic (QP) whistler mode emissions [Hospodarsky et al. 2012], electron cyclotron harmonic (ECH) emissions [Menietti et al. 2008a, 2008b, 2012; Tao et al. 2010], and upper hybrid resonance (UHR) emissions [Persoon et al. 2005, 2006a, 2006b, 2009, 2013, 2015] are observed. At higher magnetic latitudes (> ~25°), auroral hiss is detected [Mitchell et al. 2009a; Gurnett et al. 2009b; Kopf et al. 2010]. RPWS observations of ion cyclotron waves have also been made in the Saturn downward auroral current region. Menietti et al. [2011c] showed that these waves can be generated by the observed upward electron beams and modeling suggested that they can produce significant ion heating as has been observed in the terrestrial auroral region.

Evidence of lightning in Saturn's atmosphere is shown from observations of lightning whistlers [Akalin et al. 2006] and from observations of Saturn Electrostatic Discharges (SEDs) (see the section entitled Saturn Science—Lightning for detailed discussion of the lightning observations). A number of radio emissions are also observed, including Z- and O-mode narrowband emissions [Louarn et al. 2007; Ye et al. 2009, 2010a, 2011; Menietti et al. 2009, 2010b, 2012; Wang et al. 2010], and SKR [Kurth et al. 2005a, 2005b, 2011; Cecconi et al. 2006; Lamy et al. 2008a, 2010a; Fischer et al. 2009; Mutel et al. 2010; Menietti et al. 2011b]. Plasma waves have also been detected in association with many of the Saturnian moons, including Enceladus [Tokar et al. 2006; Gurnett et al. 2011a; Leisner et al. 2013; Pickett et al. 2015] and Rhea [Santolik et al. 2011]. The RPWS instrument also detects dust impacts on the Cassini spacecraft, providing information on the properties of dust [Kurth et al. 2006b; Wang et al. 2006; Ye et al. 2014a] and sometimes information on the electron density [Ye et al. 2014b] (see the section entitled Dust and Dusty Ring Science for a more detailed discussion of the RPWS dust results].

Whistler mode chorus emissions

Whistler mode emissions are often observed in Saturn's inner magnetosphere with many characteristics similar to chorus detected at Earth and Jupiter. Due to these similar characteristics, the majority of the literature on these emissions has called the whistler mode emission chorus even though some of the emissions lack discrete elements or fine structure [Hospodarsky et al. 2008; Menietti et al. 2013b, 2014a]. Hospodarsky et al. [2008] performed an initial survey of these emissions and characterized them into two types based on their spectral characteristics and where they were observed. The most common type was defined as magnetospheric chorus that was observed within ~30 degrees of the magnetic equator between L shells of about 4.5 to 10. This emission usually has a bandwidth of a few hundred Hz and is detected below 1/2 f_{ce} as Cassini crosses through the inner magnetosphere. A variety of fine structure is associated with the chorus, from a structureless, hiss-like emission to narrowband frequency tones rising in frequency. The rising tone structure is similar to structures associated with chorus detected at Earth and Jupiter, but the timescales of the structure detected at Saturn are usually longer than those observed at Earth or Jupiter [Hospodarsky et al. 2008].

There is a subset of the magnetospheric chorus that have rising tones with periods on the order of many minutes. These emissions have been referred to as rising whistler mode emission, QP whistler emission, or sometimes as worms. They are observed about 5% of the time when Cassini is near the magnetic equator within 5.5 R_S of Saturn, and appear to be related to electrons with energies of a few keV. The cause of the many-minute periodicity is not well understood [Hospodarsky et al. 2016]. Although Hospodarsky et al. [2008] included these many-minute period rising tone whistler mode emissions with the magnetospheric chorus emissions, their spectral characteristics are more similar to the QP whistler mode emissions detected at Earth. However, it is currently unclear if the same type of source generation can explain the Earth and Saturn QP emissions.

The second type of whistler mode chorus emission reported by Hospodarsky et al. [2008] is detected in association with local plasma injections and were defined as injection event chorus. Local plasma injection events are injections of hot, less dense plasma produced by the interchange instability in rapidly rotating magnetospheres such as Saturn. These injections flow towards the planet while the colder and denser plasma from the inner magnetosphere flows outward [Mauk et al. 2009; Rymer et al. 2009; Mitchell et al. 2009b; Paranicas et al. 2016]. Young injection events are usually easy to detect with RPWS due to the changes in the spectral properties of the plasma waves associated with the injection compared to the waves detected outside of the events [Menietti et al. 2008a, 2008b; Hospodarsky et al. 2008; Kennelly et al. 2013]. Specifically, the frequency of the UHR usually decreases due to the lower electron plasma density inside of the injection and the ECH and chorus emissions are enhanced. Injection event chorus is often observed in two bands located above and below 1/2 f_{ce}, with a gap in the emission intensity at 1/2 f_{ce}, very similar to chorus detected at the Earth. The injection event chorus often contains fine structure (primarily rising tones) at a much smaller timescale (less than a second to a few seconds) than the magnetospheric chorus, again more similar to chorus at Earth and Jupiter [Hospodarsky et al. 2008]. Menietti et al. [2008a] showed that the chorus emissions observed inside the injection region can be at least partially generated by the measured temperature anisotropies in the electron population.

The occurrence, intensity, local time, and latitude variations of both types of chorus emission at Saturn have been examined by Hospodarsky et al. [2008, 2012] and in a series of papers by Menietti et al. [2012, 2013b, 2014a, 2014b]. These studies found that the peak in chorus intensity is detected at about ±5 degrees in magnetic latitude, with the intensity decreasing at the magnetic equator. The emissions are observed at all LT, but display maximum intensity on the nightside between L of 4.5 to 7. The small scale fine structure is more likely to be observed at higher frequencies and at latitudes greater than ~5°. The injection event chorus was typically found to be more intense than the chorus outside of the injection events [Menietti et al. 2014a], and the amplitude and structure of the rising tones was found to reasonably match predictions from non-linear theories of chorus generation [Menietti et al. 2013a]. Calculations of the wave normal and Poynting vector using the WFR data show that the chorus emissions propagate away from the magnetic equator at Saturn—see Figure 7 of Hospodarsky et al. [2008]—similar to results obtained for chorus at Earth.

Intense whistler mode waves were also detected in the magnetic flux tube connected to the surface of the Saturnian moon Rhea during a close flyby on March 2, 2010 [Santolik et al. 2011]. The whistler mode emission was observed below 1/2 f_{ce}, had peak amplitudes >0.5 nT, and was found to be propagating toward Rhea. Santolik et al. [2011] showed that these waves could be generated by the loss-cone anisotropy caused by absorption of electrons by the surface of the moon. Strong, bursty electrostatic waves near the electron plasma frequency and broadband electrostatic waves at frequencies well below the ion plasma frequency were also detected during this flyby. The waves near the electron plasma frequency have many of the characteristics of Langmuir waves observed in the solar wind and are believed to be produced by a low energy (~35 eV) electron beam propagating away from Rhea. The low-frequency waves may be related to the higher frequency waves through a nonlinear three-wave interaction.

Whistler mode auroral hiss emission

Auroral hiss is produced by electron beams and, when plotted on a time-frequency spectrogram, usually exhibits a funnel shaped spectrum.

Cassini also observes at magnetic latitudes greater than about 25° at Saturn a whistler mode emission that has many of the characteristics of auroral hiss [Mitchell et al. 2009a; Gurnett et al. 2009b; Kopf et al. 2010]. Auroral hiss is produced by electron beams and, when plotted on a time-frequency spectrogram, usually exhibits a funnel shaped spectrum. Auroral hiss has only been detected by Cassini propagating away from the auroral zone of Saturn and the emission is often observed out to distances of many tens of Saturn radii (R_S). Before 2008, the emission often exhibited a modulation in its intensity with a period of about 10.6 hours in the northern hemisphere and about 10.8 hours in the southern hemisphere, very similar to the periods of the SKR emission [Gurnett et al. 2009a, 2009b]. Shorter scale periodicity on the order of one hour is also often detected, and these short scale structures are often correlated with ion conics [Mitchell et al. 2009a, 2016; Palmaerts et al. 2016]. Kopf et al. [2010] analyzed electron beams detected by the CAPS during a Cassini high latitude pass and found that the detected beams coincided with observations of auroral hiss emissions. Examination of the predicted emission growth rate demonstrated that each of the measured beams possessed large whistler-mode growth rates, sufficient to produce the observed emission intensities.

Similar auroral hiss-like emissions have also been detected near Saturn's B-ring during the SOI period [Xin et al. 2006], and near the Saturnian moon Enceladus [Gurnett et al. 2011a]. Using ray tracing and the observed spectral funnel characteristics of the emission observed on seven different Enceladus flybys, Leisner et al. [2013] found two possible source regions near the moon, the quadrant upstream of the Saturnward flow terminator and the quadrant downstream of the anti-Saturnward flow terminator. The result of similar source regions for multiple flybys separated by over five years suggests that the electron beam acceleration near the moon is a quasi-time-stationary feature of the plasma interaction.

Electrostatic ECH and UHR emissions

Electrostatic emissions detected in Saturn's inner magnetosphere include ECH and UHR emissions. ECH emissions usually occur in frequency bands at $(n + 1/2)f_{ce}$, where n is an integer. Just like the chorus emissions discussed earlier, the ECH emissions are observed on most orbits when Cassini crosses the inner magnetosphere [Menietti et al. 2017]. The ECH waves also exhibit very different spectral characteristics inside and outside of injection events. ECH emissions observed outside of injection events are primarily found in the first harmonic band centered at ~1.5 f_{ce}, with higher harmonic bands being weaker and more sporadic. Inside of injection events the ECH emissions usually increase in both intensity and the number of harmonic bands present. A number of studies have attempted to explain the characteristics of the ECH waves using the electron plasma distributions measured by CAPS [Rymer et al. 2009] both outside [Menietti et al. 2008b] and inside [Menietti et al. 2008a; Tao et al. 2010] of an injection event. Menietti et al. [2008a, 2008b] found that phase space distributions with an assumed narrow, empty loss cone of the lower energy (< 100 eV) electron populations both inside and outside the injection event could generate the observed ECH emissions. However, Tao et al. [2010] found that inside the injection events, assuming a non-empty loss cone for electrons with energy near a few hundred eV and a few keV (higher than those predicted by Menietti et al. [2008b] could produce ECH waves with the observed harmonic structure. The precise ECH wave gain in the Tao et al. [2010] and Menietti et al. [2008b] models is very sensitive to the electron distribution used, which for this event is not measured at the smallest pitch angles. These uncertainties in modeling the actual cold electron components may explain the differences in these studies.

The UHR emissions are detected on most orbits in the inner magnetosphere [Moncuquet et al. 2005; Schippers et al. 2013] and during close flybys of Saturn's moons—for example, Farrell et al. [2009], especially Titan [e.g., Modolo et al. 2007a]. Because the frequency of the UHR emissions (fuhr) is related to the electron plasma frequency (f_{pe}) by $f_{uhr}^2 = f_{pe}^2 + f_{ce}^2$, determining f_{uhr} and obtaining f_{ce} from the magnetic field strength provides the electron plasma density (n_e) from $f_{pe} = 8980\ n_e^{1/2}$. By measuring f_{uhr} for each pass through the inner magnetosphere, Persoon et al. [2009, 2013] have developed an empirical plasma density model for the Saturnian system.

Open Questions for Saturn System Science

Any mission, however extended, always raises questions based on the new knowledge gained. Here we give a brief list of open questions for radio and plasma wave science at Saturn, after Cassini.

- What is the rotation period of Saturn? How do the multiple, variable magnetospheric periods observed in radio, magnetic fields, energetic particles, plasma, aurora, and other phenomena tie to the internally-generated magnetic field at Saturn?
- Given the extraordinarily axi-symmetric magnetic field, why are there such prominent rotational modulations in Saturn's magnetosphere?

- What drives the episodic lightning on Saturn; why is there ~one Great White Spot storm per Saturnian year?
- How does the dust in the Saturnian system interact with Saturn and its atmosphere? How are the rings coupled to the planet other than through gravity?
- What is the predominant form of the electron distribution function at the source of SKR?
- How does the abundant neutral population in Saturn's magnetosphere make it different from fully or mostly ionized magnetospheres?
- What are the various populations of charged dust and molecules that balance charges in dusty media such as in the plumes of Enceladus and in Saturn's topside equatorial ionosphere?

RPWS Non-Saturn Science Results

Cruise Science

The bulk of science carried out in the cruise phase by the RPWS was at planetary targets as detailed in the following sections, although there were considerable efforts employed during cruise to check out the instrument and exercise and improve various observing modes planned for use at Saturn. However, Schippers et al. [2014, 2015] reported nanograins in the solar wind detected by the RPWS and Meyer-Vernet et al. [2009], reported nanograins originating from Jupiter's moons.

Venus

During two Cassini very close gravity-assist flybys of Venus, the first on April 26, 1998, and the second on June 24, 1999, the RPWS instrument conducted a search for high-frequency (0.125 to 16 MHz) radio impulses from Venus lightning. Despite the excellent sensitivity of the high-frequency RPWS receiver (down to the cosmic background), no impulses were detected [Gurnett et al. 2001]. During a subsequent close gravity-assist flyby of Earth on August 18, 1999, radio signals from lightning were observed essentially continuously at all radial distances inside of about 14 Earth radii, with maximum occurrence rates up to about 30 pulses per minute. If Venus lightning exists then it must be much weaker and at much lower frequencies than terrestrial lightning.

Earth

Cassini executed a flyby of Earth on August 18, 1999, in order to gain sufficient energy to get to Saturn. However, the flyby also offered an opportunity to understand how some of the instruments, including RPWS, perform in a planetary magnetosphere nearly five years prior to arrival at Saturn [Kurth et al. 2001b]. The Earth flyby provided the opportunity to test a number of observation modes and capabilities to determine their efficacy in time to make adjustments prior to the prime mission.

In addition, the flyby provided a swift flyby of Earth that allowed a unique set of observations of terrestrial magnetospheric radio and plasma wave phenomena.

Figure RPWS-21 shows an overview of the RPWS observations during the Earth flyby. The trajectory brings Cassini into the magnetosphere just past noon local time and carries it down the magnetotail in the post-midnight sector. Closest approach to Earth was just under 1200 km. As one would expect, the RPWS observed broadband electrostatic waves at the bow shock, electron cyclotron harmonics and whistler mode chorus in the outer radiation belts and emissions between the plasma frequency and upper hybrid frequency in the ionosphere. Evidence for electron phase space holes was found in the near-Earth plasma sheet. At higher frequencies auroral kilometric radiation was observed on the night side indicating a series of auroral substorms and fixed frequency narrowband lines from man-made terrestrial radio stations were observed. Even Jovian hectometric radiation was observed from a position far downstream from Earth.

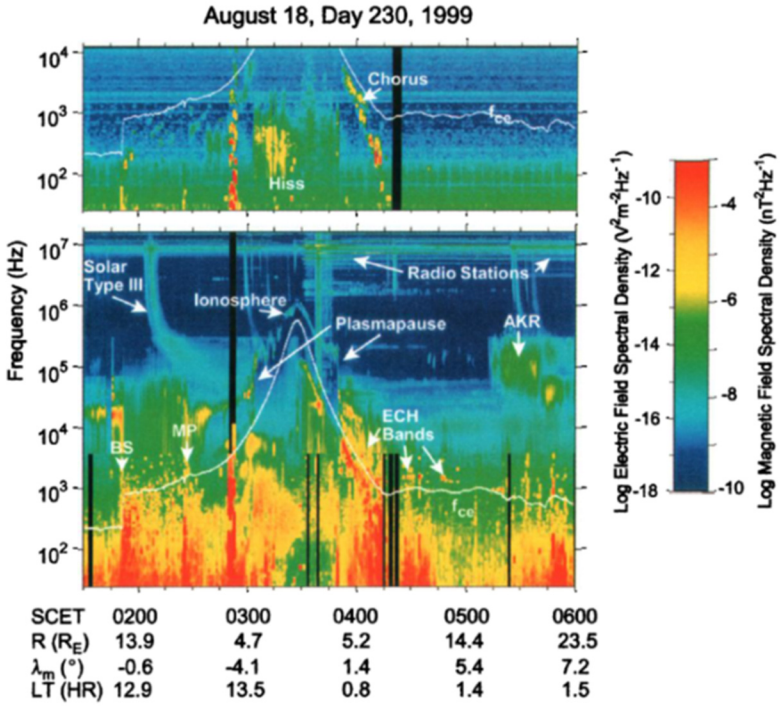

Figure RPWS-21. An overview of RPWS observations of the Earth flyby with magnetic fields shown in the *Top panel* and electric fields below. The white trace is the electron cyclotron frequency fce derived from |*B*|. *BS* refers to the bow shock, *MP* refers to the magnetopause, *ECH* refers to electron cyclotron harmonics, and *AKR* refers to auroral kilometric radiation.

Using a number of techniques, the plasma density was measured. The electron plasma frequency and upper hybrid resonance frequency are characteristic frequencies of the plasma dependent on the electron density. RPWS also includes a Langmuir probe that can determine the electron density and temperature. Finally, a relaxation sounder was used to stimulate the plasma frequency.

Wideband waveform measurements were used in various regions of the magnetosphere to acquire examples of chorus and ECH bands. These are also necessary to identify solitary-like structures associated with electron phase space holes.

Another feature of the RPWS instrument that was tested during the Earth flyby was the capability of determining the wave normal angle of whistler mode waves using 5-channel WFR measurements of three magnetic and two electric sensors. Hospodarsky et al. [2001b] used the WFR measurements to examine the propagation characteristics of a lightning whistler, chorus, and electromagnetic emissions in the magnetosheath, presumably lion roars.

Hospodarsky et al. [2001b] determined that the whistler analyzed was also detected at Palmer Station in Antarctica. The chorus waves were observed near the magnetic equator and appeared to reverse their direction of propagation at the equator, consistently propagating away from the equator where it is assumed the chorus source is located. The lion roars were found to consistently propagate nearly along the magnetic field but varied from burst to burst with some propagating near parallel and others near antiparallel to the field, suggesting multiple sources.

As mentioned above, Cassini detected intense, fixed frequency emissions at close range to Earth in the frequency range above about 1 MHz that are attributed to man-made radio transmissions. Fischer and Rucker [2006] studied the occurrence of these in detail and demonstrated that most of the emissions could be identified with shortwave radio bands. A few brief detections of scientific transmitters including the High-frequency Active Auroral Research Program (HAARP) and the Russian SURA station—see also Tokarev et al. [2006]. Fischer and Rucker point out an interesting quiet period when Cassini was near closest approach over the Pacific Ocean where a combination of the rarity of transmitters in this location and ionospheric propagation characteristics effectively shielded Cassini from the radio transmission for a period of about 20 minutes.

Jupiter

Cassini flew by Jupiter on December 30, 2000, on its way to Saturn. Arriving from the pre-noon sector, closest approach occurred in the afternoon sector at 138 Jovian radii (~10^7 km) from the planet, and was followed by an exploration of the dusk flank of the Jovian magnetosphere. In spite of the large distance of the flyby, several Cassini- Magnetospheres and Plasma Science (MAPS) instruments including RPWS recorded high-quality data for about 6 months around closest approach. These observations benefited from the simultaneous presence of Galileo in orbit around Jupiter, enabling two-point measurements, and were complemented by remote observations by HST, Chandra, and ground-based radio observations (e.g., with the Nançay decameter array, France). This resulted in a very rich data set that was the basis of many publications and will be further exploited in the coming years.

The distant observations were well adapted to the study of the complex zoo of Jupiter's magnetospheric radio emissions, nicely covered by the Kronos receiver of RPWS, an example of which is given in Figure RPWS-22. An early overview is given in [Lecacheux 2001]. The intensity

spectrum of all Jovian radio components was accurately measured [Zarka et al. 2004a] through calibration on the Galactic background and Nançay observations, demonstrating in particular the absence of peak at 10 MHz in the decameter spectrum. The beaming of the decametric (DAM) and hectometric (HOM) components (a widely opened hollow cone of a few degrees thickness) were measured via two point Cassini-Wind measurements [Kaiser et al. 2000] as well as frequency-longitude statistics and modelling [Imai et al. 2008, 2011a, 2011b]. The HOM low-frequency cutoff measured by Ulysses and Cassini provided constraints of its source location, in the outer regions of the Io plasma torus [Zarka et al. 2001a].

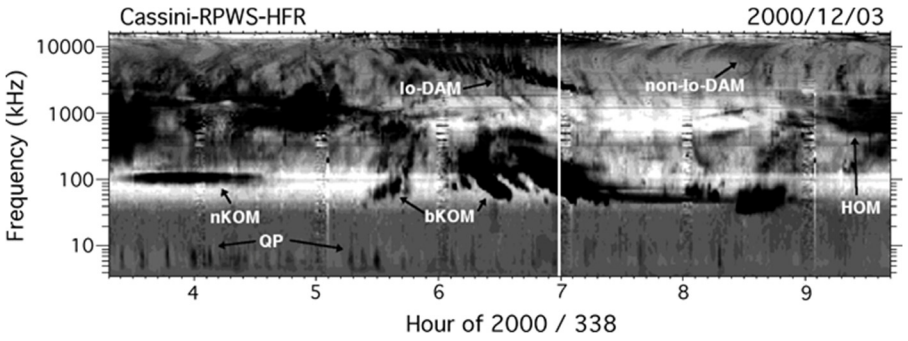

Figure RPWS-22. Jovian low-frequency radio emissions detected on December 3, 2000, by the RPWS experiment onboard Cassini approaching Jupiter. Frequency range is 3.5 kHz to 16.1 MHz. The Io-induced decameter emission (Io-DAM) appears here down to about 2 MHz, while weaker Io-independent (non-Io-DAM) arcs merge with the HOM component detected down to ~400 kHz. The auroral broadband kilometer (bKOM) component is detected down to ~40 kHz. The narrowband emission (nKOM) about 100 kHz is generated at or near the plasma frequency f_{pe} in Io's torus. The QP bursts, spaced by 5 to > 15 min, are detected in the ~5 to 20 kHz range. Distance to Jupiter was 383 R_J (2.7×10^7 km) at the time of this observation.

The six month series of continuous homogeneous measurements provided unique measurements of time variations of the radio emission. Burst of auroral (non-Io) DAM emission were found to reoccur at a period slightly longer than the system III rotation period [Panchenko et al. 2010, 2013; Panchenko and Rucker 2011]. Gurnett et al. [2002] found from Cassini and Galileo observations that Jupiter's auroral radio and UV emissions were triggered by interplanetary shocks inducing magnetospheric compressions, in disagreement with theoretical predictions [Southwood and Kivelson 2001]. Hess et al. [2014] reconciled these views by a finer analysis of dawn and dusk radio emissions seen by Cassini, Galileo and Nançay, only dusk emissions being driven by both compressions and dilatations of the magnetosphere. They also used radio observations to deduce the subcorotation velocity of the magnetospheric plasma. Clarke et al. [2009] compared the effect of solar wind compressions on radio and UV aurora at Jupiter and Saturn, and found a weaker effect at Jupiter. Radio (non-Io-DAM, HOM, and bKOM) and UV comparisons are used quite systematically in the study of Jupiter's aurora [Clarke et al. 2004, 2005; Pryor et al. 2005]. Comparison of Galileo/Jupiter and Cassini/Saturn observations also revealed similar energetic events where auroral radio intensifications are related to centrifugal plasma ejections, from the Io torus at Jupiter and from the equatorial plasma sheet at Saturn [Louarn et al. 2007].

Cassini, Galileo, and Voyager radio observations were used to try to demonstrate the influence of satellites other than Io on DAM emissions. Marginal results were obtained statistically [Hospodarsky et al. 2001a], whereas clear evidence was obtained for Europa and Ganymede by comparison of observations with modelled dynamic spectra [Louis et al. 2017a]. The ExPRES simulation tool developed in Meudon [Hess et al. 2008] and the experienced gained with Cassini on Jupiter's radio emissions were used to build simulations preparing the re-exploration of the Jovian magnetosphere by the electrostatic energy analyzer (ESA) Juice mission [Cecconi et al. 2012].

Fast recording modes of RPWS (spectral and waveform) allowed us to characterize the fine structure of Jovian radio emissions in the kilometer (bKOM) to decameter range [Kurth et al. 2001a; Lecacheux et al. 2001], including zebra-like patterns in the bKOM emission. Those were tentatively interpreted by bubble-like plasma inhomogeneities [Farrell et al. 2004] or the double plasma resonance mechanism involving ion cyclotron waves [Zlotnik et al. 2016]. Similar patterns have been observed at decameter wavelengths [Panchenko et al. 2016, 2018].

At the very low-frequency end of the radio spectrum (below a few 10s of kHz), Cassini together with Ulysses and Galileo characterized the Jovian Quasi-Periodic bursts [Kaiser et al. 2001, 2004], stereoscopic observations demonstrated their strobe-like behavior and wide beaming [Hospodarsky et al. 2004], and direction-finding techniques localized their sources at high latitude regions of the magnetopause, implying complex propagation [Hospodarsky et al. 2004; Kimura et al. 2012]. QP bursts were tentatively related to the so-called Jovian anomalous continuum radiation [Ye et al. 2012]. Propagation of radio waves near the edges of the Io plasma torus were shown to generate the HOM attenuation lane, an intensity gap oscillating between ~1 and ~3 MHz, described by Boudjada et al. [2011] and modelled by Menietti et al. [2003] and Imai et al. [2015]. Occultations of Jovian radio emissions were used to probe the Io plasma torus [Boudjada et al. 2014a].

Analysis of local low-frequency plasma waves recorded by RPWS was used to study the Jovian dust flank magnetopause and bow shock [Kurth et al. 2002; Szego et al. 2003], magnetosheath [Bebesi et al. 2010, 2011] and pre-shock [Szego et al. 2006]. The magnetopause was found to be in the process of being compressed by a solar wind pressure increase at the time of the Cassini flyby [Kurth et al. 2002]. Langmuir waves were detected upstream of the bow shock, and their level compared with that at other planets: the ratio of the energy density of the waves electric field to the plasma was found to increase with distance from the Sun [Hospodarsky et al. 2006].

Z-mode radiation and electron cyclotron harmonics (at low latitudes) and whistler-mode chorus (at higher latitudes) were measured [Menietti et al. 2012, 2016a] and their effect on electron acceleration was evaluated [de Soria-Santacruz et al. 2017]. RPWS spectral and waveform measurements also permitted to detect nanodust particles in the interplanetary medium, of likely Jovian origin [Meyer-Vernet et al. 2009; Schippers et al. 2014, 2015].

Observations of Jupiter radio emissions were used to calibrate the Direction-Finding (actually Gonio-Polarimetric) capability of RPWS/Kronos [Vogl et al. 2001, 2004], which proved extremely successful at Saturn. Early use of this directional capability permitted to check the origin of lightning-like signals observed in Cassini's inbound leg to Saturn, which proved to be Jovian radio bursts [Fischer et al. 2006c].

Overall, the Cassini RPWS experiment was very successful at Jupiter. The obtained results were reported in several review papers about comparisons of radio waves [Zarka 2000, 2004; Zarka and Kurth 2005; de Pater and Kurth 2007; Rucker et al. 2014] and plasma waves [Hospodarsky et al. 2012] at the magnetized planets, as well as in reviews about auroras [Badman et al. 2014], magnetospheric processes [Blanc et al. 2002; Seki et al. 2015], or dust detection [Meyer-Vernet et al. 2017]. They greatly helped to prepare the magnetospheric measurements of the Juno mission in Jovian polar orbit [Bagenal et al. 2017]. Two PhD theses were largely based on Cassini RPWS measurements at Jupiter [Cecconi 2004; Imai 2016].

ACRONYMS

Note: For a complete list of Acronyms, refer to Cassini Acronyms – Attachment A.

A/D	analog-to-digital converter
AKR	auroral kilometric radiation
AO	Announcement of Opportunity
AU	astronomical unit
bKOM	broadband kilometer
CA	closest approach
CAPS	Cassini Plasma Science
CDA	Cosmic Dust Analyzer
CIR	corotating interaction region
CM	central meridian
CMI	cyclotron maser instability
DAM	decametric
DOY	day of year
ECH	electron cyclotron harmonic
ELS	electron spectrometer
ENA	energetic neutral atom
ESA	electrostatic energy analyzer
EUV	extreme ultraviolet
FUV	far ultraviolet
FWHM	full width at half-maximum
GCR	galactic cosmic ray
GWS	great white spot
HAARP	High-frequency Active Auroral Research Program
HFR	high frequency receiver
HGA	high gain antenna
HOM	hectometric
HRD	high-rate detector
HST	Hubble Space Telescope
ICME	interplanetary coronal mass ejection
IMF	interplanetary magnetic field
IMS	ion mass spectrometer
INCA	Ion and Neutral Camera
IR	infrared
ISS	Imaging Science Subsystem
LEMMS	Low-Energy Magnetospheric Measurement System
LFR	low frequency receiver
LP	Langmuir probe

LPT	Linear Prediction Theory
LT	local time
MAPS	Magnetospheres and Plasma Science
MFR	medium frequency receiver
MHD	magneto-hydrodynamic
MIMI	Magnetospheric Imaging Instrument
NB	narrowbanded
nKOM	narrowband kilometer
PPO	planetary period oscillation
PRA	Planetary Radio Astronomy
QP	quasi-periodic
RH	right-handed
RPC	ring plasma cavity
RPWS	Radio and Plasma Wave Science
RS	Saturn radii
SCET	spacecraft event time
SED	Saturn electrostatic discharges
SEP	solar energetic particle
SKR	Saturn kilometric radiation
SLS	Space Launch System
SOI	Saturn orbit insertion
TM	Traceability Matrix
UHR	upper hybrid resonance
UT	universal time
UV	ultraviolet
UVIS	Ultraviolet Imaging Spectrograph
VIMS	Visual and Infrared Mapping Spectrometer
WBR	wideband receiver
WFR	waveform receiver

REFERENCES

Disclaimer: The partial list of references below correspond with in-text references indicated in this report. For all other Cassini references, refer to Attachment B – References & Bibliographies; Attachment C – Cassini Science Bibliographies; the sections entitled References contributed by individual Cassini instrument and discipline teams located in Volume 1 Sections 3.1 and 3.2 Science Results; and other resources outside of the Cassini Final Mission Report.

Achilleos, N., C. Bertucci, C. T. Russell, G. B. Hospodarsky, A. M. Rymer, C. S. Arridge, M. E. Burton, M. K. Dougherty, S. Hendricks, E. J. Smith, B. T. Tsurutani, (2006), Orientation, location, and velocity of Saturn's bow shock: Initial results from the Cassini spacecraft, Journal of Geophysical Research, 111, A03201, doi: 10.1029/2005JA011297.

Ågren, K., (2012), On the formation and structure of the ionosphere of Titan, Ph.D. Thesis, Uppsala University, Uppsala, Sweden.

Ågren, K., N. J. T. Edberg, J.-E. Wahlund, (2012), Detection of negative ions in the deep ionosphere of Titan during the Cassini T70 flyby, Geophysical Research Letters, 39, L10201, doi: 10.1029/2012GL051714.

Ågren, K., D. J. Andrews, S. C. Buchert, A. J. Coates, S. W. H. Cowley, M. K. Dougherty, N. J. T. Edberg, P. Garnier, G. R. Lewis, R. Modolo, H. Opgenoorth, G. Provan, L. Rosenqvist, D. L. Talboys, J.-E. Wahlund, A. Wellbrock, (2011), Detection of currents and associated electric fields in Titan's ionosphere from Cassini data, Journal of Geophysical Research, 116, A04313, doi: 10.1029/2010JA016100.

Ågren, K., J.-E. Wahlund, P. Garnier, R. Modolo, J. Cui, M. Galand, I. Muller-Wodarg, (2009), On the ionospheric structure of Titan, Planetary and Space Science, 57, 1821–1827, doi: 10.1016/j.pss.2009.04.012.

Ågren, K., J.-E. Wahlund, R. Modolo, D. Lummerzheim, M. Galand, I. Muller-Wodarg, P. Canu, W. S. Kurth, T. E. Cravens, R. V. Yelle, J. H. Waite, Jr., A. J. Coates, G. R. Lewis, D. T. Young, C. Bertucci, M. Dougherty, (2007), On magnetospheric electron impact ionisation and dynamics in Titan's ram-side and polar ionosphere - A Cassini Case Study, Annales Geophysicae, 25, 2359–2369, doi: 10.5194/angeo-25-2359-2007.

Akalin, F., D. A. Gurnett, T. F. Averkamp, A. M. Persoon, O. Santolik, W. S. Kurth, G. B. Hospodarsky, (2006), First whistler observed in the magnetosphere of Saturn, Geophysical Research Letters, 33, L20107, doi: 10.1029/2006GL027019.

Akalin, F., (2005), Observation of a whistler in the magnetosphere of Saturn, M.S. Thesis, University of Iowa, Iowa City, Iowa.

Amatucci, W. E., P. W. Schuck, D. N. Walker, P. M. Kintner, S. Powell, B. Holback, D. Leonhardt, (2001), Contamination-free sounding rocket Langmuir probe, Review of Scientific Instruments, 72, 2052–2057.

Andre, N., M. Blanc, S. Maurice, P. Schippers, E. Pallier, T. I. Gombosi, K. C. Hansen, D. T. Young, F. J. Crary, S. Bolton, E. C. Sittler, H. T. Smith, R. E. Johnson, R. A. Baragiola, A. J. Coates, A. M. Rymer, M. K. Dougherty, N. Achilleos, C. S. Arridge, S. M. Krimigis, D. G. Mitchell, N. Krupp, D. C. Hamilton, I. Dandouras, D. A. Gurnett, W. S. Kurth, P. Louarn, R. Srama, S. Kempf, J. H. Waite, L. W. Esposito, J. T. Clarke, (2008), Identification of Saturn's magnetospheric regions and associated plasma processes: Synopsis of Cassini observations during orbit insertion, Reviews of Geophysics, 46, RG4008, doi: 10.1029/2007RG000238.

Andre, N., A. M. Persoon, J. Goldstein, J. L. Burch, P. Louarn, G. R. Lewis, A. M. Rymer, A. J. Coates, W. S. Kurth, E. C. Sittler, Jr., M. F. Thomsen, F. J. Crary, M. K. Dougherty, D. A. Gurnett, D. T. Young, (2007), Magnetic signatures of plasma-depleted flux tubes in the Saturnian inner magnetosphere, Geophysical Research Letters, 34, L14108, doi: 10.1029/2007GL030374.

Andrews, D. J., S. W. H. Cowley, M. K. Dougherty, L. Lamy, G. Provan, and D. J. Southwood, (2012), Planetary period oscillations in Saturn's magnetosphere: Evolution of magnetic oscillation properties from southern summer to post-equinox, Journal of Geophysical Research, 117, A04224, doi: 10.1029/2011JA017444.

Andrews, D. J., B. Cecconi, S. W. H. Cowley, M. K. Dougherty, L. Lamy, G. Provan, P. Zarka, (2011), Planetary period oscillations in Saturn's magnetosphere: Evidence in magnetic field phase data for rotational modulation of Saturn kilometric radiation emissions, Journal of Geophysical Research, 116, A09206, doi: 10.1029/2011JA016636.

Andrews, D. J., A. J. Coates, S. W. H. Cowley, M. K. Dougherty, L. Lamy, G. Provan, P. Zarka, (2010), Magnetospheric period oscillations at Saturn: Comparison of equatorial and high-latitude magnetic field periods with north and south SKR periods, Journal of Geophysical Research, 115, A12252, doi: 10.1029/2010JA015666.

Aplin, K. and G. Fischer, (2019), Atmospheric electricity in the solar system, Oxford Research Encyclopedia, Planetary Science, Oxford University Press, doi: 10.1093/acrefore/9780190647926.013.112.

Aplin, K. L. and G. Fischer, (2017), Lightning detection in planetary atmospheres, Weather, 72, 2, 46–50, doi: 10.1002/wea.2817.

Arridge, C. S., J. P. Eastwood, C. M. Jackman, G.-K. Poh, J. A. Slavin, M. F. Thomsen, N. Andre, X. Jia, A. Kidder, L. Lamy, A. Radioti, D. B. Reisenfeld, N. Sergis, M. Volwerk, A. P. Walsh, P. Zarka, A. J. Coates, M. K. Dougherty, (2016a), Cassini in situ observations of long duration magnetic reconnection in Saturn's magnetotail, Nature Physics, 12, 268–271, doi: 10.1038/nphys3565.

Arridge, C. S., J. M. Jasinski, N. Achilleos, Y. V. Bogdanova, E. J. Bunce, S. W. H. Cowley, A. N. Fazakerley, K. K. Khurana, L. Lamy, J. S. Leisner, E. Roussos, C. T. Russell, P. Zarka, A. J. Coates, M. K. Dougherty, G. H. Jones, S. M. Krimigis, N. Krupp, (2016b), Cassini observations of Saturn's southern polar cusp, Journal of Geophysical Research, 121, 3006–3030, doi: 10.1002/2015JA021957.

Arridge, C. S., N. André, H. J. McAndrews, E. J. Bunce, M. H. Burger, K. C. Hansen, H.-W. Hsu, R. E. Johnson, G. H. Jones, S. Kempf, K. K. Khurana, N. Krupp, W. S. Kurth, J. S. Leisner, C. Paranicas, E. Roussos, C. T. Russell, P. Schippers, E. C. Sittler, H. T. Smith, M. F. Thomsen, M. K. Dougherty, (2011), Mapping magnetospheric equatorial regions at Saturn from Cassini Prime Mission Observations, Space Science Reviews, 164, Nos. 1–4, 1–83, doi: 10.1007/s11214-011-9850-4.

Azari, A. R., X. Jia, M. W. Liemohn, G. B. Hospodarsky, G. Provan, S.-Y. Ye, S. W. H. Cowley, C. Paranicas, N. Sergis, A. M. Rymer, M. F. Thomsen, D. G. Mitchell, (2019), Are Saturn's interchange injections organized by rotational longitude? Journal of Geophysical Research, 124, 1806–1822, doi: 10.1029/2018Ja026196.

Azari, A. R., M. W. Liemohn, X. Jia, M. F. Thomsen, D. G. Mitchell, N. Sergis, A. M. Rymer, G. B. Hospodarsky, C. Paranicas, J. Vandegriff, (2018), Interchange injections at Saturn: Statistical survey of energetic H^+ sudden flux intensifications, Journal of Geophysical Research, 123, 4692–4711, doi: 10.1029/2018JA025391.

Bader, A., S. V. Badman, Z. H. Yao, J. Kinrade, W. R. Pryor, (2019), Observations of continuous quasiperiodic auroral pulsations on Saturn in high time-resolution UV auroral imagery, Journal of Geophysical Research, 124, 2451–2465, doi: 10.1029/2018JA026320.

Badman, S. V., G. Provan, E. J. Bunce, D. G. Mitchell, H. Melin, S. W. H. Cowley, A. Radioti, W. S. Kurth, W. R. Pryor, J. D. Nichols, S.L. Jinks, T. S. Stallard, R. H. Brown, K. H. Baines, M. K. Dougherty, (2016), Saturn's auroral morphology and field-aligned currents during a solar wind compression, Icarus, 263, 83–93, doi: 10.1016/j.icarus.2014.11.014.

Badman, S. V., G. Branduardi-Raymont, M. Galand, S. L. G. Hess, N. Krupp, L. Lamy, H. Melin, C. Tao, (2014), Auroral processes at the giant planets: Energy deposition, emission mechanisms, morphology and spectra, Space Science Reviews, 187, Issue 1–4, doi: 10.1007/s11214-014-0042-x.

Badman, S. V., N. Achilleos, C. S. Arridge, K. H. Baines, R. H. Brown, E. J. Bunce, A. J. Coates, S. W. H. Cowley, M. K. Dougherty, M. Fujimoto, G. Hospodarsky, S. Kasahara, T. Kimura, H. Melin, D. G. Mitchell, T. Stallard, C. Tao, (2012a), Cassini observations of ion and electron beams at Saturn and their relationship to infrared auroral arcs, Journal of Geophysical Research, 117, A01211, doi: 10.1029/2011JA017222.

Badman, S. V., N. Achilleos, C. S. Arridge, K. H. Baines, R. H. Brown, E. J. Bunce, A. J. Coates, S. W. H. Cowley, M. K. Dougherty, M. Fujimoto, G. Hospodarsky, S. Kasahara, T. Kimura, H. Melin, D. G. Mitchell, T. Stallard, C. Tao, (2012b), Correction to Cassini observations of ion and electron beams at saturn and their relationship to infrared auroral arcs, Journal of Geophysical Research, 117, A04220, doi: 10.1029/2012JA017617.

Badman, S. V., D. J. Andrews, S. W. H. Cowley, L. Lamy, G. Provan, C. Tao, S. Kasahara, T. Kimura, M. Fujimoto, H. Melin, T. Stallard, R. H. Brown, K. H. Baines, (2012c), Rotational Modulation and Local Time Dependence of Saturn's Infrared H_3^+ Auroral Intensity, Journal of Geophysical Research, 117, A09228, doi: 10.1029/2012JA017990.

Badman, S. V., S. W. H. Cowley, L. Lamy, B. Cecconi, P. Zarka, (2008a), Relationship between solar wind corotating interaction region compressions and the phasing and intensity of Saturn kilometric radiation bursts, Annales Geophysicae, 26, 3641–3651, doi: 10.5194/angeo-26-3641-2008.

Badman, S. V., S. W. H. Cowley, L. Lamy, B. Cecconi, P. Zarka, (2008b), Saturn's radio clock, Astronomy & Geophysics, No. 4, pp. 4.13–4.15, Blackwell Publishing, doi: 10.1111/j.1468-4004.2008.49413.x.

Bagenal, F., A. Adriani, F. Allegrini, S. J. Bolton, B. Bonfond, E. J. Bunce, J. E. P. Connerney, S. W. H. Cowley, R. W. Ebert, G. R. Gladstone, C. J. Hansen, W. S. Kurth, S. M. Levin, B. H. Mauk, D. J. McComas, C. P. Paranicas, D. Santos-Costas, R. M. Thorne, P. Valek, J. H. Waite, P. Zarka, (2017), Magnetospheric science objectives of the Juno Mission, Space Science Reviews, 213, 219–287, doi: 10.1007/s11214-014-0036-8.

Baines, K. H., M. L. Delitsky, T. W. Momary, R. H. Brown, B. J. Buratti, R. N. Clark, P. D. Nicholson, (2009), Storm clouds on Saturn: Lightning-induced chemistry and associated materials consistent with Cassini/VIMS spectra, Planetary and Space Science, 57, 1650–1658.

Bebesi, Z., K. Szego, A. Balogh, N. Krupp, G. Erdos, A. M. Rymer, G. R. Lewis, W. S. Kurth, D. T. Young, M. K. Dougherty, (2011), Response to– Comment on– Slow-mode shock candidate in the Jovian magnetosheath by Bebesi et al. 2010, Planetary and Space Science, 59, Issues 5–6, 445–446, doi: 10.1016/j.pss.2010.10.007.

Bebesi, Z., K. Szego, A. Balogh, N. Krupp, G. Erdos, A. M. Rymer, G. R. Lewis, W. S. Kurth, D. T. Young, M. K. Dougherty, (2010), Slow-mode shock candidate in the Jovian magnetosheath, Planetary and Space Science, 58, Issue 5, 807–813, doi: 10.1016/j.pss.2009.12.008.

Beghin, C., P. Canu, E. Karkoschka, C. Sotin, C. Bertucci, W. S. Kurth, J. J. Berthelier, R. Grard, M. Hamelin, K. Schwingenschuh, F. Simoes, (2009), New insights on Titan's plasma-driven Schumann resonance inferred from Huygens and Cassini data, Planetary and Space Science, 57, 1872–1888, doi: 10.1016/j.pss.2009.04.006.

Bertucci, C., D. C. Hamilton, W. S. Kurth, G. B. Hospodarsky, D. Mitchell, N. Sergis, N. J. T. Edberg, M. K. Dougherty, (2015), Titan's interaction with the supersonic solar wind, Geophysical Research Letters, 42, 193–200, doi: 10.1002/2014GL062106.

Bertucci, C., F. Duru, N. Edberg, M. Fraenz, C. Martinecz, K. Szego, O. Vaisberg, (2011), The induced magnetospheres of Mars, Venus, and Titan, Space Science Reviews, 162, 113–171, doi: 10.1007/s11214-011-9845-1.

Bertucci, C., N. Achilleos, M. K. Dougherty, R. Modolo, A. J. Coates, K. Szego, A. Masters, Y. Ma, F. M. Neubauer, P. Garnier, J.-E. Wahlund, D. T. Young, (2008), The magnetic memory of Titan's ionized atmosphere, Science, 321, 1475–1478, doi: 10.1126/science.1159780.

Bertucci, C., N. Achilleos, C. Mazelle, G. B. Hospodarsky, M. Thomsen, M. K. Dougherty, W. Kurth, (2007a), Low-frequency waves in the foreshock of Saturn: First results from Cassini, Journal of Geophysical Research, 112, A09219, doi: 10.1029/2006JA012098.

Bertucci, C., F. M. Neubauer, K. Szego, J.-E. Wahlund, A. J. Coates, M. K. Dougherty, D. T. Young, W. S. Kurth, (2007b), Structure of Titan's mid-range magnetic tail: Cassini Magnetometer observations during the T9 flyby, Geophysical Research Letters, 34, L24S02, doi: 10.1029/2007GL030865.

Blanc, M., S. Bolton, J. Bradley, M. Burton, T. E. Cravens, I. Dandouras, M. K. Dougherty, M. C. Festou, J. Feynman, R. E. Johnson, T. G. Gombosi, W. S. Kurth, P. C. Liewer, B. H. Mauk, S. Maurice, D. Mitchell, F. M. Neubauer, J. D. Richardson, D. E. Shemansky, E. C. Sittler, B. T. Tsurutani, Ph. Zarka, L. W. Esposito, E. Gruen, D. A. Gurnett, A. J. Kliore, S. M. Krimigis, D. Southwood, J. H. Waite, D. T. Young, (2002), Magnetospheric and plasma science with Cassini-Huygens, Space Science Reviews, 104, 253–346, doi: 10.1023/A:1023605110711.

Boudjada, M. Y., P. H. M. Galopeau, S. Sawas, H. Lammer, (2014a), Remote sensing of the Io torus plasma ribbon using natural radio occultation of the Jovian radio emission, Annales Geophysicae, 32, 1119–1128, doi: 10.5194/angeo-32-1119-2014.

Boudjada, M. Y., P. H. M. Galopeau, M. Maksimovic, H. O. Rucker, (2014b), Visibility of Type III burst source location as inferred from stereoscopic space observations, Advances in Radio Science, 12, 167–170, doi: 10.5194/ars-12-167-2014.

Boudjada, M. Y., P. H. M. Galopeau, H. O. Rucker, A. Lecacheux, N. Mebarki, W. Macher, W. Voller, (2011), Morphological aspects of the attenuation bands associated with Jovian hectometric radiation, Journal of Geophysical Research, 116, A11208, doi: 10.1029/2010Ja016354.

Branduardi-Raymont, G., P. G. Ford, K. C. Hansen, L. Lamy, A. Masters, B. Cecconi, A. J. Coates, M. K. Dougherty, G. R. Gladstone, P. Zarka, (2013), Search for Saturn's x-ray aurorae at the arrival of a solar wind shock, Journal of Geophysical Research, 118, 2145–2156, doi: 10.1002/jgra.50112.

Bunce, E. J., D. C. Grodent, S. L. Jinks, D. J. Andrews, S. V. Badman, A. J. Coates, S. W. H. Cowley, M. K. Dougherty, W. S. Kurth, D. G. Mitchell, G. Provan, (2014), Cassini nightside observations of the oscillatory motion of Saturn's northern auroral oval, Journal of Geophysical Research, 119, 3528–3543, doi: 10.1002/2013JA019527.

Bunce, E. J., S. W. H. Cowley, D. L. Talboys, M. K. Dougherty, L. Lamy, W. S. Kurth, P. Schippers, B. Cecconi, P. Zarka, C. S. Arridge, A. J. Coates, (2010), Extraordinary field-aligned current signatures in Saturn's high-latitude magnetosphere: Analysis of Cassini data during Revolution 89, Journal of Geophysical Research, 115, A10238, doi: 10.1029/2010JA015612.

Bunce, E. J., S. W. H. Cowley, D. M. Wright, A. J. Coates, M. K. Dougherty, N. Krupp, W. S. Kurth, A. M. Rymer, (2005), In situ observations of a solar wind compression-induced hot plasma injection in Saturn's tail, Geophysical Research Letters, 32, L20S04, doi: 10.1029/2005GL022888.

Burch, J. L., J. Goldstein, T. W. Hill, D. T. Young, F. J. Crary, A. J. Coates, N. Andre, W. S. Kurth, E. C. Sittler, Jr., (2005), Properties of local plasma injections in Saturn's magnetosphere, Geophysical Research Letters, 32, L14S02, doi: 10.1029/2005GL022611.

Burns, J. A., D. P. Hamilton, M. R. Showalter, (2001), Dusty rings and circumplanetary dust: Observations and simple physics, In Interplanetary Dust, (eds.) E. Grün, B. A. S. Gustafson, S. Dermott, H. Fechtig, Springer, Berlin.

Carbary, J. F., W. S. Kurth, D. G. Mitchell, (2016), Short periodicities in low-frequency plasma waves at Saturn, Journal of Geophysical Research, 121, 6562–6572, doi: 10.1002/2016JA022732.

Carbary, J. F. and D. G. Mitchell, (2013), Periodicities in Saturn’s magnetosphere, Reviews of Geophysics, 51, 1–30, doi: 10.1002/rog.20006.

Carbary, J. F., D. G. Mitchell, P. C. Brandt, S. M. Krimigis, D. A. Gurnett, (2011), ENA periodicities and their phase relations to SKR emissions at Saturn, Geophysical Research Letters, 38, L16106, doi: 10.1029/2011GL048418.

Carbary, J. F., D. G. Mitchell, S. M. Krimigis, D. A. Gurnett, W. S. Kurth, (2010), Phase relations between energetic neutral atom intensities and kilometric radio emissions at Saturn, Journal of Geophysical Research, 115, A01203, doi: 10.1029/2009JA014519.

Cecconi, B., S. Hess, A. Herique, M. R. Santovito, D. Santos-Costa, P. Zarka, G. Alberti, D. Blankenship, J.-L. Bougeret, L. Bruzzone, W. Kofman, (2012), Natural radio emission of Jupiter as interferences for radar investigations of Icy Satellites of Jupiter, Planetary and Space Science, 61, 32–45, doi: 10.1016/j.pss.2011.06.012.

Cecconi, B., L. Lamy, P. Zarka, R. Prange, W. S. Kurth, P. Louarn, (2009), Goniopolarimetric study of the revolution 29 perikrone using the Cassini Radio and Plasma Wave Science instrument high-frequency radio receiver, Journal of Geophysical Research, 114, A03215, doi: 10.1029/2008JA013830.

Cecconi, B., (2009), Comment on– Spectral features of SKR observed by Cassini/RPWS: Frequency bandwidth, flux density and polarization by Patrick Galopeau et al. 2007, Journal of Geophysical Research, 114, A07206, doi: 10.1029/2007JA012970.

Cecconi, B., (2007), Influence of an extended source on goniopolarimetry (or direction finding) with Cassini and solar terrestrial relations observatory radio receivers, Radio Science, 42, RS2003, doi: 10.1029/2006RS003458.

Cecconi, B., P. Zarka, W. S. Kurth, (2006), SKR polarization and source localization with the Cassini/RPWS/HFR instrument: First results, In Planetary Radio Emissions VI, (eds.) H. O. Rucker, W. S. Kurth, G. Mann, Austrian Academy of Sciences Press, Vienna, Austria, pp. 37–49.

Cecconi, B. and P. Zarka, (2005a), Direction finding and antenna calibration through analytical inversion of radio measurements performed using a system of two or three electric dipole wire antennas on a three-axis stabilized spacecraft, Radio Science, 40, RS3003, doi: 10.1029/2004RS003070.

Cecconi, B. and P. Zarka, (2005b), Model of a variable radio period for Saturn, Journal of Geophysical Research, 110, A12203, doi: 10.1029/2005JA011085.

Cecconi, B., (2004), Étude goniopolarimétrique des émissions radio de Jupiter et Saturne à l'aide du récepteur radio de la sonde Cassini, Ph.D. Thesis, University of Paris, Meudon, France.

Clarke, J. T., J. Nichols, J.-C. Gerard, D. Grodent, K. C. Hansen, W. Kurth, G. R. Gladstone, J. Duval, S. Wannawichian, E. Bunce, S. W. H. Cowley, F. Crary, M. Dougherty, L. Lamy, D. Mitchell, W. Pryor, K. Retherford, T. Stallard, B. Zieger, P. Zarka, B. Cecconi, (2009), The response of Jupiter's and Saturn's auroral activity to the solar wind, Journal of Geophysical Research, 114, A05210, doi: 10.1029/2008JA013694.

Clarke, J. T., J.-C. Gerard, D. Grodent, S. Wannawichian, J. Gustin, J. Connerney, F. Crary, M. Dougherty, W. Kurth, S. W. H. Cowley, E. J. Bunce, T. Hill, J. Kim, (2005), Morphological differences between Saturn's ultraviolet aurorae and those of Earth and Jupiter, Nature, 433, 717–719, doi: 10.1038/nature03331.

Clarke, J. T., D. Grodent, S. W. H. Cowley, E. J. Bunce, P. Zarka, J. E. P. Connerney, T. Satoh, (2004), Jupiter's aurora, In Jupiter: the Planet, Satellites, and Magnetosphere, (eds.) F. Bagenal, W. McKinnon, T. Dowling, Cambridge University Press, Cambridge.

Coates, A. J., A. Wellbrock, G. H. Jones, J. H. Waite, P. Schippers, M. F. Thomsen, C. S. Arridge, R. L. Tokar, (2013), Photoelectrons in the Enceladus plume, Journal of Geophysical Research, 118, 5099–5108, doi: 10.1002/jgra.50495.

Coates, A. J., J.-E. Wahlund, K. Ågren, N. J. T. Edberg, J. Cui, A. Wellbrock, K. Szego, (2011), Recent results from Titan’s ionosphere, Space Science Review, 162, 85–211, doi: 10.1007/s11214-011-9826-4.

Coates, A. J., F. J. Crary, G. R. Lewis, D. T. Young, J. H. Waite, E. C. Sittler Jr., (2007), Discovery of heavy negative ions in Titan's ionosphere, Geophysical Research Letters, 34, L22103, doi: 10.1029/2007GL030978.

Crary, F. J., J. T. Clarke, M. K. Dougherty, P. G. Hanlon, K. C. Hansen, J. T. Steinberg, B. L. Barraclough, A. J. Coates, J.-C. Gerard, D. Grodent, W. S. Kurth, D. G. Mitchell, A. M. Rymer, D. T. Young, (2005), Solar wind dynamic pressure and electric field as the main factors controlling Saturn's aurorae, Nature, 433, 720–722, doi: 10.1038/nature03333.

Cravens, T., L. Moore, H. J. Waite, R. Perryman, M. Perry, J.-E. Wahlund, A. M. Persoon, W. S. Kurth, (2018), The ion composition of Saturn's equatorial ionosphere as observed by Cassini, Geophysical Research Letters 46, no. 12, 6315-6321.

Cravens, T. E., M. Richard, Y. J. Ma, C. Bertucci, J. G. Luhmann, S. Ledvina, I. P. Robertson, J.-E. Wahlund, K. Ågren, J. Cui, I. Müller-Wodarg, J. H. Waite, M. Dougherty, J. Bell, D. Ulusen, (2010), Dynamical and magnetic field time constants for Titan’s ionosphere: Empirical estimates and comparisons with Venus, Journal of Geophysical Research, 115, A08319, doi: 10.1029/2009JA015050.

Cravens, T. E., I. P. Robertson, J. H. Waite, R. V. Yelle, V. Vuitton, A. J. Coates, J.-E. Wahlund, K. Ågren, M. S. Richard, V. de La Haye, A. Wellbrock, F. M. Neubauer, (2009a), Model-data

comparisons for Titan's nightside ionosphere, Icarus, 199, 174–188, doi: 10.1016/j.icarus.2008.09.005.

Cravens, T. E., R. V. Yelle, J.-E. Wahlund, D. E. Shemansky, A. F. Nagy, (2009a), Composition and structure of the ionosphere and thermosphere, In Titan from Cassini-Huygens, (eds.) R. H. Brown, J.-P. Lebreton, J. H. Waite, Springer, Dordrecht, doi: 10.1007/978-1-420-9215-2_11, pp. 259-295.

Cravens, T. E., I. P. Robertson, J. H. Waite, R. V. Yelle, W. T. Kasprzak, C. N. Keller, S. A. Ledvina, H. B. Niemann, J. G. Luhmann, R. L. McNutt, W.-H. Ip, V. De La Haye, I. Mueller-Wodarg, J.-E. Wahlund, V. G. Anicich, V. Vuitton, (2006), Composition of Titan's ionosphere, Geophysical Research Letters, 33, L07105, doi: 10.1029/2005GL025575.

Cravens, T. E., I. P. Robertson, J. Clark, J.-E. Wahlund, J. H. Waite, Jr., S. A. Ledvina, H. B. Niemann, R. V. Yelle, W. T. Kasprzak, J. G. Luhmann, R. L. McNutt, W.-H. Ip, V. De La Haye, I. Muller-Wodarg, D. T. Young, A. J. Coates, (2005), Titan's ionosphere: Model comparisons with Cassini Ta data, Geophysical Research Letters, 32, L12108, doi: 10.1029/2005GL023249.

Cui, J., M. Galand, R. V. Yelle, J.-E. Wahlund, K. Ågren, J. H. Waite, Jr., M. K. Dougherty, (2010), Ion transport in Titan's upper atmosphere, Journal of Geophysical Research, 115, A06314, doi: 10.1029/2009JA014563.

Cui, J., M. Galand, R. V. Yelle, V. Vuitton, J.-E. Wahlund, P. P. Lavvas, I. C. F. Muller-Wodarg, T. E. Cravens, W. T. Kasprzak, J. H. Waite, Jr., (2009), Diurnal variations of Titan's ionosphere, Journal of Geophysical Research, 114, A06310, doi: 10.1029/2009JA014228.

de Pater, I. and W. S. Kurth, (2007), The solar system at radio wavelengths, In Encyclopedia of the Solar System, 2nd Edition, (eds.) L.-A. McFadden, P. Weissman, T. Johnson, Academic Press/Elsevier, San Diego, pp. 695–718.

de Soria-Santacruz, M., Y. Y. Shprits, A. Drozdov, J. D. Menietti, H. B. Garrett, H. Zhu, A. C. Kellerman, R. B. Horne, (2017), Interactions between energetic electrons and realistic whistler mode waves in the Jovian magnetosphere, Journal of Geophysical Research, 122, 5355–5364, doi: 10.1002/2017JA023975.

Desai, R. T., A. J. Coates, A. Wellbrock, V. Vuitton, F. J. Crary, D. Gonzalez-Caniulef, O. Shebanits, G. H. Jones, G. R. Lewis, J. H. Waite, S. A. Taylor, D. O. Kataria, J.-E. Wahlund, N. J. T. Edberg, E. C. Sittler, (2017), Carbon chain anions and the growth of complex organic molecules in Titan's ionosphere, Astrophysical Journal Letters, 844, doi: 10.3847/2041-8212/aa/7851.

Desch, M. D., G. Fischer, M. L. Kaiser, W. M. Farrell, W. S. Kurth, D. A. Gurnett, P. Zarka, A. Lecacheux, C. C. Porco, A. P. Ingersoll, U. Dyudina, (2006), Cassini RPWS and imaging observations of Saturn lightning, In Planetary Radio Emissions VI, (eds.) H. O. Rucker, W. S. Kurth, G. Mann, Austrian Academy of Sciences Press, Vienna, Austria, pp. 103–110.

Desch, M. D. and M. L. Kaiser, (1990), Upper limit set for level of lightning activity on Titan, Nature, 343, 442–444.

Dong, Y., T. W. Hill, S.-Y. Ye, (2015), Characteristics of Ice grains in the Enceladus plume from Cassini observations, Journal of Geophysical Research, 120, 915–937, doi: 10.1002/2014JA020288.

Dougherty, M. K., K. K. Khurana, F. M. Neubauer, C. T. Russell, J. Saur, J. S. Leisner, M. E. Burton, (2006), Identification of a dynamic atmosphere at Enceladus with the Cassini magnetometer, Science, 311, 1406–1409, doi: 10.1126/science.1120985.

Dyudina, U. A., A. P. Ingersoll, S. P. Ewald, C. C. Porco, G. Fischer, Y. Yair, (2013), Saturn's visible lightning, its radio emissions, and the structure of the 2009–2011 lightning storms, Icarus, 225, 1029–1037, doi: 10.1016/j.icarus.2013.07.013.

Dyudina, U. A., A. P. Ingersoll, S. P. Ewald, C. C. Porco, G. Fischer, W. S. Kurth, R. A. West, (2010), Detection of visible lightning on Saturn, Geophysical Research Letters, 37, L09205, doi: 10.1029/2010GL043188.

Dyudina, U. A., A. P. Ingersoll, S. P. Ewald, C. C. Porco, G. Fischer, W. S. Kurth, M. D. Desch, A. Del Genio, J. Barbara, J. Ferrier, (2007), Lightning storms on Saturn observed by Cassini ISS and RPWS during 2004–2006, Icarus, 190, 545–555, doi: 10.1016/j.icarus.2007.03.035.

Edberg, N. J. T., E. Vigren, D. Snowden, L. H. Regoli, O. Shebanits, J.-E. Wahlund, D. J. Andrews, C. Bertucci, J. Cui, (2019), Titan's variable ionosphere during the T118-T119 Cassini flybys, Geophysical Research Letters, 45, 8721–8728, doi: 10.1029/2018GL078436.

Edberg, N. J. T., D. J. Andrews, C. Bertucci, D. A. Gurnett, M. Holmberg, C. M. Jackman, W. S. Kurth, J. D. Menietti, H. Opgenoorth, O. Shebanits, E. Vigren, and J.-E. Wahlund, (2015), Effects of Saturn's magnetospheric dynamics on Titan's ionosphere, Journal of Geophysical Research, 120, 8884–8898, doi: 10.1002/2015JA021373.

Edberg, N. J. T., D. J. Andrews, O. Shebanits, K. Ågren, J.-E. Wahlund, H. J. Opgenoorth, E. Roussos, P. Garnier, T. E. Cravens, S. V. Badman, R. Modolo, C. Bertucci, M. K. Dougherty, (2013a), Extreme densities in Titan's ionosphere during the T85 magnetosheath encounter, Geophysical Research Letters, 40, 1–5, doi: 10.1002/grl.50579.

Edberg, N. J. T., D. J. Andrews, O. Shebanits, K. Ågren, J.-E. Wahlund, H. J. Opgenoorth, T. E. Cravens, Z. Girazian, (2013b), Solar cycle modulation of Titan's ionosphere, Journal of Geophysical Research, 118, 5255–5264, doi: 10.1002/jgra.50463.

Edberg, N. J. T., K. Ågren, J.-E. Wahlund, M. W. Morooka, D. J. Andrews, S. W. H. Cowley, A. Wellbrock, A. J. Coates, C. Bertucci, M. K. Dougherty, (2011), Structured ionospheric outflow during the Cassini T55–T59 Titan flybys, Planetary and Space Science, 59, 788–797, doi: 10.1016/j.pss.2011.03.007.

Edberg, N. J. T., J.-E. Wahlund, K. Ågren, M. W. Morooka, R. Modolo, C. Bertucci, M. K. Dougherty, (2010), Electron density and temperature measurements in the cold plasma environment of Titan: Implications for atmospheric escape, Geophysical Research Letters, 37, L20105, doi: 10.1029/2010GL044544.

Encrenaz, T., J.-P. Bibring, M. Blanc, A. Barucci, F. Roques, P. Zarka, (2004), The solar system, 3rd edition, Astronomy and Astrophysics Library, Springer, Germany.

Engelhardt, I. A. D., J.-E. Wahlund, D. J. Andrews, A. I. Erikkson, S. Ye, W. S. Kurth, D. A. Gurnett, M. W. Morooka, W. M. Farrell, M. K. Dougherty, (2015), Plasma regions, charged dust, and field-aligned currents near Enceladus, Planetary and Space Science, 117, 453–469, doi: 10.1016/j.pss.2015.09.010.

Ergun, R. E., C. W. Carlson, J. P. McFadden, R. J. Strangeway, M. V. Goldman, D. L. Newman, (2003), Fast auroral snapshot satellite observations of very low frequency saucers, 10, 454, doi: 10.1063/1.1530160.

Eriksson, A. I., T. Nilsson, J.-E. Wahlund, (2012), Interpretation of Langmuir probe data obtained close to a spacecraft, In Proceedings of the 39th EPS Conference/16th International Congress on Plasma Physics, (eds.) S. Ratynskaya, L. Blomberg, A. Fasoli, European Physical Society, Stockholm, Sweden, ISBN 2-914771-79-7, vol. 36F, P4.185.

Farrell, W. M., L. Z. Hadid, M. W. Morooka, W. S. Kurth, J.-E. Wahlund, R. J. MacDowall, A. H. Sulaiman, A. M. Persoon, D. A. Gurnett, (2018), Saturn's plasma density depletions along magnetic field lines connected to the main rings, Geophys. Res. Lett., 45, 8104–8110, doi: 10.1029/2018GL078137.

Farrell, W. M., J.-E. Wahlund, M. Morooka, W. S. Kurth, D. A. Gurnett, R. J. MacDowall, (2017a), Ion trapping to dust grains: Simulation applications to the Enceladus plume, Journal of Geophysical Research: Planets, 122, Issue 4, 729–743, doi: 10.1002/2016JE005235.

Farrell, W. M., W. S. Kurth, D. A. Gurnett, A. M. Persoon, R. J. MacDowall, (2017b), Saturn's rings and associated ring plasma cavity: Evidence for slow ring erosion, Icarus, 292, 48–52, doi: 10.1016/j.icarus.2017.03.022.

Farrell, W. M., J.-E. Wahlund, M. Morooka, D. A. Gurnett, W. S. Kurth, R. J. MacDowall, (2014), An estimate of dust pickup current at Enceladus, Icarus, 239, 217–221, doi: 10.1016/j.icarus.2014.05.034.

Farrell, W. M., J.-E. Wahlund, M. Morooka, D. A. Gurnett, W. S. Kurth, R. J. MacDowall, (2012), The electromagnetic pickup of submicron-sized dust above Enceladus' northern hemisphere, Icarus, 219, 498–501, doi: 10.1016/j.icarus.2012.02.033.

Farrell, W. M., W. S. Kurth, R. L. Tokar, J.-E. Wahlund, D. A. Gurnett, Z. Wang, R. J. MacDowall, M. W. Morooka, R. E. Johnson, J. H. Waite, Jr., (2010), Modification of the plasma in the near-vicinity of Enceladus by the enveloping dust, Geophysical Research Letters, 37, L20202, doi: 10.1029/2010GL044768.

Farrell, W. M., W. S. Kurth, D. A. Gurnett, R. E. Johnson, M. L. Kaiser, J.-E. Wahlund, J. H. Waite, Jr., (2009), Electron density dropout near Enceladus in the context of water-vapor and water-ice, Geophysical Research Letters, 36, L10203, doi: 10.1029/2008GL037108.

Farrell, W. M., M. L. Kaiser, D. A. Gurnett, W. S. Kurth, A. M. Persoon, J.-E. Wahlund, P. Canu, (2008), Mass unloading along the inner edge of the Enceladus Plasma torus, Geophysical Research Letters, 35, L02203, doi: 10.1029/2007GL032306.

Farrell, W. M., M. L. Kaiser, G. Fischer, P. Zarka, W. S. Kurth, D. A. Gurnett, (2007), Are Saturn electrostatic discharges really superbolts? A temporal dilemma, Geophysical Research Letters, 34, L06202, doi: 10.1029/2006GL028841.

Farrell, W. M., M. D. Desch, M. L. Kaiser, W. S. Kurth, D. A. Gurnett, (2006), Changing Electrical nature of Saturn's rings: Implications for spoke formation, Geophysical Research Letters, 33, L07203, doi: 10.1029/2005GL024922.

Farrell, W. M., M. D. Desch, M. L. Kaiser, A. Lecacheux, W. S. Kurth, D. A. Gurnett, B. Cecconi, P. Zarka, (2005a), A nightside source of Saturn's kilometric radiation: Evidence for an inner magnetosphere energy driver, Geophysical Research Letters, 32, L18107, doi: 10.1029/2005GL023449.

Farrell, W. M., W. S. Kurth, M. L. Kaiser, M. D. Desch, D. A. Gurnett, P. Canu, (2005b), Narrowband Z-mode emissions interior to Saturn's plasma torus, Journal of Geophysical Research, 110, A10204, doi: 10.1029/2005JA011102.

Farrell, W. M., M. L. Kaiser, W. S. Kurth, M. D. Desch, D. A. Gurnett, G. B. Hospodarsky, R. J. MacDowall, (2004), Remote sensing of possible plasma density bubbles in the inner Jovian dayside magnetosphere, Journal of Geophysical Research, 109, A09S14, doi: 10.1029/2003JA010130.

Farrell, W. M., D. A. Gurnett, D. L. Kirchner, W. S. Kurth, L. J. C. Woolliscroft, (1993), Data compression for the Cassini Radio and Plasma Wave experiment, 1993 Space and Earth Science Data Compression Workshop, NASA Conference Publication 3183, p. 111, Snowbird, UT.

Felici, M., C. S. Arridge, A. J. Coates, S. V. Badman, M. K. Dougherty, C. M. Jackman, W. S. Kurth, H. Melin, D. G. Mitchell, D. B. Reisenfeld, N. Sergis, (2016), Cassini observations of ionospheric plasma in Saturn's magnetotail lobes, Journal of Geophysical Research, 121, 338–357, doi: 10.1002/2001JA021648.

Feyerabend, M., S. Simon, F. M. Neubauer, U. Motschmann, C. Bertucci, N. J. T. Edberg, G. B. Hospodarsky, W. S. Kurth, (2016), Hybrid simulation of Titan's interaction with the supersonic solar wind during Cassini's T96 flyby, Geophysical Research Letters, 43, 35–42, doi: 10.1002/2015GL066848.

Fischer, G. J. P. Pagaran, P. Zarka, M. Delcroix, U. A. Dyudina, W. S. Kurth, D. A. Gurnett, (2018), Analysis of a long-lived, two-cell lightning storm on Saturn, Astronomy & Astrophysics, 621, A113, doi:10.1051/0004-6361/201833014.

Fischer, G., D. A. Gurnett, W. S. Kurth, S.-Y. Ye, J. B. Groene, (2015), Saturn kilometric radiation periodicity after equinox, Icarus, 254, 72–91, doi: 10.1016/icarus.2015.03.014.

Fischer, G., (2015), Im Kontext: Blitze am Saturn, In Physik fuer Wissenschaftler und Ingenieure (7. Auflage), (eds.) P. A. Tipler, G. Mosca, J. Wagner, Springer-Verlag, Berlin-Heidelberg, pp. 752–753.

Fischer, G., W. Macher, M. Panchenko, (2014a), Space-based radio observations of Saturn at IWF, In Planetary Radio Emissions 7.5, Planetary Retirement Edition, (eds.) N. I. Kömle, G. Fischer, W. Macher, Living Edition Publishers, Pöllauberg, pp. 55–70.

Fischer, G., S.-Y. Ye, J. B. Groene, A. P. Ingersoll, K. Sayanagi, J. D. Menietti, W. S. Kurth, D. A. Gurnett, (2014b), A possible influence of the Great White Spot on Saturn kilometric radiation periodicity, Annales Geophysicae, 32, 1463–1476, doi: 10.5194/angeo-32-1463-2014.

Fischer, G., D. A. Gurnett, Y. Yair, (2011a), Extraterrestrial lightning and its past and future investigation, lightning; properties, formation and types, (eds.) M. D. Wood, NOVA Science Publishers, Inc., New York.

Fischer, G., D. A. Gurnett, P. Zarka, L. Moore, U. Dyudina, (2011b), Peak electron densities in Saturn's ionosphere derived from the low-frequency cutoff of Saturn lightning, Journal of Geophysical Research, 116, A04315, doi: 10.1029/2010JA016187.

Fischer, G., W. S. Kurth, D. A. Gurnett, P. Zarka, U. A. Dyudina, A. P. Ingersoll, S. P. Ewald, C. C. Porco, A. Wesley, C. Go, M. Delcroix, (2011c), A giant thunderstorm on Saturn, Nature, 475, 75–77, doi: 10.1038/nature10205.

Fischer, G., U. A. Dyudina, W. S. Kurth, D. A. Gurnett, P. Zarka, T. Barry, M. Delcroix, C. Go, D. Peach, R. Vandebergh, A. Wesley, (2011d), Overview of Saturn lightning observations, In Planetary Radio Emissions VII, (eds.) H. O. Rucker, W. S. Kurth, P. Louarn, G. Fischer, Austrian Academy of Sciences, Vienna, Austria, pp. 135–144.

Fischer, G. and D. A. Gurnett, (2011), The search for Titan lightning radio emissions, Geophysical Research Letters, 38, L08206, doi: 10.1029/2011GL047316.

Fischer, G., B. Cecconi, L. Lamy, S. Ye, U. Taubenschuss, W. Macher, P. Zarka, W. S. Kurth, D. A. Gurnett, (2009), Elliptical polarization of Saturn Kilometric radiation observed from high latitudes, Journal of Geophysical Research, 114, A08216, doi: 10.1029/2009JA014176.

Fischer, G., D. A. Gurnett, W. S. Kurth, F. Akalin, P. Zarka, U. A. Dyudina, W. M. Farrell, M. L. Kaiser, (2008), Atmospheric electricity at Saturn, Space Science Reviews, 137, 271–285, doi: 10.1007/s11214-008-9370-z.

Fischer, G., W. S. Kurth, U. A. Dyudina, M. L. Kaiser, P. Zarka, A. Lecacheux, A. P. Ingersoll, D. A. Gurnett, (2007a), Analysis of a giant lightning storm on Saturn, Icarus, 190, 528–544, doi: 10.1016/j.icarus.2007.04.002.

Fischer, G., D. A. Gurnett, W. S. Kurth, W. M Farrell, M. L. Kaiser, P. Zarka, (2007b), Nondetection of Titan lightning radio emissions with Cassini/RPWS after 35 close Titan flybys, Geophysical Research Letters, 34, L22104, doi: 10.1029/2007GL031668.

Fischer, G., D. A. Gurnett, A. Lecacheux, W. Macher, and W. S. Kurth, (2007c), Polarization measurements of Saturn electrostatic discharges with Cassini/RPWS below a frequency of 2 MHz, Journal of Geophysical Research, 112, A12308, doi: 10.1029/2007JA012592.

Fischer, G., M. D. Desch, P. Zarka, M. L. Kaiser, D. A. Gurnett, W. S. Kurth, W. Macher, H. O. Rucker, A. Lecacheux, W. M. Farrell, B. Cecconi, (2006a), Saturn lightning recorded by Cassini/RPWS in 2004, Icarus, 183, 1, 135–152, doi: 10.1016/j.icarus.2006.02.010.

Fischer, G., W. Macher, M. D. Desch, M. L. Kaiser, P. Zarka, W. S. Kurth, W. M. Farrell, A. Lecacheux, B. Cecconi, D. A. Gurnett, (2006b), On the intensity of Saturn lightning, In Planetary Radio Emissions VI, (eds.) H. O. Rucker, W. S. Kurth, G. Mann, Austrian Academy of Sciences Press, Vienna, Austria, pp. 123–132.

Fischer, G., W. Macher, D. A. Gurnett, M. D. Desch, A. Lecacheux, P. Zarka, W. S. Kurth, M L. Kaiser, (2006c), The discrimination between Jovian radio emissions and Saturn electrostatic discharges, Geophysical Research Letters, 33, L21201, doi: 10.1029/2006GL026766.

Fischer, G. and H. O. Rucker, (2006), Man-made radio emissions recorded by Cassini/RPWS during Earth flyby, In Planetary Radio Emissions VI, (eds.) H. O. Rucker, W. S. Kurth, G. Mann, Austrian Academy of Sciences Press, Vienna, Austria, pp. 299–306.

Fischer, G., (2004), Energy dissipation and HF radiation of lightning on Titan and Earth, Ph.D. Thesis, Karl-Franzens Universitat, Graz, Austria.

Fischer, G., T. Tokano, W. Macher, H. Lammer, H. O. Rucker, (2004), Energy dissipation of possible Titan lightning strokes, Planetary and Space Science, 52, 447–458.

Fischer, G., W. Macher, H. O. Rucker, H. P. Ladreiter, D. F. Vogl, Cassini RPWS Team, (2001), Wire-grid modeling of Cassini spacecraft of the determination of effective antenna length vectors of the RPWS antennas, In Planetary Radio Emissions V, (eds.) H. O. Rucker, M. L. Kaiser, Y. Leblanc, Austrian Academy of Sciences Press, Vienna, Austria, pp. 347–356.

Fletcher, L. N., B. E. Hesman, R. K. Achterberg, P. G. J. Irwin, G. Bjoraker, N. Gorius, J. Hurley, J. Sinclair, G. S. Orton, J. Legarreta, E. Garcia-Melendo, A. Sanchez-Lavega, P. L. Read, A. A. Simon-Miller, F. M. Flasar, (2012), The origin and evolution of Saturn’s 2011–2012 Stratospheric Vortex, Icarus, 221, 560–586.

Galand, M., A. J. Coates, T. E. Cravens, J.-E. Wahlund, (2013), Titan's ionosphere, In Titan – Interior, surface, atmosphere and space environment, (eds.) I. C. F. Müller-Wodarg, C. A. Griffith, E. Lellouch, T. E. Cravens, Cambridge University Press, Cambridge.

Galand, M., R. Yelle, J. Cui, J.-E. Wahlund, V. Vuitton, A. Wellbrock, A. Coates, (2010), Ionization sources in Titan's deep ionosphere, Journal of Geophysical Research, 115, A07312, doi: 10.1029/2009JA015100.

Galand, M., R. V. Yelle, A. J. Coates, H. Backes, J.-E. Wahlund, (2006), Electron temperature of Titan's sunlit ionosphere, Geophysical Research Letters, 33, L21101, doi: 10.1029/2006GL027488.

Galopeau, P. H. M., M. Y. Boudjada, A. Lecacheux, (2009), Reply to– Comment by B. Cecconi on– Spectral features of SKR observed by Cassini/RPWS: Frequency bandwidth, flux density and polarization, Journal of Geophysical Research, 114, A07207, doi: 10.1029/2008JA013177.

Galopeau, P. H. M., M. Y. Boudjada, A. Lecacheux, (2007), Spectral features of SKR observed by Cassini/RPWS: Frequency bandwidth, flux density and polarization, Journal of Geophysical Research, 112, A11213, doi: 10.1029/2007JA012573.

Garnier, P., M. K. G. Holmberg, J.-E. Wahlund, G. R. Lewis, P. Schippers, A. Coates, D. A. Gurnett, J. H. Waite, I. Dandouras, (2014), Deriving the characteristics of warm electrons (100 - 500 eV) in the magnetosphere of Saturn with the Cassini Langmuir probe, Planetary and Space Science, 104, 173–184, doi: 10.1016/j.pss.2014.09.008.

Garnier, P., M. Holmberg, J.-E. Wahlund, G. Lewis, S. R. Grimald, M. Thomsen, D. A. Gurnett, A. J. Coates, F. Crary, I. Dandouras, (2013), The influence of the secondary electrons induced by energetic electrons impacting the Cassini Langmuir probe at Saturn, Journal of Geophysical Research, 118, 7054–7073, doi: 10.1002/2013JA019114.

Garnier, P., J.-E. Wahlund, M. K. G. Holmberg, M. Morooka, S. Grimald, A. Eriksson, P. Schippers, D. A. Gurnett, S. M. Krimigis, N. Krupp, A. J. Coates, F. Crary, G. Gustafsson, (2012), The detection of energetic electrons with the Cassini Langmuir probe at Saturn, Journal of Geophysical Research, 117, A10292, doi: 10.1029/2011JA017298.

Garnier, P., I. Dandouras, D. Toublanc, E. C. Roelof, P. C. Brandt, D. G. Mitchell, S. M. Krimigis, N. Krupp, D. C. Hamilton, J.-E. Wahlund, (2010), Statistical analysis of the energetic ion and ENA data for the Titan environment, Planetary and Space Science, 58, 1811–1822, doi: 10.1016/j.pss.2010.08.009.

Garnier, P., J.-E. Wahlund, L. Rosenqvist, R. Modolo, K. Ågren, N. Sergis, P. Canu, M. Andre, D. A. Gurnett, W. S. Kurth, S. M. Krimigis, A. J. Coates, M. K. Dougherty, J. H. Waite, (2009), Titan's ionosphere in the magnetosheath: Cassini RPWS results during the T32 flyby, Annales Geophysicae, 27, 4257–4272, doi: 10.5194/angeo-27-4257-2009.

Garnier, P., I. Dandouras, D. Toublanc, E. C. Roelof, P. C. Brandt, D. G. Mitchell, S. M. Krimigis, N. Krupp, D. C. Hamilton, O. Dutuit, J.-E. Wahlund, (2008), The lower exosphere of Titan: Energetic neutral atoms absorption and imaging, Journal of Geophysical Research, 113, A10216, doi: 10.1029/2008JA013029.

Gautier, A. L., B. Cecconi, P. Zarka, G. Fischer, (2011), Propagation of Saturn's radio lightning studied by three-dimensional ray tracing, In EPSC-DPS Joint Meeting, p. 917.

Gérard, J.-C., D. Grodent, S. W. H. Cowley, D. G. Mitchell, W. S. Kurth, J. T. Clarke, E. J. Bunce, J. D. Nichols, M. K. Dougherty, F. J. Crary, A. J. Coates, (2006), Saturn's auroral morphology and activity during quiet magnetospheric conditions, Journal of Geophysical Research, 111, A12210, doi: 10.1029/2006JA011965.

Goertz, C. K., (1989), Dusty plasmas in the solar system, Reviews of Geophysics, 27, 271–292.

Gombosi, T. I., T. P. Armstrong, C. S. Arridge, K. K. Khurana, S. M. Krimigis, N. Krupp, A. M. Persoon, M. F. Thomsen, (2009), Saturn's magnetospheric configuration, In Saturn from Cassini-Huygens, (eds.) M. K. Dougherty, L. W. Esposito, S. M. Krimigis, Springer, Dordrecht, pp. 203–255, doi: 10.1007/978-1-4020-9217-6_9.

Grün, E., C. K. Goertz, G. E. Morfill, O. Havnes, (1992), Statistics of Saturn's spokes, Icarus, 99, 191–201.

Gu, X., R. M. Thorne, B. Ni, S.-Y. Ye, (2013), Resonant diffusion of energetic electrons by narrowband Z mode waves in Saturn's inner magnetosphere, Geophysical Research Letters, 40, 255–261, doi: 10.1029/2012GL054330.

Gurnett, D. A. and A. Bhattacharjee, (2017), Introduction to plasma physics with space, laboratory, and astrophysical applications, 2nd Edition, Cambridge University Press, Cambridge, UK.

Gurnett, D. A. and W. R. Pryor, (2012), Auroral processes associated with Saturn's moon Enceladus, In Auroral phenomenology and magnetospheric processes: Earth and other planets, (eds.) A. Keiling, E. Donovan, F. Bagenal, T. Karlsson, American Geophysical Union Geophysical Monograph Series, Washington DC, vol. 197, pp. 305–313, doi: 10.1029/2011BK001174.

Gurnett, D. A., T. F. Averkamp, P. Schippers, A. M. Persoon, G. B. Hospodarsky, J. S. Leisner, W. S. Kurth, G. H. Jones, A. J. Coates, F. J. Crary, M. K. Dougherty, (2011a), Auroral hiss, electron beams and standing Alfven wave currents near Saturn's moon Enceladus, Geophysical Research Letters, 38, L06102, doi: 10.1029/2011GL046854.

Gurnett, D. A., J. B. Groene, T. F. Averkamp, W. S. Kurth, S.-Y. Ye, G. Fischer, (2011b), A SLS4 longitude system based on a tracking filter analysis of the rotational modulation of Saturn kilometric radiation, In Planetary Radio Emissions VII, (eds.) H. O. Rucker, W. S. Kurth, P. Louarn, G. Fischer, Austrian Academy of Sciences, Vienna, Austria, pp. 51–63.

Gurnett, D. A., A. M. Persoon, J. B. Groene, W. S. Kurth, M. Morooka, J.-E. Wahlund, J. D. Nichols, (2011c), The rotation of the plasmapause-like boundary at high latitudes in Saturn's magnetosphere and its relation to the eccentric rotation of the northern and southern auroral ovals, Geophysical Research Letters, 38, L21203, doi: 10.1029/2011GL049547.

Gurnett, D. A., (2011), An overview of the time-dependent rotational modulation of Saturnian radio emissions, abstract, In Planetary Radio Emissions VII, (eds.) H. O. Rucker, W. S. Kurth, P. Louarn, G. Fischer, Austrian Academy of Sciences, Vienna, Austria, p. 37.

Gurnett, D. A., A. M. Persoon, A. J. Kopf, W. S. Kurth, M. W. Morooka, J.-E. Wahlund, K. K. Khurana, M. K. Dougherty, D. G. Mitchell, S. M. Krimigis, N. Krupp, (2010a), A plasmapause-like density boundary at high latitudes in Saturn's magnetosphere, Geophysical Research Letters, 37, L16806, doi: 10.1029/2010GL044466.

Gurnett, D. A., J. B. Groene, A. M. Persoon, J. D. Menietti, S.-Y. Ye, W. S. Kurth, R. J. MacDowall, A. Lecacheux, (2010b), The reversal of the rotational modulation rates of the north and south components of Saturn kilometric radiation near equinox, Geophysical Research Letters, 37, L24101, doi: 10.1029/2010GL045796.

Gurnett, D. A., A. Lecacheux, W. S. Kurth, A. M. Persoon, J. B. Groene, L. Lamy, P. Zarka, J. F. Carbary, (2009a), Discovery of a north-south asymmetry in Saturn's radio rotation period, Geophysical Research Letters, 36, L16102, doi: 10.1029/2009GL039621.

Gurnett, D. A., A. M. Persoon, J. B. Groene, A. J. Kopf, G. B. Hospodarsky, W. S. Kurth, (2009b), A north-south difference in the rotation rate of auroral hiss at Saturn: Comparison to Saturn's kilometric radio emission, Geophysical Research Letters, 36, L21108, doi: 10.1029/2009GL040774.

Gurnett, D. A., (2009), The search for life in the solar system, Transactions of the American Clinical and Climatological Association, 120, 299–325, doi: PMCID:PMC2744519.

Gurnett, D. A., A. M. Persoon, W. S. Kurth, J. B. Groene, T. F. Averkamp, M. K. Dougherty, D. J. Southwood (2007), The variable rotation period of the inner region of Saturn's plasma disk, Science, 316, No. 5823, 442–445, doi: 10.1016/science.1138562.

Gurnett, D. A., W. S. Kurth, G. B. Hospodarsky, A. M. Persoon, T. F. Averkamp, B. Cecconi, A. Lecacheux, P. Zarka, P. Canu, N. Cornilleau-Wehrlin, P. Galopeau, A. Roux, C. Harvey, P. Louarn, R. Bostrom, G. Gustafsson, J.-E. Wahlund, M. D. Desch, W. M. Farrell, M. L. Kaiser, K. Goetz, P. J. Kellogg, G. Fischer, H.-P. Ladreiter, H. Rucker, H. Alleyne, A. Pedersen, (2005), Radio and plasma wave observations at Saturn from Cassini's approach and first orbit, Science, 307, 1255–1259, doi: 10.1126/science.1105356.

Gurnett, D. A., W. S. Kurth, D. L. Kirchner, G. B. Hospodarsky, T. F. Averkamp, P. Zarka, A. Lecacheux, R. Manning, A. Roux, P. Canu, N. Cornilleau-Wehrlin, P. Galopeau, A. Meyer, R. Bostrom, G. Gustafsson, J.-E. Wahlund, L. Aahlen, H. O. Rucker, H. P. Ladreiter, W. Macher, L. J. C. Woolliscroft, H. Alleyne, M. L. Kaiser, M. D. Desch, W. M. Farrell, C. C. Harvey, P. Louarn, P. J. Kellogg, K. Goetz, A. Pedersen, (2004), The Cassini radio and plasma wave science investigation, Space Science Reviews, 114, 395–463, doi: 10.1007/s11214-004-1434-0.

Gurnett, D. A., W. S. Kurth, G. B. Hospodarsky, A. M. Persoon, P. Zarka, A. Lecacheux, S. J. Bolton, M. D. Desch, W. M. Farrell, M. L. Kaiser, H.-P. Ladreiter, H. O. Rucker, P. Galopeau, P. Louarn, D. T. Young, W. R. Pryor, M. K. Dougherty, (2002), Control of Jupiter's radio emission and aurorae by the solar wind, Nature, 415, 985–987, doi: 10.1038/415985a.

Gurnett, D. A., P. Zarka, R. Manning, W. S. Kurth, G. B. Hospodarsky, T. F. Averkamp, M. L. Kaiser, W. M. Farrell, (2001), Non-detection at Venus of high-frequency radio signals characteristic of terrestrial lightning, Nature, 409, 313–315, doi: doi: 10.1038/35053009.

Gustafsson, G. and J.-E. Wahlund, (2010), Electron temperatures in Saturn's plasma disc, Planetary and Space Science, 58, 1018–1025, doi: 10.1016/j.psss.2010.03.007.

Gustin, J., J.-C. Gerard, D. Grodent, G. R. Gladstone, J. T. Clarke, W. R. Pryor, V. Dols, B. Bonfond, A. Radioti, L. Lamy, J. M. Ajello, (2013), effects of methane on giant planet's UV emissions and implications for the auroral characteristics, Journal of Molecular Spectroscopy, 291, 108–117, doi: 10.1016/j.jms.2013.03.010.

Guzman, M., R. Lorenz, D. Hurley, W. Farrell, J. Spencer, C. Hansen, T. Hurford, J. Ibea, P. Carlson, C. P. McKay, (2018), Collecting amino acids in the Enceladus plume, International Journal of Astrobiology, 18, 47–59, doi: 10.1017/S1473550417000544.

Hadid, L. Z., M. W. Morooka, J.-E. Wahlund, A. M. Persoon, D. Andrews, O. Shebanits, W. S. Kurth, E. Vigren, N. J. T. Edberg, A. F. Nagy, A. I. Ericksson, (2018), Saturn's Ionosphere: Electron Density Altitude Profiles and D-ring Interaction from the Cassini Grand Finale, Geophysical Research Letters, vol. 46, Issue 15, pp. 9362–9369, doi: 10.1029/2018GL078004.

Hadid, L. Z., M. W. Morooka, J.-E. Wahlund, L. Moore, T. E. Cravens, M. M. Hedman, N. J. T. Edberg, E. Vigren, J. H. Waite, R. Perryman, W. S. Kurth, W. M. Farrell, A. I. Eriksson, (2018), Ring shadowing effects on Saturn's ionosphere: Implications for ring opacity and plasma transport, Geophysical Research Letters, 45, 10084–10184, doi: 10.1029/2018GL079150.

Hadid, L., (2017), In-situ observations of compressible turbulence in planetary magnetosheaths and solar wind, Ph.D. Thesis, University of Paris-Saclay, France.

Hamilton, D. P., (1993), Motion of dust in a planetary magnetosphere - orbit-averaged equations for oblateness, electromagnetic, and radiation forces with application to Saturn's E ring, Icarus, 101, 244–264.

Hansen, K. C., A. J. Ridley, G. B. Hospodarsky, M. K. Dougherty, T. I. Gombosi, G. Toth, (2005), Global MHD simulations of Saturn's magnetosphere at the time of Cassini approach, Geophysical Research Letters, 32, L20S06, doi: 10.1029/2005GL022835.

Hedman, M. M., J. A. Burns, D. P. Hamilton, M. R. Showalter, (2012), The Three-dimensional structure of Saturn's E ring, Icarus, 217, 322–338, doi: 10.1016/j.icarus.2011.11.006.

Hedman, M. M., J. A. Burns, M. S. Tiscareno, C. C. Porco, G. Jones, E. Roussos, N. Krupp, C. Paranicas, S. Kempf, (2007), The source of Saturn’s G ring, Science, 317, 653, doi: 10.1126/science.1143964.

Hess, S., E. Echer, P. Zarka, L. Lamy, P. Delamere, (2014), Multi-instrument study of the Jovian radio emissions triggered by solar wind shocks and inferred magnetospheric subcorotation rates, Planetary and Space Science, 99, 136–148, doi: 10.1016/j.pss.2014.05.015.

Hess, S., B. Cecconi, P. Zarka, (2008), Modeling of Io-Jupiter decameter arcs, emission beaming and energy source, Geophysical Research Letters, 35, 13, doi: 10.1029/2008GL033656.

Hill, T. W., M. F. Thomsen, R. L. Tokar, A. J. Coates, G. R. Lewis, D. T. Young, F. J. Crary, et al., 92012), Charged nanograins in the Enceladus plume, Journal of Geophysical Research: Space Physics, 117, no. A5 (2012).

Hill, T. W., M. F. Thomsen, R. L. Tokar, A. J. Coates, G. R. Lewis, D. T. Young, F. J. Crary, R. A. Baragiola, R. E. Johnson, Y. Dong, R. J. Wilson, G. H. Jones, J.-E. Wahlund, D. G. Mitchell, M. Horányi, (2011), Charged nanograins in the Enceladus plume, Journal of Geophysical Research, vol. 117, Issue A5, doi: 10.1029/2011JA017218.

Holmberg, M. K. G., O. Shebanits, J.-E. Wahlund, M. W. Morooka, E. Vigren, N. André, P. Garnier, A. M. Persoon, V. Génot, L. K. Gilbert, (2017), Density structures, dynamics, and seasonal and solar cycle modulations of Saturn's inner plasma disk, Journal of Geophysical Research, 122, 12258–12273, doi: 10.1002/2017JA024311.

Holmberg, M. K. G., J.-E. Wahlund, E. Vigren, T. A. Cassidy, D. J. Andrews, (2016), Transport and chemical loss rates in Saturn's inner plasma disk, Journal of Geophysical Research, 121, 2321–2334, doi: 10.1002/2015JA021784.

Holmberg, M. K. G., J.-E. Wahlund, M. W. Morooka, (2014), Dayside/nightside asymmetry of ion densities and velocities in Saturn's inner magnetosphere, Geophysical Research Letters, 41, 3717–3723, doi: 10.1002/2014GL060229.

Holmberg, M. K. G., J.-E. Wahlund, M. W. Morooka, A. M. Persoon, (2012), Ion densities and velocities in the inner plasma torus of Saturn, Planetary and Space Science, 73, 151–160, doi: 10.1016/j.pss.2012.09.016.

Holmberg, M. K. G., (2013), On the structure and dynamics of Saturn's inner plasma disk, Licentiate Thesis (Ph.D.), Uppsala University, Uppsala, Sweden.

Holmberg, M. K. G., (2010), Determination of solar EUV intensity and ion flux from Langmuir probe current characteristics, M.S. Thesis, Uppsala University, Uppsala, Sweden.

Horányi, M., (1996), Charged dust dynamics in the solar system, Annual Review of Astronomy and Astrophysics, 34, 383–418, doi: 10.1146/annurev.astro.34.1.383.

Hospodarsky, G. B., J. D. Menietti, D. Píša, W. S. Kurth, D. A. Gurnett, A. M. Persoon, J. Leisner, T. F. Averkamp, (2016), Plasma wave observations with Cassini at Saturn, Chapter 22, In Magnetosphere-Ionosphere Coupling in the Solar System, (eds.) C. R. Chappell, R. W. Schunk, P. M. Banks, J. L. Burch, R. M. Thorne, Wiley & Sons, Inc., pp. 277–289, doi: 10.1002/9781119066880.

Hospodarsky, G. B., J. S. Leisner, K. Sigsbee, J. D. Menietti, W. S. Kurth, D. A. Gurnett, C. A. Kletzing, O. Santolik, (2012), Plasma wave observations at Earth, Jupiter, and Saturn, In Dynamics of Earth's Radiation Belts and Inner Magnetosphere, (eds.) D. Summers, I. R. Mann, D. N. Baker, M. Schulz, American Geophysical Union Geophysical Monograph Series, Washington DC, vol. 199, pp. 415–430, doi: 10.1029/2012GM001342.

Hospodarsky, G. B., T. F. Averkamp, W. S. Kurth, D. A. Gurnett, M. K. Dougherty, O. Santolik, (2011), Observations of chorus at Saturn by Cassini (abstract), In Planetary Radio Emissions VII, (eds.) H. O. Rucker, W. S. Kurth, P. Louarn, G. Fischer, Austrian Academy of Sciences, Vienna, Austria, pp. 127.

Hospodarsky, G. B., T. F. Averkamp, W. S. Kurth, D. A. Gurnett, J. D. Menietti, O. Santolik, M. K. Dougherty, (2008), Observations of chorus at Saturn using the Cassini Radio and Plasma Wave Science Instrument, Journal of Geophysical Research, 113, A12206, doi: 10.1029/2008JA013237.

Hospodarsky, G. B., W. S. Kurth, D. A. Gurnett, P. Zarka, P. Canu, M. Dougherty, G. H. Jones, A. Coates, A. Rymer, (2006), Observations of Langmuir waves detected by the Cassini spacecraft, In Planetary Radio Emissions VI, (eds.) H. O. Rucker, W. S. Kurth, G. Mann, Austrian Academy of Sciences Press, Vienna, Austria, pp. 67–79.

Hospodarsky, G. B., W. S. Kurth, B. Cecconi, D. A. Gurnett, M. L. Kaiser, M. D. Desch, P. Zarka, (2004), Simultaneous observations of Jovian quasi-periodic radio emissions by the Galileo and

Cassini spacecraft, Journal of Geophysical Research, 109, A09S07, doi: 10.1029/2003JA010263.

Hospodarsky, G. B., I. W. Christopher, J. D. Menietti, W. S. Kurth, D. A. Gurnett, T. F. Averkamp, J. B. Groene, P. Zarka, (2001a), Control of Jovian radio emissions by the Galilean moons as observed by Cassini and Galileo, In Planetary Radio Emissions V, (eds.) H. O. Rucker, M. L. Kaiser, Y. Leblanc, Austrian Academy of Sciences Press, Vienna, Austria, pp. 155–164.

Hospodarsky, G. B., T. F. Averkamp, W. S. Kurth, D. A. Gurnett, M. Dougherty, U. Inan, T. Wood, (2001b), Wave normal and poynting vector calculations using the Cassini Radio and Plasma Wave instrument, Journal of Geophysical Research, 106, 30253–30269, doi: 10.1029/10.1029/2001JA900114.

Hsu, H.-W., J. Schmidt, S. Kempf, F. Postberg, G. Moragas-Klostermeyer, M. Seiss, H. Hoffmann, M. Burton, S.-Y. Ye, W. S. Kurth, M. Horanyi, N. Khawaja, F. Spahn, D. Schirdewahn, J. O'Donoghue, L. Moore, J. Cuzzi, G. H. Jones, R. Srama, (2018), In situ collection of dust grains falling from Saturn's rings into its atmosphere, Science, 362, Issue 6410, eaat3185, doi: 10/1126/science.aat3195.

Hsu, H.-W., S. Kempf, S. V. Badman, W. S. Kurth, F. Postberg, R. Srama, (2016), Interplanetary magnetic field structure at Saturn inferred from nanodust measurements during the 2013 auroral campaign, Icarus, 263, 10–16, doi: 10.1016/j.icarus.2015.02.022.

Imai, M., (2016), Characteristics of Jovian low-frequency radio emissions during the Cassini and Voyager flyby of Jupiter, Ph.D. Thesis, Kyoto University, Kyoto, Japan.

Imai, M., A. Lecacheux, M. Moncuquet, F. Bagenal, C. A. Higgins, K. Imai, J. R. Thieman, (2015), Modeling Jovian hectometric attenuation lanes during the Cassini flyby of Jupiter, Journal of Geophysical Research, 120, 1888–1907, doi: 10.1002/2014JA020815.

Imai, M., A. Lecacheux, K. Imai, C. A. Higgins, J. R. Thieman, (2011a), Jupiter's decametric and hectomectric radio emissions observed by Voyager PRA and Cassini RPWS, In Planetary Radio Emissions VII, (eds.) H. O. Rucker, W. S. Kurth, P. Louarn, G. Fischer, Austrian Academy of Sciences, Vienna, Austria, pp. 167–176.

Imai, M., K. Imai, C. A. Higgins, J. R. Thieman, (2011b), Comparison between Cassini and Voyager observations of Jupiter’s decametric and hectometric radio emissions, Journal of Geophysical Research, 116, A12233, doi: 10.1029/2011JA016456.

Imai, M., K. Imai, C. A. Higgins, J. R. Thieman, (2008), Angular beaming model of Jupiter's decametric radio emissions based on Cassini RPWS data analysis, Geophysical Research Letters, 35, L17103, doi: 10.1029/2008GL034987.

Jackman, C. M., M. F. Thomsen, D. G. Mitchell, N. Sergis, C. S. Arridge, M. Felici, S. V. Badman, C. Paranicas, X. Jia, G. B. Hospodarsky, M. Andriopoulou, K. K. Khurana, A. W. Smith, M. K. Dougherty, (2015), Field depolarization in Saturn’s magnetotail with planetward ion flows and energetic particle flow bursts: Evidence of quasi-steady connection, Journal of Geophysical Research, 120, 3603–3617, doi: 10.1002/2015JA020995.

Jackman, C. M., C. S. Arridge, J. A. Slavin, S. E. Milan, L. Lamy, M. K. Dougherty, A. J. Coates, (2010), In situ observations of the effect of a solar wind compression on Saturn's magnetotail, Journal of Geophysical Research, 115, A10240, doi: 10.1029/2010JA015312.

Jackman, C. M., L. Lamy, M. P. Freeman, P. Zarka, B. Cecconi, W. S. Kurth, S. W. H. Cowley, M. K. Dougherty, (2009), On the character and distribution of lower-frequency radio emissions at Saturn, and their relationship to substorm-like events, Journal of Geophysical Research, 114, A08211, doi: 10.1029/2008JA013997.

Jackman, C. M., N. Achilleos, E. J. Bunce, B. Cecconi, J. T. Clarke, S. W. H. Cowley, W. S. Kurth, P. Zarka, (2005), Interplanetary conditions and magnetospheric dynamics during the cassini orbit insertion fly-through of Saturn's magnetosphere, Journal of Geophysical Research, 110, A10212, doi: 10.1029/2005JA011054.

Jacobsen, K. S., J.-E. Wahlund, A. Pedersen, (2009), Cassini Langmuir probe measurements in the inner magnetosphere of Saturn, Planetary and Space Science, 57, 48–52, doi: 10.1016/j.pss.2008.10.012.

Jasinski, J. M., C. S. Arridge, L. Lamy, J. S. Leisner, M. F. Thomsen, D. G. Mitchell, A. J. Coates, A. Radioti, G. H. Jones, E. Roussos, N. Krupp, D. Grodent, M. K. Dougherty, J. H. Waite, (2014), Cusp observation at Saturn's high latitude magnetosphere by the Cassini spacecraft, Geophysical Research Letters, 41, 1382–1388, doi: 10.1002/2014GL059319.

Jia, X., M. G. Kivelson, T. I. Gombosi, (2012), Driving Saturn’s magnetospheric periodicities from the upper atmosphere/ionosphere, Journal of Geophysical Research, 117, A04215, doi: 10.1029/2011JA017367.

Jia, Y.-D., C. T. Russell, K. Khurana, H. Y. Wei, Y. J. Ma, J. S. Leisner, A. M. Persoon, M. K. Dougherty, (2011), Cassini magnetometer observations over the Enceladus poles, Geophysical Research Letters, 38, L19109, doi: 10.1029/2011GL049013.

Jia, Y.-D., C. T. Russell, K. K. Khurana, G. Toth, J. S. Leisner, T. I. Gombosi, (2010a), The interaction of Saturn's magnetosphere and its moons 1: Interaction between corotating plasma and standard obstacles, Journal of Geophysical Research, 115, A04214, doi: 10.1029/2009JA014630.

Jia, Y.-D., C. T. Russell, K. K. Khurana, Y. J. Ma, W. Kurth, T. I. Gombosi, (2010b), Interaction of Saturn's magnetosphere and its moons: 3. Time variation of the Enceladus plume, Journal of Geophysical Research, 115, A12243, doi: 10.1029/2010JA015534.

Jinks, S., E. Bunce, S. Cowley, G. Provan, T. Yeoman, C. Arridge, M. Dougherty, D. Gurnett, N. Krupp, W. Kurth, D. Mitchell, M. Morooka, J.-E. Wahlund, (2014), Cassini multi-instrument assessment of Saturn's polar cap boundary, Journal of Geophysical Research, 119, 8161–8177, doi: 10.1002/2014JA020367.

Jones, G. H., C. S. Arridge, A. J. Coates, G. R. Lewis, S. Kanani, A. Wellbrock, D. T. Young, F. J. Crary, R. L. Tokar, R. J. Wilson, T. W. Hill, R. E. Johnson, D. G. Mitchell, J. Schmidt, S. Kempf, U. Beckmann, C. T. Russell, Y. D. Jia, M. K. Dougherty, J. H. Waite, B. A. Magee,

(2009), Fine jet structure of electrically charged grains in Enceladus' plume, Geophysical Research Letters, 36, L16204, doi: 10.1029/2009GL038284.

Jones, G. H., E. Roussos, N. Krupp, U. Beckmann, A. J. Coates, F. Crary, I. Dandouras, V. Dikarev, M. K. Dougherty, P. Garnier, C. J. Hansen, A. R. Hendrix, G. B. Hospodarsky, R. E. Johnson, S. Kempf, K. Khurana, S. M. Krimigis, H. Krüger, W. S. Kurth, A. Lagg, H. J. McAndrews, D. G. Mitchell, C. Paranicas, F. Postberg, C. T. Russell, J. Saur, M. Seis, F. Spahn, R. Srama, D. F. Strobel, R. Tokar, J.-E. Wahlund, R. J. Wilson, J. Woch, D. Young, (2008), The dust halo of Saturn's largest icy moon: Evidence of rings at Rhea?, Science, 319, 1380–1384, doi: 10.1126/science.1151524.

Kaiser, M. L., W. M. Farrell, W. S. Kurth, G. B. Hospodarsky, D. A. Gurnett, (2004), New observations from Cassini and Ulysses of Jovian VLF radio emissions, Journal of Geophysical Research, 109, A09S08, doi: 10.1029/2003JA010233.

Kaiser, M. L., W. M. Farrell, M. D. Desch, G. B. Hospodarsky, W. S. Kurth, D. A. Gurnett, (2001), Ulysses and Cassini at Jupiter: Comparison of the quasi-periodic radio bursts, In Planetary Radio Emissions V, (eds.) H. O. Rucker, M. L. Kaiser, Y. Leblanc, Austrian Academy of Sciences Press, Vienna, Austria, pp. 41–48.

Kaiser, M. L., P. Zarka, W. S. Kurth, G. B. Hospodarsky, D. A. Gurnett, (2000), Cassini and wind stereoscopic observations of Jovian nonthermal radio emissions: Measurement of beam widths, Journal of Geophysical Research, 105, 16053–16062, doi: 10.1029/1999JA000414.

Kaiser, M. L., J. E. P. Connerney, M. D. Desch, (1983), Atmospheric storm explanation of Saturnian electrostatic discharges, Nature, 303, 50–53.

Karlsson, R., W. Macher, U. Taubenschuss, H. O. Rucker, Cassini/RPWS Team, (2007), In flight calibration of the Cassini Radio and Plasma Wave Science (RPWS) antennas after the Huygens probe release, In Proceedings of the Nordic Shortwave Conference HF07 (in Faro, Gotland), pp. 3.4.1–3.4.9.

Kasaba, Y., T. Kimura, D. Maruno, A. Morioka, B. Cecconi, L. Lamy, C. M. Jackman, C. Tao, H. Kita, H. Misawa, T. Tsuchiya, A. Kumamoto, (2017), A flux comparison of northern and southern Saturn kilometric radio bursts during southern summer, In Planetary Radio Emissions VIII, (eds.) G. Fischer, G. Mann, M. Panchenko, P. Zarka, Austrian Academy of Sciences Press, Vienna, Austria, pp. 205–215.

Kellett, S., C. Arridge, E. Bunce, A. Coates, S. Cowley, M. Dougherty, A. Persoon, N. Sergis, R. Wilson, (2011), Saturn's ring current: Local time dependence and temporal variability, Journal of Geophysical Research, 116, A05220, doi: 10.1029/2010JA016216.

Kellett, S., C. Arridge, E. Bunce, A. Coates, S. Cowley, M. Dougherty, A. Persoon, N. Sergis, R. Wilson, (2010), Nature of the ring current in Saturn's dayside magnetosphere, Journal of Geophysical Research, 115, A08201, doi: 10.1029/2009JA015146.

Kelley, M. C., S. Pancoast, S. Close, Z. Z. Wang, (2012), Analysis of electromagnetic and electrostatic effects of particle impacts on spacecraft, Advances in Space Research, 49, Issue 6, doi: 10.1016/j.asr.2011.12.023, 1029-1033.

Kellogg, P., D. A. Gurnett, G. B. Hospodarsky, W. S. Kurth, M. Dougherty, R. Forsyth, (2003a), Ion isotropy and ion resonant waves in the solar wind: Corrected Cassini observations, Journal of Geophysical Research, 108(A1), 1045, doi: 10.1029/2002JA009312.

Kellogg, P., D. A. Gurnett, G. B. Hospodarsky, W. S. Kurth, M. Dougherty, R. Forsyth, (2003b), Electric fluctuations and ion isotropy, AIP Conference Proceedings, American Institute of Physics, vol. 679, Issue 1, pp. 383–388, doi: 10.1063/1.1618618.

Kellogg, P. J., D. A. Gurnett, G. B. Hospodarsky, W. S. Kurth, (2001a), Ion isotropy and ion resonant waves in the solar wind: Cassini observations, Geophysical Research Letters, 28, 87–90, doi: 10.1029/10.1029/2000GL012100.

Kellogg, P. J., D. A. Gurnett, G. B. Hospodarsky, W. S. Kurth, (2001b), Comment on– Ion isotropy and ion resonant waves in the solar wind: Cassini observations, Geophysical Research Letters, 28, 4061–4061.

Kempf, S., U. Beckmann, G. Moragas-Klostermeyer, R. Srama, T. Economou, J. Schmidt, F. Spahn, E. Grün, (2008), The E ring in the vicinity of Enceladus I: Spatial distribution and properties of the ring particles, Icarus, 193, 420–437, doi: 10.1016/j.icarus.2007.06.027.

Kennelly, T., J. S. Leisner, G. B. Hospodarsky, D. A. Gurnett, (2013), Ordering of injection events within Saturnian SLS longitude and local time, Journal of Geophysical Research, 118, 832–838, doi: 10.1002/jgra.50152.

Khan, H., S. W. H. Cowley, E. Kolesnikova, M. Lester, M. J. Brittnacher, T. J. Hughes, W. J. Hughes, W. S. Kurth, D. J. McComas, L. Newitt, C. J. Owen, G. D. Reeves, H. J. Singer, C. W. Smith, D. J. Southwood, J. F. Watermann, (2001), Observations of two complete substorm cycles during the Cassini Earth swing-by: Cassini magnetometer data in a global context, Journal of Geophysical Research, 106, 30,141–30,175, doi: 10.1029/2001JA900049.

Kimura, T., L. Lamy, C. Tao, S. Badman, S. Kasahara, B. Cecconi, P. Zarka, A. Morioka, Y. Miyoshi, D. Maruno, Y. Kasaba, M. Fujimoto, (2013), Long-term modulations of Saturn's auroral radio emissions by the solar wind and seasonal variations controlled by the solar ultraviolet flux, Journal of Geophysical Research, 118, 7019–7035, doi: 10.1002/2013JA018833.

Kimura, T., B. Cecconi, P. Zarka, Y. Kasaba, F. Tsuchiva, H. Misawa, A. Morioka, (2012), Polarization and direction of arrival of Jovian quasiperiodic bursts observed by Cassini, Journal of Geophysical Research, 117, A11209, doi: 10.1029/2012JA017506.

Kinrade, J., S. V. Badman, E. J. Bunce, C. Tao, G. Provan, S. W. H. Cowley, A. Grocott, R. L. Gray, D. Grodent, T. Kimura, J. D. Nichols, C. S. Arridge, A. Radioti, J. T. Clarke, F. J. Crary, W. R. Pryor, H. Melin, K. H. Baines, M. K. Dougherty, (2017), An Isolated, bright cusp aurora at Saturn, Journal of Geophysical Research, 122, 6121–6138, doi: 10/1002/2016JA023792.

Kivelson, M. G. and X. Jia, (2018), Coupled SKR emissions in Saturn's northern and southern ionospheres, Geophysical Research Letters, 45, 2893–2900, doi: 10.1002/2017GL075425.

Konovalenko, A. A., N. N. Kalinichenko, H. O. Rucker, A. Lecacheux, G. Fischer, P. Zarka, V. V. Zakharenko, K. Y. Mylostna, J.-M. Griessmeier, E. P. Abranin, I. S. Falkovich, K. M. Sidorchuk,

W. S. Kurth, M. L. Kaiser, D. A. Gurnett, (2013), Earliest recorded ground-based decameter wavelength observations of Saturn's lightning during the giant E-storm detected by Cassini spacecraft in early 2006, Icarus, 224, 14–23, doi: 10.1016/j.icarus.2012.07.024.

Kopf, A. J., D. A. Gurnett, J. D. Menietti, R. L. Mutel, W. M. Farrell, (2011), A statistical study of kilometric radiation fine structure striations observed at Jupiter and Saturn, Magnetospheres of the Outer Planets Conference, July 11–15, 2011, Hosted by John Clarke, sponsored by Boston University, Session 5 Aurora, #53, Kopf_AJ_MOP-1.ppt.

Kopf, A. J., (2010), A multi-instrument study of auroral hiss at Saturn, Ph.D. Thesis, University of Iowa, Iowa City, Iowa.

Kopf, A. J., D. A. Gurnett, J. D. Menietti, P. Schippers, C. S. Arridge, G. B. Hospodarsky, W. S. Kurth, S. Grimald, N. Andre, A. J. Coates, M. K. Dougherty, (2010), Electron beams as the source of whistler-mode auroral hiss at Saturn, Geophysical Research Letters, 37, L09102, doi: 10.1029/2010GL042980.

Kriegel, H., S. Simon, U. Motschmann, J. Saur, F. M. Neubauer, A. M. Persoon, M. K. Dougherty, D. A. Gurnett, (2011), Influence of negatively charged plume grains on the structure of Enceladus' Alfven wings: Hybrid simulations versus Cassini Magnetometer data, Journal of Geophysical Research, 116, A102233, doi: 10.1029/2011JA016842.

Krupp, N., E. Roussos, C. Paranicas, D. G. Mitchell, P. Kollmann, S. Ye, W. S. Kurth, K. R. Khurana, R. Perryman, H. Waite, R. Srama, D. C. Hamilton, (2017), Energetic electron measurements near Enceladus by Cassini during 2005–2015, Icarus, 306, 256–274, doi: 10.1016/j.icarus.2017.10.022.

Kurth, W. S., G. B. Hospodarsky, D. A. Gurnett, L. Lamy, M. K. Dougherty, J. Nichols, E. J. Bunce, W. Pryor, K. H. Baines, U. Dyudina, T. Stallard, H. Melin, F. J. Crary, (2016), Saturn kilometric radiation intensities during the Saturn auroral campaign of 2013, Icarus, 263, 2–9, doi: 10.1016/j.icarus.2015.01.003.

Kurth, W. S., D. A. Gurnett, J. D. Menietti, R. L. Mutel, M. G. Kivelson, E. J. Bunce, S. W. H. Cowley, D. L. Talboys, M. K. Dougherty, C. Arridge, A. Coates, S. Grimald, L. Lamy, P. Zarka, B. Cecconi, P. Schippers, N. Andre, P. Louarn, D. Mitchell, J. S. Leisner, M. Morooka, (2011), A close encounter with a Saturn kilometric radiation source region, In Planetary Radio Emissions VII, (eds.) H. O. Rucker, W. S. Kurth, P. Louarn, G. Fischer, Austrian Academy of Sciences, Vienna, Austria, pp. 75–86.

Kurth, W. S., E. J. Bunce, J. T. Clarke, F. J. Crary, D. C. Grodent, A. P. Ingersoll, U. A. Dyudina, L. Lamy, D. G. Mitchell, A. M. Persoon, W. R. Pryor, J. Saur, T. Stallard, (2009), Auroral processes, Chapter 12, In Saturn from Cassini-Huygens, (eds.) M. K. Dougherty, L. W. Esposito, S. M. Krimigis, Springer, Dordrecht, pp. 333–374, doi: 10.1007/978-1-4020-9217-6_12.

Kurth, W. S.,T. F. Averkamp, D. A. Gurnett, J. B. Groene, A. Lecacheux, (2008), An update to a Saturn longitude system based on kilometric radio emissions, Journal of Geophysical Research, 113, A05222, doi: 10.1029/2007JA012861.

Kurth, W. S., A. Lecacheux, T. F. Averkamp, J. B. Groene, D. A. Gurnett, (2007), A Saturnian longitude system based on a variable kilometric radiation period, Geophysical Research Letters, 34, L02201, doi: 10.1029/2006GL028336.

Kurth, W. S., B. Cecconi, D. A. Gurnett, M. L. Kaiser, P. Zarka, A. Lecacheux, (2006a), Is Titan a radio source?, In Planetary Radio Emissions VI, (eds.) H. O. Rucker, W. S. Kurth, G. Mann, Austrian Academy of Sciences Press, Vienna, Austria, pp. 133–142.

Kurth, W. S., T. F. Averkamp, D. A. Gurnett, Z. Wang, (2006b), Cassini RPWS Observations of dust in Saturn's E ring, Planetary and Space Science, 54, 988–998, doi: 10.1016/j.pss.2006.05011.

Kurth, W. S., D. A. Gurnett, J. T. Clarke, P. Zarka, M. D. Desch, M. L. Kaiser, B. Cecconi, A. Lecacheux, W. M. Farrell, P. Galopeau, J.-C. Gerard, D. Grodent, R. Prange, M. K. Dougherty, F. J. Crary, (2005a), An Earth-like correspondence between Saturn's auroral features and radio emission, Nature, 433, 722–725, doi: 10.1038/nature03334.

Kurth, W. S., G. B. Hospodarsky, D. A. Gurnett, B. Cecconi, P. Louarn, A. Lecacheux, P. Zarka, H. O. Rucker, M. Boudjada, M. L. Kaiser, (2005b), High spectral and temporal resolution observations of Saturn kilometric radiation, Geophysical Research Letters, 32, L20S07, doi: 10.1029/2005GL022648.

Kurth, W. S., (2003), Cassini, The World Book Encyclopedia, 3, 276–277.

Kurth, W. S., D. A. Gurnett, G. B. Hospodarsky, W. M. Farrell, A. Roux, M. K. Dougherty, S. P. Joy, M. G. Kivelson, R. J. Walker, F. J. Crary, C. J. Alexander, (2002), The dusk flank of Jupiter's Magnetosphere, Nature, 415, 991–994, doi: 10.1038/415991a.

Kurth, W. S., G. B. Hospodarsky, D. A. Gurnett, A. Lecacheux, P. Zarka, M. D. Desch, M. L. Kaiser, W. M. Farrell, (2001a), High-resolution observations of low-frequency Jovian radio emissions by Cassini, In Planetary Radio Emissions V, (eds.) H. O. Rucker, M. L. Kaiser, Y. Leblanc, Austrian Academy of Sciences Press, Vienna, Austria, pp. 15–28.

Kurth, W. S., G. B. Hospodarsky, D. A. Gurnett, M. L. Kaiser, J.-E. Wahlund, A. Roux, P. Canu, P. Zarka, Y. Tokarev, (2001b), An overview of observations by the Cassini radio and plasma wave investigation at Earth, Journal of Geophysical Research, 106, 30,239-30,252, doi: 10.1029/2001JA900033.

Kurth, W. S. and P. Zarka, (2001), Saturn radio waves, In Planetary Radio Emissions V, (eds.) H. O. Rucker, M. L. Kaiser, Y. Leblanc, Austrian Academy of Sciences Press, Vienna, Austria, pp. 247–259.

Ladreiter, H. P., P. Zarka, A. Lecacheux, W. Macher, H. O. Rucker, R. Manning, D. A. Gurnett, W. S. Kurth, (1995), Analysis of electromagnetic wave direction finding performed by spaceborne antennas using singular value decomposition techniques, Radio Science, 30, 1699–1712, doi: 10.1029/95RS02479.

Lammer, H., J. H. Bredehöft, A. Coustenis, M. L. Khodachenko, L. Kaltenegger, O. Grasset, D. Prieur, F. Raulin, P. Ehrenfreund, M. Yamauchi, J.-E. Wahlund, J.-M. Grießmeier, G. Stangl,

C. S. Cockell, Yu. N. Kulikov, J. L. Grenfell, H. Rauer, (2009), What makes a planet habitable? Astronomy and Astrophysics Review, 17, 181–249, doi: 10.1007/s00159-009-0019-z.

Lammer, H., T. Tokano, G. Fischer, W. Stumptner, G. J. Molina-Cuberos, K. Schwingenschuh, H. O. Rucker, (2001a), Lightning activity on Titan: Can Cassini detect it?, Planetary and Space Science, 49, 561–574, doi: 10.1016/S0032-0633(00)00171-9.

Lammer, H., T. Tokano, G. Fischer, G. J. Molina-Cuberos, W. Stumptner, K. Schwingenschuh, H. O. Rucker, (2001b), Detection capability of Cassini for thundercloud generated lightning discharges on Titan, In Planetary Radio Emissions V, (eds.) H. O. Rucker, M. L. Kaiser, Y. Leblanc, Austrian Academy of Sciences Press, Vienna, Austria, pp. 261–270.

Lamy, L., P. Zarka, B. Cecconi, R. Prange, W. S. Kurth, G. B. Hospodarsky, A. M. Persoon, M. Morooka, J.-E. Wahlund, G. J. Hunt, (2018a), The low frequency source of Saturn's kilometric radiation, Science, 362, Issue 6410, eaat2027, doi: 10.1126/science.aat2027.

Lamy, L., R. Prange, C. Tao, T. Kim, S. V. Badman, P. Zarka, B. Cecconi, W. S. Kurth, W. Pryor, E. J. Bunce, A. Radioti, (2018b), Saturn's northern aurorae at solstice from HST observations coordinated with Cassini's Grand Finale, Geophysical Research Letters, 45, 9353–9362, doi: 10.1029/2018GL078211.

Lamy, L., (2017), The Saturnian kilometric radiation before the Cassini Grand Finale, In Planetary Radio Emissions VIII, G. Fischer, G. Mann, M. Panchenko, P. Zarka, (eds.) Austrian Academy of Sciences Press, Vienna, Austria, pp. 171–190.

Lamy, L., R. Prange, W. Pryor, J. Gustin, S. V. Badman, H. Melin, T. Stallard, D. G. Mitchell, P. C. Brandt, (2013), Multispectral simultaneous diagnosis of Saturn's aurorae throughout a planetary rotation, Journal of Geophysical Research, 118, 4817–4843, doi: 10.1002/jgra.50404.

Lamy, L., B. Cecconi, P. Zarka, P. Canu, P. Schippers, W. S. Kurth, R. L. Mutel, D. A. Gurnett, D. Menietti, P. Louarn, (2011a), Emission and propagation of Saturn kilometric radiation: Magnetoionic modes, beaming pattern, and polarization state, Journal of Geophysical Research, 116, A04212, doi: 10.1029/2010JA016195.

Lamy, L., (2011), Variability of southern and northern periodicities of Saturn Kilometric Radiation, In Planetary Radio Emissions VII, (eds.) H. O. Rucker, W. S. Kurth, P. Louarn, G. Fischer, Austrian Academy of Sciences, Vienna, Austria, pp. 38–50.

Lamy, L., P. Schippers, P. Zarka, B. Cecconi, C. Arridge, M. K. Dougherty, P. Louarn, N. Andre, W. S. Kurth, R. L. Mutel, D. A. Gurnett, A. J. Coates, (2010a), Properties of Saturn kilometric radiation measured within its source region, Geophysical Research Letters, 37, L12104, doi: 10.1029/2010GL043415.

Lamy, L., P. Zarka, B. Cecconi, R. Prange, (2010b), Auroral kilometric radiation diurnal, semi-diurnal, and shorter-term modulations disentangled by Cassini/RPWS, Journal of Geophysical Research, 115, A09221, doi: 10.1029/2010JA015434.

Lamy, L., P. Schippers, P. Zarka, B. Cecconi, C. S. Arridge, M. K. Dougherty, P. Louarn, N. Andre, W. S. Kurth, R. L. Mutel, D. A. Gurnett, A. J. Coates, (2010c), Properties of Saturn

kilometric radiation measured within its source region (abstract), In Planetary Radio Emissions VII, (eds.) H. O. Rucker, W. S. Kurth, P. Louarn, G. Fischer, Austrian Academy of Sciences, Vienna, Austria, p. 97.

Lamy, L., B. Cecconi, R. Prange, P. Zarka, J. D. Nichols, J. T. Clarke, (2009), An auroral oval at the footprint of Saturn's kilometric radio sources, colocated with the UV aurorae, Journal of Geophysical Research, 114, A10212, doi: 10.1029/2009JA014401.

Lamy, L., P. Zarka, B. Cecconi, R. Prange, W. S. Kurth, D. A. Gurnett, (2008a), Saturn kilometric radiation: Average and statistical properties, Journal of Geophysical Research, 113, A07201, doi: 10.1029/2007JA012900.

Lamy, L., P. Zarka, B. Cecconi, S. Hess, R. Prange, (2008b), Modeling of Saturn kilometric radiation arcs and equatorial shadow zone, Journal of Geophysical Research, 113, A10213, doi: 10.1029/2008JA013464.

Lamy, L., (2008), Etudes des emissions radio aurorales de Saturne, modelisation et aurores UV, Ph.D. Thesis, l'Universite Pierre et Marie Curie, Meudon, France.

Lavvas, P. P., R. V. Yella, T. Koskinen, A. Bazin, V. Vuitton, E. Vigren, M. Galand, A. Wellbrock, A. J. Coates, J.-E. Wahlund, F. Crary, D. Snowden, (2013), Aerosol growth in Titan’s ionosphere, In Proceedings of the National Academy of Sciences, doi: 10.1073/pnas.1217059110.

Lecacheux, A., W. S. Kurth, R. Manning, (2001), Sub-second time scales in Jovian radio emissions as measured by Cassini/RPWS: Comparison with ground-based observations, In Planetary Radio Emissions V, (eds.) H. O. Rucker, M. L. Kaiser, Y. Leblanc, Austrian Academy of Sciences Press, Vienna, Austria, pp. 29–39.

Lecacheux, A., (2001), Radio observations during the Cassini flyby of Jupiter, In Planetary Radio Emissions (eds.) V, H. O. Rucker, M. L. Kaiser, Y. Leblanc, Austrian Academy of Sciences Press, Vienna, Austria, pp. 1–13.

Leisner, J. S., G. B. Hospodarsky, D. A. Gurnett, (2013), Enceladus auroral hiss observations: Implications for electron beam locations, Journal of Geophysical Research, 118, 160–166, doi: 10.1029/2012JA018213.

Lewis, G. R., C. S. Arridge, D. R. Linder, L. K. Gilbert, D. O. Kataria, A. J. Coates, A. Persoon, G. A. Collinson, N. Andre, P. Schippers, J.-E. Wahlund, M. Morooka, G. H. Jones, A. M. Rymer, D. T. Young, D. G. Mitchell, A. Lagg, S. A. Livi, (2010), The calibration of the Cassini-Huygens CAPS electron spectrometer, Planetary and Space Science, 58, 427–436, doi: 10.1016/j.pss.2009.11.008.

Li, C. and A.P. Ingersoll, (2015), Moist convection in hydrogen atmospheres and the frequency of Saturn’s giant storms, Nature Geoscience, 8, 398–403.

Livi, R., J. Goldstein, J. L. Burch, F. Crary, A. M. Rymer, D. G. Mitchell, A. M. Persoon, (2014), Multi-instrument analysis of plasma parameters in Saturn's equatorial, inner magnetosphere using corrections for corrections for spacecraft potential and penetrating background radiation, Journal of Geophysical Research, 119, 3683–3707, doi: 10.1002/2013JA019616.

Louarn, P., W. S. Kurth, D. A. Gurnett, G. B. Hospodarsky, A. M. Persoon, B. Cecconi, A. Lecacheux, P. Zarka, P. Canu, A. Roux, H. O. Rucker, W. M. Farrell, M. L. Kaiser, N. Andre, C. Harvey, M. Blanc, (2007), Observation of similar radio signatures at Saturn and Jupiter: Implications for the magnetospheric dynamics, Geophysical Research Letters, 34, L20113, doi: 10.1029/2007GL030368.

Louis, C. K., L. Lamy, P. Zarka, B. Cecconi, S. L. G. Hess, (2017a), Detection of Jupiter decametric emissions controlled by Europa and Ganymede with Voyager/PRA and Cassini/RPWS, Journal of Geophysical Research, 122, 9228–9247, doi: 10.1002/2016JA023779.

Louis, C., L. Lamy, P. Zarka, B. Cecconi, M. Imai, W. Kurth, G. Hospodarsky, S. Hess, X. Bonnin, S. Bolton, J. Connerney, S. Levin, (2017b), Io-Jupiter decametric arcs observed by Juno/Waves compared to ExPRES simulations, Geophysical Research Letters, vol. 44, Issue 18, pp 9225–9232, doi: 10.1002/2017GL073036.

Luhmann, J. G., D. Ulusen, S. A. Ledvina, K. Mandt, B. Magee, J. H. Waite, J. Westlake, T. E. Cravens, I. Robertson, N. J. T. Edberg, K. Ågren, J.-E. Wahlund, Y.-J. Ma, H. Y. Wei, C. T. Russell, M. K. Dougherty, (2012), Investigating magnetospheric interaction effects on Titan's ionosphere with the Cassini orbiter Ion Neutral Mass Spectrometer, Langmuir probe, and magnetometer observations during targeted flybys, Icarus, 2192, Issue 2, 534–555, doi: 10.1016/j.icarus.2012.03.015.

Ma, Y.-J., C. T. Russell, A. F. Nagy, G. Toth, M. K. Dougherty, A. Wellbrock, A. J. Coates, P. Garnier, J.-E. Wahlund, T. E. Cravens, M. S. Richard, F. J. Crary, (2011), The importance of thermal electron heating in Titan’s ionosphere: Comparison with Cassini T34 flyby, Journal of Geophysical Research, 116, A10213, doi: 10.1029/2011JA016657.

Ma, Y.-J., C. T. Russell, A. F. Nagy, G. Toth, C. Bertucci, M. K. Dougherty, F. M. Neubauer, A. Wellbrock, A. J. Coates, P. Garnier, J.-E. Wahlund, T. E. Cravens, F. J. Crary, (2009), Time-dependent global MHD simulations of Cassini T32 flyby: From magnetosphere to magnetosheath, Journal of Geophysical Research, 114, A03204, doi: 10.1029/2008JA013676.

Ma, Y.-J., A. F. Nagy, G. Toth, T. E. Cravens, C. T. Russell, T. I. Gombosi, J.-E. Wahlund, F. J. Crary, A. J. Coates, C. L. Bertucci, F. M. Neubauer, (2007), 3D global multi-species Hall-MHD simulation of the Cassini T9 flyby, Geophysical Research Letters, 34, L24S10, doi: 10.1029/2007GL031627.

Ma, Y.-J., A. F. Nagy, T. E. Cravens, I. V. Sokolov, K. C. Hansen, J.-E. Wahlund, F. J. Crary, A. J. Coates, M. K. Dougherty, (2006), Comparisons between MHD model calculations and observations of Cassini flybys of Titan, Journal of Geophysical Research, 111, A05207, doi: 10.1029/2005JA011481.

Madanian, H., T. E. Cravens, M. S. Richard, J. H. Waite Jr., N. J. T. Edberg, J. H. Westlake, J.-E. Wahlund, (2016), Solar cycle variations in ion composition in the dayside ionosphere of Titan, Journal of Geophysical Research, 121, 8013–8037, doi: 10.1002/2015JA022274.

Mandt, K. E., D. A. Gell, M. Perry, J. H. Waite, F. Crary, D. Young, B. A. Magee, J. H. Westlake, T. Cravens, W. Kasprzak, G. Miller, J.-E. Wahlund, K. Ågren, N. J. T. Edberg, A. N. Heays, B. R. Lewis, S. T. Gibson, V. de la Haye, M-C. Liang, (2012), Ion densities and composition of Titan's upper atmosphere derived from the Cassini Ion Neutral Mass Spectrometer: Analysis methods and comparison of measured ion densities to photochemical model simulations, Journal of Geophysical Research, 117, E10006, doi: 10.1029/2012JE004139.

Mann, I. and A. Czechowski, (2012), Causes and consequences of the existence of nanodust in interplanetary space, In Nanodust in the solar system: Discoveries and interpretations, Astrophysics and Space Science Library, Springer-Verlag, Berlin, p. 385, doi: 10.1007/978-3-642-27543-2_10.

Mann, I., E. Murad, A. Czechowski, (2007), Nanoparticles in the inner solar system, Planetary and Space Science, 55, 1000–1009, doi: 10.1016/j.pss.2006.11.015.

Marty, B., T. Guillot, Athena Coustenis, N. Achilleos, Y. Alibert, S. Asmar, D. Atkinson, S. Atreya, G. Babasides, K. Baines, T. Balint, D. Banfield, S. Barber, B. Bézard, G. L. Bjoraker, M. Blanc, S. Bolton, N, Chanover, S. Charnoz, E. Chassefière, J. E. Colwell, E. Deangelis, M. K. Dougherty, P. Drossart, F. M. Flasar, T. Fouchet, R. Frampton, I. Franchi, D. Gautier, L. Gurvits, R. Hueso, B. Kazeminejad, S. M. Krimigis, A. Jambon, G. Jones, Y. Langevin, M. Leese, E. Lellouch, J. Lunine, A. Milillo, P. Mahaffy, B. Mauk, A. Morse, M. Moreira, X. Moussas, C. Murray, I. Mueller-Wodarg, T. C. Owen, S. Pogrebenko, R. Prangé, P. Read, A. Sánchez-Lavega, P. Sarda, D. Stam, G. Tinetti, P. Zarka, J. Zarnecki, (2008), Kronos: Exploring the Depths of Saturn With Probes and Remote Sensing Through an International Mission, Experimental Astronomy, doi: 10.1007/s10686-008-9094-9, pp. 8–37.

Masters, A., A. H. Sulaiman, L. Stawarz, B. Reville, N. Sergis, M. Fujimoto, D. Burgess, A. J. Coates, M. K. Dougherty, (2017), An In Situ comparison of electron acceleration at collisionless shocks under differing upstream magnetic field orientations, Astrophysical Journal, 843, doi: 10.3847/1538-4357/aa76ea.

Masters, A., A. H. Sulaiman, N. Sergis, L. Stawarz, M. Fujimoto, A. J. Coates, M. K. Dougherty, (2016), Suprathermal electrons at Saturn's bow shock, Astrophysical Journal, 826, doi: 10.3847/0004-637X/826/1/48.

Masters, A., L. Stawarz, M. Fujimoto, S. J. Schwartz, N. Sergis, M. F. Thomsen, A. Retino, H. Hasegawa, B. Zieger, G. R. Lewis, A. J. Coates, P. Canu, M. K. Dougherty, (2013a), Electron acceleration to relativistic energies at a strong quasi-parallel shock wave, Nature Physics, 9, 164–167, doi: 10.1038/nphys2541.

Masters, A., L. Stawarz, M. Fujimoto, S. J. Schwartz, N. Sergis, M. F. Thomsen, A. Retino, H. Hasegawa, B. Zieger, G. R. Lewis, A. J. Coates, P. Canu, M.K. Dougherty, (2013b), In situ observations of high-mach number collisionless shocks in space plasmas, Plasma Physics and Controlled Fusion, 55, 124035, doi: 10.1088/0741-3335/55/12/124035.

Masters, A., H. J. McAndrews, J. T. Steinberg, M. F. Thomsen, C. S. Arridge, M. K. Dougherty, L. Billingham, S. J. Schwartz, N. Sergis, G. B. Hospodarsky, A. J. Coates, (2009), Hot flow

anomalies at Saturn's bow shock, Journal of Geophysical Research, 114, A08217, doi: 10.1029/2009JA014112.

Masters, A., N. Achilleos, M. K. Dougherty, J. A. Slavin, G. B. Hospodarsky, C. S. Arridge, A. J. Coates, (2008), An empirical model of Saturn's bow shock: Cassini observations of shock location and shape, Journal of Geophysical Research, 113, A10210, doi: 10.1029/2008JA013276.

Mauk, B. H., D. C. Hamilton, T. W. Hill, G. B. Hospodarsky, R. E. Johnson, C. Paranicas, E. Roussos, C. T. Russell, D. E. Shemansky, E. C. Sittler, Jr., R. M. Thorne, (2009), Fundamental Plasma Processes in Saturn's Magnetosphere, in Saturn from Cassini-Huygens, (eds.), M. K. Dougherty, L. W. Esposito, and S. M. Krimigis, pp. 281–331, Springer, Dordrecht, doi: 10.1007/978-1-4020-9217-6_11.

McGhee, C. A., R. G. French, L. Dones, J. N. Cuzzi, H. J. Salo, R. Danos, (2005), HST Observations of the Spokes in Saturn’s B Ring, Icarus, 173, 508–521.

Mendillo, M., L. Moore, J. Clarke, I. Mueller-Wodarg, W. S. Kurth, M. L. Kaiser, (2005), Effects of ring shadowing on the detection of electrostatic discharges at Saturn, Geophysical Research Letters, 32, L05107, doi: 10.1029/2004GL021934.

Menietti, J. D., T. F. Averkamp, S.-Y. Ye, A. M. Persoon, M. W. Morooka, J. B. Groene, W. S. Kurth, (2018a), Extended survey of Saturn Z-mode wave intensity through Cassini's Final Orbits, Geophysical Research Letters, 45, 7330–7336, doi: 10.1029/2018GL079287.

Menietti, J. D., T. V. Averkamp, S.-Y. Ye, A. Sulaiman, M. Morooka, A. M. Persoon, G. B. Hospodarsky, W. S. Kurth, D. A. Gurnett, J.-E. Wahlund, (2018b), Analysis of intense Z-mode emission observed during the Cassini proximal orbits, Geophysical Research Letters, 45, 6766–6772, doi: 10.1002/2018GL077354.

Menietti, J. D., T. F. Averkamp, W. S. Kurth, S.-Y. Ye, D. A. Gurnett, B. Cecconi, (2017), Survey of Saturn electrostatic cyclotron harmonic wave intensity, Journal of Geophysical Research, 122, 8214–8227, doi: 10.1002/2017JA023929.

Menietti, J. D., J. B. Groene, T. F. Averkamp, R. B. Horne, E. E. Woodfield, Y. Y. Shprits, M. de Soria-Santacruz Pich, D. A. Gurnett, (2016a), Survey of whistler mode chorus intensity at Jupiter, Journal of Geophysical Research, 121, 10, 9758–9770, doi: 10.1002/2016JA022969.

Menietti, J. D., P. H. Yoon, D. Píša, S.-Y. Ye, O. Santolik, C. S. Arridge, D. A. Gurnett, A. J. Coates, (2016b), Source region and growth analysis of narrowband Z-mode emission at Saturn, Journal of Geophysical Research, 121, 12, 11929–11942, doi: 10.1002/2016JA022913.

Menietti, J. D., T. F. Averkamp, S.-Y. Ye, R. B. Horne, E. E. Woodfield, Y. Y. Shprits, D. A. Gurnett, J.-E. Wahlund, (2015), Survey of Saturn Z-mode emission, Journal of Geophysical Research, 120, 6176–6187, doi: 10.1002/2015JA021426.

Menietti, J. D., G. B. Hospodarsky, Y. Shprits, D. A. Gurnett, (2014a), Saturn chorus latitudinal variations, Journal of Geophysical Research, 119, Issue 6, 4656–4667, doi: 10.1002/2014JA019914.

Menietti, J. D., T. F. Averkamp, J. B. Groene, R. Horne, Y. Shprits, E. Woodfield, G. B. Hospodarsky, D. A. Gurnett, (2014b), Survey analysis of chorus intensity at Saturn, Journal of Geophysical Research, 119, 8415–8425, doi: 10.1002/2014JA020523.

Menietti, J. D., Y. Katoh, G. B. Hospodarsky, D. A. Gurnett, (2013a), Frequency drift of Saturn chorus emission compared to nonlinear theory, Journal of Geophysical Research, 118, 982–990, doi: 10.1002/jgra.50165.

Menietti, J. D., P. Schippers, Y. Katoh, J. S. Leisner, G. B. Hospodarsky, D. A. Gurnett, O. Santolik, (2013b), Saturn chorus intensity variations, Journal of Geophysical Research, 118, 1–11, doi: 10.1002/jgra.50529.

Menietti, J. D., Y. Shprits, R. Horne, E. Woodfield, G. B. Hospodarsky, D. A. Gurnett, (2012), Chorus, ECH, and Z-mode emissions observed at Jupiter and Saturn and possible electron acceleration, Journal of Geophysical Research, 117, A12214, doi: 10.1029/2012JA018187.

Menietti, J. D., R. L. Mutel, P. Schippers, S.-Y. Ye, O. Santolik, W. S. Kurth, D. A. Gurnett, B. Cecconi, (2011a), Saturn kilometric radiation near a source center on day 73, 2008, In Planetary Radio Emissions VII, (eds.) H. O. Rucker, W. S. Kurth, P. Louarn, G. Fischer, Austrian Academy of Sciences, Vienna, Austria, pp. 87–96.

Menietti, J. D., R. L. Mutel, P. Schippers, S.-Y. Ye, D. A. Gurnett, L. Lamy, (2011b), Analysis of Saturn kilometric radiation near a source center, Journal of Geophysical Research, 116, A12222, doi: 10.1029/2011JA017056.

Menietti, J. D., P. Schippers, O. Santolik, D. A. Gurnett, F. Crary, A. J. Coates, (2011c), Ion cyclotron harmonics in the Saturn downward current auroral region, Journal of Geophysical Research, 116, A12234, doi: 10.1029/2011JA017102.

Menietti, J. D., S.-Y. Ye, C. W. Piker, B. Cecconi, (2010a), The influence of Titan on Saturn kilometric radiation, Annales Geophysicae, 28, 395–406, doi: 10.5194/angeo-28-395-2010.

Menietti, J. D., P. H. Yoon, S.-Y. Ye, B. Cecconi, A. M. Rymer, (2010b), Source mechanism of Saturn narrowband emission, Annales Geophysicae, 28, 1013–1021, doi: 10.5194/angeo-28-1013-2010.

Menietti, J. D., S.-Y. Ye, P. H. Yoon, O. Santolik, A. M. Rymer, D. A. Gurnett, A. J. Coates, (2009), Analysis of narrowband emission observed in the Saturn magnetosphere, Journal of Geophysical Research, 114, A06206, doi: 10.1029/2008JA013982.

Menietti, J. D., O. Santolik, A. M. Rymer, G. B. Hospodarsky, A. M. Persoon, D. A. Gurnett, A. J. Coates, D. T. Young, (2008a), Analysis of plasma waves observed within local plasma injections seen in Saturn's magnetosphere, Journal of Geophysical Research, 113, A05213, doi: 10.1029/2007JA012856.

Menietti, J. D., O. Santolik, A. M. Rymer, G. B. Hospodarsky, D. A. Gurnett, A. J. Coates, (2008b), Analysis of plasma waves observed in the inner Saturn magnetosphere, Annales Geophysicae, 26, 2631–2644, doi: 10.5194/angeo-26-2631-2008.

Menietti, J. D., P. H. Yoon, D. A. Gurnett, (2007a), Possible eigenmode trapping in density enhancements in Saturn's inner magnetosphere, Geophysical Research Letters, 34, L04103, doi: 10.1029/2006GL028647.

Menietti, J. D., J. B. Groene, T. F. Averkamp, G. B. Hospodarsky, W. S. Kurth, D. A. Gurnett, P. Zarka, (2007b), Influence of Saturnian moons on Saturn kilometric radiation, Journal of Geophysical Research, 112, A08211, doi: 10.1029/2007JA012331.

Menietti, J. D. and W. S. Kurth, (2006), Ordered fine structure in radio emission observed by Cassini, Cluster, and Polar, In Planetary Radio Emissions VI, (eds.) H. O. Rucker, W. S. Kurth, and G. Mann, Austrian Academy of Sciences Press, Vienna, Austria, pp. 265–272.

Menietti, J. D., D. A. Gurnett, G. B. Hospodarsky, C. A. Higgins, W. S. Kurth, P. Zarka, (2003), Modeling radio emission attenuation lanes observed by the Galileo and Cassini spacecraft, Planetary and Space Science, 51, 533–540, doi: 10.1016/S0032-0633(03)00078-3.

Meyer-Vernet, N., M. Moncuquet, K. Issautier, P. Schippers, (2017), Frequency range of dust detection in space with radio and plasma wave receivers: Theory and application to interplanetary nanodust impacts on Cassini, Journal of Geophysical Research, 122, 8–22, doi: 10.1002/2016JA023081.

Meyer-Vernet, N., Z. Czechowski, I. Mann, M. Maksimovic, A. Lecacheux, K. Goetz, M. L. Kaiser, O. C. St. Cyr, S. D. Bale, G. Le Chat, (2010), Detection of fast nanoparticles in the solar wind, 12th International Solar Wind Conference, AIP Conference Proceedings, American Institute of Physics Publishing, vol. 1216, pp. 502–505,doi: 10.1063/1.3395912.

Meyer-Vernet, N., A. Lecacheux, M. L. Kaiser, D. A. Gurnett, (2009), Detecting nanoparticles at radio frequencies: Jovian dust stream impacts on Cassini/RPWS, Geophysical Research Letters, 36, L03103, doi: 10.1029/2008GL036752.

Mitchell, D. G., M. E. Perry, D. C. Hamilton, J. H. Westlake, P. Kollmann, H. T. Smith, J. F. Carbary, J. H. Waite, R. Perryman, H.-W. Hsu, J.-E. Wahlund, M. W. Morooka, L. Z. Hadid, A. M. Persoon, W. S. Kurth, (2018), Dust grains fall from Saturn's D-ring into its equatorial upper atmosphere, Science, 362, Issue 6410, eaat2236, doi:10.1126/science.aat2236.

Mitchell, D. G., J. F. Carbary, E. J. Bunce, A. Radioti, S. V. Badman, W. R. Pryor, G. B. Hospodarsky, W. S. Kurth, (2016), Recurrent pulsations in Saturn's high latitude magnetosphere, Icarus, 263, 94–100, doi: 10.1016/j.icarus.2014.10.028.

Mitchell, D. G., P. C. Brandt, J. F. Carbary, W. S. Kurth, S. M. Krimigis, C. Paranicas, N. Krupp, D. C. Hamilton, B. H. Mauk, G. B. Hospodarsky, M. K. Dougherty, W. R. Pryor, (2015), Injection, interchange, and reconnection: Energetic particle observations in Saturn's magnetosphere, Chapter 19, In Magnetotails in the solar system, Geophysical Monograph 207, (eds.) A. Keiling, C. M. Jackman P. A. Delamere, American Geophysical Union and John Wiley & Sons, Inc., pp. 327-343.

Mitchell, D. G., W. S. Kurth, G. B. Hospodarsky, N. Krupp, J. Saur, B. H. Mauk, J. F. Carbary, S. M. Krimigis, M. K. Dougherty, D. C. Hamilton, (2009a), Ion conics and electron beams

associated with auroral processes on Saturn, Journal of Geophysical Research, 114, A02212, doi: 10.1029/2008JA013621.

Mitchell, D. G., J. F. Carbary, S. W. H. Cowley, T. W. Hill, P. Zarka, (2009b), The dynamics of Saturn's magnetosphere, In Saturn from Cassini-Huygens, (eds.) M. K. Dougherty, L. W. Esposito, S. M. Krimigis, Springer, Dordrecht, pp. 257–279, doi: 10.1007/978-1-4020-9217-6_10.

Mitchell, D. G., S. M. Krimigis, C. Paranicas, P. C. Brandt, J. F. Carbary, E. C. Roelof, W. S. Kurth, D. A. Gurnett, J. T. Clarke, J. D. Nichols, J.-C. Gerard, D. C. Grodent, M. K. Dougherty, W. R. Pryor, (2009c), Recurrent energization of plasma in the midnight-to-dawn quadrant of Saturn's magnetosphere, and its relationship to auroral UV and radio emissions, Planetary and Space Science, 57, 1732–1742, doi: 10.1016/j.pss.2009.04.002.

Mitchell, D. G., P. C. Brandt, E. C. Roelof, J. Dandouras, S. M. Krimigis, B. H. Mauk, C. P. Paranicas, N. Krupp, D. C. Hamilton, W. S. Kurth, P. Zarka, M. K. Dougherty, E. J. Bunce, D. E. Shemansky, (2005), Energetic ion acceleration in Saturn's magnetotail: Substorms at Saturn?, Geophysical Research Letters, 32, L20S01, doi: 10.1029/2005GL022647.

Modolo, R. and G. M. Chanteur, (2008), A global hybrid model for Titan's interaction with the Kronian plasma: Application to the Cassini Ta flyby, Journal of Geophysical Research, 113, A01317, doi: 10.1029/2007JA012453.

Modolo, R., G. Chanteur, J.-E. Wahlund, P. Canu, W. S. Kurth, D. A. Gurnett, A. P. Matthews, C. Bertucci, (2007a), Plasma environment in the wake of Titan from hybrid simulation: A case study, Geophysical Research Letters, 34, L24S07, doi: 10.1029/2007GL030489.

Modolo, R., J.-E. Wahlund, R. Bostrom, P. Canu, W. S. Kurth, D. A. Gurnett, G. R. Lewis, A. J. Coates, (2007b), Far plasma wake of Titan from the RPWS observations: A case study, Geophysical Research Letters, 34, L24S04, doi: 10.1029/2007GL030482.

Molina-Cuberos, G. J., H. Lammer, W. Stumptner, K. Schwingenschuh, H. O. Rucker, J. J. Lopez-Moreno, R. Rodrigo, T. Tokano, (2001), Ionospheric layer induced by meteoric ionization in Titan's atmosphere, Planetary and Space Science, 49, 143–153, doi: 10.1016/S0032-0633(00)00133-1.

Moncuquet, M., N. Meyer-Vernet, A. Lecacheux, B. Cecconi, W. S. Kurth, (2006), Quasi Thermal Noise in Bernstein waves at Saturn, In Planetary Radio Emissions VI, (eds.) H. O. Rucker, W. S. Kurth, G. Mann, Austrian Academy of Sciences Press, Vienna, Austria, pp. 93–100.

Moncuquet, M., A. Lecacheux, N. Meyer-Vernet, B. Cecconi, W. S. Kurth, (2005), Quasi thermal noise spectroscopy in the inner magnetosphere of Saturn with Cassini/RPWS: Electron temperatures and density, Geophysical Research Letters, 32, L20S02, doi: 10.1029/2005GL022508.

Moore, L., T. E. Cravens, I. Mueller-Wodarg, M. Perry, J. H. Waite, R. Perryman, A. Nagy, D. Mitchell, A. Persoon, J.-E. Wahlund, M. W. Morooka, (2018), Models of Saturn's equatorial ionosphere based on in situ data from Cassini's Grand Finale, Geophysical Research Letters, 45, 9398–9407, doi: 10.1029/2018GL078162.

Moore, L., G. Fischer, I. Mueller-Wodarg, M. Galand, M. Mendillo, (2012), Diurnal variation of electron density in the Saturn ionosphere: Model comparisons with Saturn Electrostatic Discharge (SED) observations, Icarus, 221, 508–516, doi: 10.1016/j.icarus.2012.08.010.

Morooka, M. W., J.-E. Wahlund, L. Hadid, A. I. Ericksson, N. J. T. Edberg, E. Vigren, D. J. Andrews, A. M. Persoon, W. S. Kurth, D. A. Gurnett, W. M. Farrell, J. H. Waite, R. S. Perryman, M. Perry, (2019), Saturn's dusty ionosphere, Journal of Geophysical Research, 124, 1679–1697, doi: 10.1029/2018JA026154.

Morooka, M. W., J.-E. Wahlund, D. Andrews, A. M. Persoon, S.-Y. Ye, W. S. Kurth, D. A. Gurnett, W. M. Farrell, (2018), The dusty plasma disk around the Janus/Epimetheus ring, Journal of Geophysical Research, 123, 4668–4678, doi: 10.1002/2017JA024917.

Morooka, M. W., J.-E. Wahlund, D. Andrews, A. M. Persoon, S.-Y. Ye, W. S. Kurth, D. A. Gurnett, W. M. Farrell, (2018), Cassini RPWS dust observation near Janus and Epimetheus orbits, Journal of Geophysical Research: Space Physics, 123, no. 6, 4952–4960, doi: 10.1029/2017JA025112.

Morooka, M. W., J.-E. Wahlund, M. Shafiq, W. M. Farrell, D. A. Gurnett, W. S. Kurth, A. M. Persoon, M. Andre, A. I. Ericksson, M. Holmberg, (2011), Dusty plasma in the vicinity of Enceladus, Journal of Geophysical Research, 116, A12221, doi: 10.1029/2011JA017038.

Morooka, M. W., R. Modolo, J.-E. Wahlund, M. Andre, A. I. Eriksson, A. M. Persoon, D. A. Gurnett, W. S. Kurth, A. J. Coates, G. R. Lewis, K. K. Khurana, M. Dougherty, (2009), The electron density of Saturn's magnetosphere, Annales Geophysicae, 27, 2971–2991, doi: angeo-27-2971-2009.

Mousis, O., R. Hueso, J.-P. Beaulieu, S. Bouley, B. Carry, F. Colas, A. Klotz, C. Pellier, J.-M. Petit, P. Rousselot, M. Ali-Dib, W. Beisker, M. Birlan, C. Buil, A. Delsanti, E. Frappa, H. B. Hammel, A. C. Levasseur-Regourd, G. S. Orton, A. Sanchez-Lavega, A. Santerne, P. Tanga, J. Vaubailoon, B. Zanda, D. Baratoux, T. Böhm, V. Boudon, A. Bouquet, L. Buzzi, J.-L. Dauvergne, A. Decock, M. Delcroix, P. Drossart, N. Esseiva, G. Fischer, L. N. Fletcher, S. Foglia, J. M. Gomez-Forrellad, J. Guarro-Flo, D. Herald, E. Jehin, F. Kugel, J.-P. Lebreton, J. Lecacheux, A. Leroy, L. Maquet, G. Masi, A. Maury, F. Meyer, S. Perez-Hoyos, A. S. Rajpurohit, C. Rinner, J. H. Rogers, F. Roques, R. W. Schmude, B. Sicardy, B. Tregon, M. Vanhuysse, A. Wesley, T. Widemann, (2014), Instrumental methods for professional and amateur collaborations in planetary astronomy, Experimental Astronomy, vol. 38, Issue 1–2, pp. 91–191, doi: 10.1007/s10686-014-9379-0.

Mutel, R. L., J. D. Menietti, D. A. Gurnett, W. Kurth, P. Schippers, C. Lynch, L. Lamy, C. Arridge, B. Cecconi, (2010), CMI growth rates for Saturnian kilometric radiation, Geophysical Research Letters, 37, L19105, doi: 10.1029/2010GL044940.

Mylostna, K., V. Zakharenko, A. Konovalenko, V. Kolyadin, P. Zarka, J.-M. Griessmeier, G. Litvinenko, M. Sidorchuk, H. O. Rucker, G. Fischer, B. Cecconi, A. Coffre, L. Denis, V. Nikolaenko, V. Shevchenko, (2013), Study of Saturn electrostatic discharges in a wide range of time scales, Odessa Astronomical Publication, 26, p. 251.

Nichols, J. D., S. V. Badman, K. H. Baines, R. H. Brown, E. J. Bunce, J. T. Clarke, S. W. H. Cowley, F. J. Crary, M. K. Dougherty, J.-C. Gerard, A. Grocott, D. Grodent, W. S. Kurth, H. Melin, D. G. Mitchell, W. R. Pryor, T. S. Stallard, (2014), Dynamic auroral storms on Saturn as observed by the Hubble Space Telescope, Geophysical Research Letters, 41, 3323–3330, doi: 10.1002/2014GL060186.

Nichols, J. D., B. Cecconi, J. T. Clarke, S. W. H. Cowley, J.-C. Gerard, A. Grocott, D. Grodent, L. Lamy, P. Zarka, (2010), Variation of Saturn's UV aurora with SKR phase, Geophysical Research Letters, 37, L15102, doi: 10.1029/2010GL044057.

Nichols, J. D., S. V. Badman, E. J. Bunce, J. T. Clarke, S. W. H. Cowley, F. J. Crary, M. K. Dougherty, G.-C. Gerard, D. Grodent, K. C. Hansen, W. S. Kurth, D. G. Mitchell, W. R. Pryor, T. S. Stallard, D. L. Talboys, S. Wannawichian, (2009), Saturn's equinoctial auroras, Geophysical Research Letters, 36, L24102, doi: 10.1029/2009GL041491.

Nilsson, T., (2009), Modeling of Cassini Langmuir probe measurements, M.S. Thesis, Uppsala University, Uppsala, Sweden.

Nordheim, T. A., G. H. Jones, E. Roussos, J. S. Leisner, A. J. Coates, W. S. Kurth, K. K. Khurana, N. Krupp, M. K. Dougherty, J. H. Waite, (2014), Detection of a strongly negative surface potential at Saturn's moon Hyperion, Geophysical Research Letters, 41, 7011–7018, doi: 10.1002/2014GL061127.

Olson, J., N. Brenning, J.-E. Wahlund, H. Gunell, (2010), On the interpretation of Langmuir probe data inside a spacecraft sheath, Review of Scientific Instruments, 81, 105–106, doi: 10.1063/1.3482155.

Omidi, N., A. H. Sulaiman, W. Kurth, H. Madanian, T. Cravens, N. Sergis, M. K. Dougherty, N. J. Edberg, (2017), A single deformed bow shock for Titan-Saturn system, Journal of Geophysical Research, 122, 11058–11075, doi: 10.1002/2017JA024672.

Omidi, N., R. Tokar, T. Averkamp, D. Gurnett, W. Kurth, Z. Wang, (2012), Flow stagnation at Enceladus: The effects of neutral gas and charged dust, Journal of Geophysical Research, 117, A06230, doi: 10.1029/2011JA017488.

Omidi, N., C. T. Russell, R. L. Tokar, W. M. Farrell, W. S. Kurth, D. A. Gurnett, Y. D. Jia, L. S. Leisner, (2010), Hybrid simulations of plasma-neutral-dust interactions at Enceladus, In Pickup Ions Throughout the Heliosphere and Beyond, (eds.) J. A. le Roux, V. Florinski, G. Zank, AIP Conference Proceedings, American Institute of Physics Publishing, pp. 237–242.

Palmaerts, B., A. Radioti, D. Grodent, Z. H. Yao, T. J. Bradley, E. Roussos, L. Lamy, E. J. Bunce, S.W.H. Cowley, N. Krupp, W. S. Kurth, J.-C. Gerard, W. R. Pryor, (2018), Auroral storm and polar arcs at Saturn: Final Cassini/UVIS auroral observations, Geophysical Research Letters, 45, 6832–6842, doi: 10.1029/2018GL078094.

Palmaerts, B., E. Roussos, N. Krupp, W. S. Kurth, D. G. Mitchell, J. N. Yates, (2016), Statistical analysis and multi-instrument overview of the quasi-periodic 1-hour pulsations in Saturn's outer magnetosphere, Icarus, 271, 1–18, doi: 10.1016/j.icarus.2016.01.025.

Panchenko, M., S. Rošker, H. O. Rucker, A. Brazhenko, P. Zarka, G. Litvinenko, V. E. Shaposhnikov, A. A. Konovalenko, V. Melnik, A. V. Franzuzenko, J. Schiemel, (2018), Zebra pattern in decametric radio emission of Jupiter, Astronomy and Astrophysics, 610, A69.

Panchenko, M., S. Rošker, H. O. Rucker, A. Brazhenko, A. A. Konovalenko, G. Litvinenko, P. Zarka, V. Melnik, V. E. Shaposhnikov, A. V. Franzuzenko, (2016), Zebra-like fine spectral structures in Jovian decametric radio emission, In Planetary Radio Emissions VIII, (eds.) G. Fischer, G. Mann, M. Panchenko, P. Zarka, Austrian Academy Science Press, Vienna, Austria, pp. 103–114.

Panchenko, M., G. Fischer, W. Macher, (2014), Space-based observations of Jupiter's radio emission at IWF, In Planetary Radio Emissions 7.5, Planetary Retirement Edition, (eds.) N. I. Kömle, G. Fischer, W. Macher, Living Edition Publishers, Pöllauberg, 71–78.

Panchenko, M., H. O. Rucker, W. M. Farrell, (2013), Periodic bursts of Jovian non-Io decametric radio emission, Planetary and Space Science, 77, 100, 3–11, doi: 10.1016/j.pss.2012.08.015.

Panchenko, M. and H. O. Rucker, (2011), New type of periodic bursts of non-Io Jovian decametric radio emission, In Planetary Radio Emissions VII, (eds.) H. O. Rucker, W. S. Kurth, P. Louarn, G. Fischer, Austrian Academy of Sciences, Vienna, Austria, pp. 157–166.

Panchenko, M., H. O. Rucker, M. L. Kaiser, O. C. St. Cyr, J.-L. Bougeret, K. Goetz, S. D. Bale, (2010), New periodicity in Jovian decametric radio emission, Geophysical Research Letters, 37, L05106, doi: 10.1029/2010GL042488.

Paranicas, C., M. F. Thomsen, N. Achilleos, M. Andriopoulou, S. V. Badman, G. Hospodarsky, C. M. Jackman, X. Jia, T. Kennelly, K. Khurana, P. Kollman, N. Krupp, P. Louarn, E. Roussos, N. Sergis, (2016), Effects of radial motion on interchange injections at Saturn, Icarus, 264, 342–351, doi: 10.1016/j.icarus.2015.10.002.

Persoon, A. M., W. S. Kurth, D. A. Gurnett, J. B. Groene, A. Sulaiman, J.-E. Wahlund, M. W. Morooka, L. Z. Hadid, A. F. Nagy, J. H. Waite, T. E. Cravens, (2019), Electron density distributions in Saturn's ionosphere, Geophysical Research Letters, 46, 3061–3068, doi: 10.1029/2018GL078020.

Persoon, A. M., D. A. Gurnett, W. S. Kurth, J. B. Groene, (2015), Evidence for a seasonally dependent ring plasma in the region between Saturn's A-ring and Enceladus' orbit, Journal of Geophysical Research, 120, 6276–6285, doi: 10.1002/2015JA021180.

Persoon, A. M., D. A. Gurnett, J. S. Leisner, W. S. Kurth. J. B. Groene, J. B. Faden, (2013), The plasma density distribution in the inner region of Saturn's magnetosphere, Journal of Geophysical Research, 118, 1–5, doi: 10.1002/jgra.50182.

Persoon, A. M., D. A. Gurnett, J. S. Leisner, M. Morooka, J.-E. Wahlund, J. B. Groene, W. S. Kurth, G. B. Hospodarsky, (2011), The location of the high-density boundary in Saturn's inner magnetosphere (extended abstract), In Planetary Radio Emissions VII, (eds.) H. O. Rucker, W. S. Kurth, P. Louarn, G. Fischer, Austrian Academy of Sciences, Vienna, Austria, pp. 129–132.

Persoon, A. M., D. A. Gurnett, O. Santolik, W. S. Kurth, J. B. Faden, J. B. Groene, G. R. Lewis, A. J. Coates, R. J. Wilson, R. L. Tokar, J.-E. Wahlund, M. Moncuquet, (2009), A diffusive

equilibrium model for the plasma density in Saturn's magnetosphere, Journal of Geophysical Research, 114, A04211, doi: 10.1029/2008JA013192.

Persoon, A. M., D. A. Gurnett, W. S. Kurth, J. B. Groene, (2006a), A simple scale height model of the electron density in Saturn's plasma disk, Geophysical Research Letters, 33, L18106, doi: 10.1029/2006GL027090.

Persoon, A. M., D. A. Gurnett, W. S. Kurth, G. B. Hospodarsky, J. B. Groene, P. Canu, M. K. Dougherty, (2006b), An electron density model for Saturn's inner magnetosphere, In Planetary Radio Emissions VI, (eds.) H. O. Rucker, W. S. Kurth, G. Mann, Austrian Academy of Sciences Press, Vienna, Austria, pp. 81–91.

Persoon, A. M., D. A. Gurnett, W. S. Kurth, G. B. Hospodarsky, J. B. Groene, P. Canu, M. K. Dougherty, (2005), Equatorial electron density measurements in Saturn's inner magnetosphere, Geophysical Research Letters, 32, L23105, doi: 10.1029/2005GL024294.

Pickett, J. S., W. S. Kurth, D. A. Gurnett, R. L. Huff, J. B. Faden, T. F. Averkamp, D. Píša, G. H. Jones (2015), Electrostatic solitary waves observed at Saturn by Cassini inside 10 R_S near Enceladus, Journal of Geophysical Research, 120, 6569–6580, doi: 10.1002/2015JA021305.

Píša, D., A. H. Sulaiman, O. Santolik, G. B. Hospodarsky, W. S. Kurth, D. A. Gurnett, (2018), First observations of lion roar emission in Saturn’s magnetosheath, Geophysical Research Letters, 45, 486–492, doi: 10.1002/2017GL075919.

Píša, D., O. Santolik, G. B. Hospodarsky, W. S. Kurth, D. A. Gurnett, J. Soucek, (2016), Spatial distribution of Langmuir waves observed upstream of Saturn's bow shock by Cassini, Journal of Geophysical Research, 121, 7771–7784, doi: 10.1002/2016JA022912.

Píša, D., G. B. Hospodarsky, W. S. Kurth, O. Santolik, J. Soucek, D. A. Gurnett, A. Masters, M. E. Hill, (2015), Statistics of Langmuir wave amplitudes observed inside Saturn's foreshock by the Cassini spacecraft, Journal of Geophysical Research, 120, 2531–2542, doi: 10.1002/2014JA020560.

Pitman, K. M., B. J. Buratti, J. A. Mosher, J. M. Bauer, T. W. Momary, R. H. Brown, P. D. Nicholson, M. M. Hedman, (2008), First high solar phase angle observations of Rhea using Cassini VIMS: Upper limits on water vapor and geologic activity, The Astrophysical Journal Letters, 680, L65, doi: 10.1086/589745.

Plankensteiner, K., H. Reiner, B. M. Rode, T. Mikoviny, A. Wisthaler, A. Hansel, T. D. Mark, G. Fischer, H. Lammer, H. O. Rucker, (2007), Discharge experiments chemical evolution on the surface of Titan – Simulation experiments, Icarus, 187, 616–619, doi: 10.1016/j.icarus.2006.12.018.

Porco, C. C., P. Helfenstein, P. C. Thomas, A. P. Ingersoll, J. Wisdom, R. West, G. Neukum, et al., (2006), Cassini observes the active south pole of Enceladus, Science, 311, 1393–1401, doi: 10.1126/science.1123013.

Porco, C. C., E. Baker, J. Barbara, K. Beurle, A. Brahic, J. A. Burns, S. Charnoz, N. Cooper, D. D. Dawson, A. D. Del Genio, T. Denk, L. Dones, U. Dyudina, M. W. Evans, B. Giese, K. Grazier, P. Helfenstein, A. P. Ingersoll, R. A. Jacobson, T. V. Johnson, A. McEwen, C. D.

Murray, G. Neukum, W. M. Owen, J. Perry, T. Roatsch, J. Spitale, S. Squyres, P. Thomas, M. Tiscareno, E. Turtle, A. R. Vasavada, J. Veverka, R. Wagner, R. West, (2005), Cassini imaging science: Initial results on Saturn's atmosphere, Science, 307, 1243–1247.

Provan, G., L. Lamy, S. W. H. Cowley, E. J. Bunce, (2019), Planetary period oscillations in Saturn's magnetosphere: Comparison of magnetic and SKR modulation periods and phases during northern summer to the end of the Cassini Mission, Journal of Geophysical Research, 124, 1157–1172, doi: 10.1029/2018JA026079.

Provan, G., S. W. H. Cowley, L. Lamy, E. J. Bunce, G. J. Hunt, P. Zarka, M. K. Dougherty, (2016), Planetary period oscillations in Saturn's magnetosphere: Coalescence and reversal of northern and southern periods in late northern spring, Journal of Geophysical Research, 121, 10, 9829–9862, doi: 10.1002/2016JA023056.

Provan, G., C. Tao, S. W. H. Cowley, M. K. Dougherty, A. J. Coates, (2015), Planetary period oscillations in Saturn's magnetosphere: Examining the relationship between abrupt changes in behavior and solar wind-induced magnetospheric compressions and expansions, Journal of Geophysical Research, 120, 9524–9544, doi: 10.1002/ 2015JA021642.

Provan, G., L. Lamy, S. W. H. Cowley, M. K. Dougherty, (2014), Planetary period oscillations in Saturn's magnetosphere: Comparison of magnetic oscillations and SKR modulations in the post-equinox interval, Journal of Geophysical Research, 119, 7380–7401, doi: 10.1002/2014JA020011.

Provan, G., D. J. Andrews, B. Cecconi, S. W. H Cowley, M. K. Dougherty, L. Lamy, P. M. Zarka, (2011), Magnetospheric period magnetic field oscillations at Saturn: Equatorial phase "jitter" produced by superposition of southern and northern period oscillations, Journal of Geophysical Research, 116, A04225, doi: 10.1029/2010JA016213.

Pryor, W., A. M. Rymer, D. G. Mitchell, T. W. Hill, D. T. Young, J. Saur, G. H. Jones, S. Jacobsen, S. W. H. Cowley, B. H. Mauk, A. J. Coates, J. Gustin, D. Grodent, J.-C. Gerard, L. Lamy, J. D. Nichols, S. M. Krimigis, L. W. Esposito, M. K. Dougherty, A. J. Jouchoux, A. F. Stewart, W. E. McClintock, G. M. Holsclaw, J. M. Ajello, J. E. Colwell, A. R. Hendrix, F. J. Crary, J. T. Clarke, X. Zhou, (2011), The auroral footprint of Enceladus on Saturn, Nature, 472, 331–333, doi: 10.1038/nature09928.

Pryor, W. R., A. I. F. Stewart, L. W. Esposito, W. E. McClintock, J. E. Colwell, A. J. Jouchoux, A. J. Steffl, D. E. Shemansky, J. M. Ajello, R. A. West, C. J. Hansen, B. T. Tsurutani, W. S. Kurth, G. Hospodarsky, D. A. Gurnett, J. T. Clarke, D. Grodent, M. K. Dougherty, (2005), Cassini UVIS observations of Jupiter's auroral variability, Icarus, 178, 312–326, doi: 10.1016/j.icarus.2005.05.021.

Reed, J. J., C. M. Jackman, L. Lamy, D. Whiter, W. Kurth, (2018), Low frequency extensions of the Saturn kilometric radiation as a proxy for magnetospheric dynamics, Journal of Geophysical Research, 123, 443–463, doi: 10.1002/2017JA024499.

Richard, M. S., T. E. Cravens, C. Wylie, D. Webb, Q. Chediak, R. Perryman, K. Mandt, J. Westlake, J. H. Waite Jr., I. Robertson, B. A. Magee, N. J. T. Edberg, (2015), An empirical

approach to modeling ion production rates in Titan's ionosphere I: Ion production rates on the dayside and globally, Journal of Geophysical Research, 120, 1264–1280, doi: 10.1002/2013JA019706.

Richard, M. S., T. E. Cravens, I. P. Robertson, J. H. Waite, J.-E. Wahlund, F. J. Crary, A. J. Coates, (2011), Energetics of Titan’s ionosphere: Model comparisons with Cassini data, Journal of Geophysical Research, 116, A09310, doi: 10.1029/2011JA016603.

Rief, G., (2013), Numerical calibration of the Cassini RPWS antenna system, M.S. Thesis, Karl-Franzens-Universitat, Graz, Austria.

Robertson, I. P., T. E. Cravens, J. H. Waite Jr., R. V. Yelle, V. Vuitton, A. J. Coates, J.-E. Wahlund, K. Ågren, B. Magee, K. Mandt, M. S. Richard, (2009), Structure of Titan's ionosphere: Model comparisons with Cassini data, Planetary and Space Science, 57, 1834–1846, doi: 10.1016/j.pss.2009.07.011.

Rodriguez-Martinez, M., X. Blanco-Cano, C. T. Russell, J. S. Leisner, R. J. Wilson, M. K. Dougherty, (2010), Harmonic growth of ion-cyclotron waves in Saturn's magnetosphere, Journal of Geophysical Research, 115, A09207, doi: 10.1029/2009JA015000.

Romanelli, N., R. Modolo, E. Dubinin, J.-J. Berthelier, C. Bertucci, J.-E. Wahlund, F. Leblanc, P. Canu, N. J. T. Edberg, H. Waite, W. Kurth, D. Gurnett, A. Coates, M. Dougherty, (2014), Outflow and plasma acceleration in Titan's induced magnetotail: Evidence of magnetic tension forces, Journal of Geophysical Research, 119, 9992–10005 doi: 10.1002/2014JA020391.

Rosenqvist, L., J.-E. Wahlund, K. Ågren, R. Modolo, H. J. Opgenoorth, D. Strobel, I. Muller-Wodarg, P. Garnier, C. Bertucci, (2009), Titan Ionospheric conductivities from Cassini measurements, Planetary and Space Science, 57, 1828–1833, doi: 10.1016/j.pss.2009.01.007.

Roussos, E., C. M. Jackman, M. F. Thomsen, W. S. Kurth, S. V. Badman, C. Paranicas, P. Kollmann, N. Krupp, R. Bucik, D. G. Mitchell, S. M. Krimigis, D. C. Hamilton, A. Radioti, (2018), Solar Energetic Particles (SEP) and Galactic Cosmic Rays (GCR) as tracers of solar wind conditions near Saturn: Event lists and applications, Icarus, 300, 47–71, doi: 10.1016/j.icarus.2017.08.040.

Roussos, E., N. Krupp, D. G. Mitchell, C. Paranicas, S. M. Krimigis, M. Andriopoulou, W. S. Kurth, S. V. Badman, A. Masters, M. K. Dougherty, (2016), Quasi-periodic injections of relativistic electrons in Saturn's outer magnetosphere, Icarus, 263, 101–116, doi: 10.1016/j.icarus.2015.04.017.

Roussos, E., P. Kollmann, N. Krupp, C. Paranicus, S. M. Krimigis, D. G. Mitchell, A. M. Persoon, D. A. Gurnett, W. S. Kurth, H. Kriegel, S. Simon, K. K. Khurana, G. H. Jones, J.-E. Wahlund, M. K. G. Holmberg, (2012), Energetic electron observations of Rhea's magnetospheric interaction, Icarus, 221, Issue 1, 116–134, doi: 10.1016/j.icarus.2012.07.006.

Royer, E. M., E. L. W. Esposito, F. Crary, J.-E. Wahlund, (2018), Enhanced airglow signature observed at Titan in response to its fluctuating magnetospheric environment, Geophysical Research Letters, 45, 8864–8870, doi: 10.1029/2018GL078870.

Rucker, H. O., M. Panchenko, C. Weber, (2014), Planetary radio astronomy: Earth, giant planets, and beyond, advances in radio science, 12, 211–220, doi: 10.5194/ars-12-211-2014.

Rucker, H. O., M. Panchenko, K. C. Hansen, U. Taubenschuss, M. Y. Boudjada, W. S. Kurth, M. K. Dougherty, J. T. Steinberg, P. Zarka, P. H. M. Galopeau, D. J. McComas, C. H. Barrow, (2008), Saturn kilometric radiation as a monitor for the solar wind?, Advances in Space Research, 42, 40–47, doi: 10.1016/j.asr.2008.02.008.

Rucker, H. O., W. Macher, S. Albrecht, (1997), Experimental and theoretical investigations on the Cassini RPWS antennas, In Planetary Radio Emissions IV, (eds.) H. O. Rucker, S. J. Bauer, A. Lecacheux, Osterreichischen Akademie Der Wissenschaften, Wien, Austria, pp. 327–337.

Rucker, H. O., W. Macher, R. Manning, H. P. Ladreiter, (1996), Cassini model rheometry, Radio Science, 31, 1299–1311, doi: 10.1029/10.1029/96RS01972.

Rymer, A. M., B. H. Mauk, T. W. Hill, N. Andre, D. G. Mitchell, C. Paranicas, D. T. Young, H. T. Smith, A. M. Persoon, J. D. Menietti, G. B. Hospodarsky, A. J. Coates, M. K. Dougherty, (2009), Cassini evidence for rapid interchange transport at Saturn, Planetary and Space Science, 57, 1779–1784, doi: 10.1016/j.pss.2009.04.010.

Sakai, S., T. E. Cravens, N. Omidi, M. E. Perry, J. H. Waite Jr., (2016), Ion energy distributions and densities in the plume of Enceladus, Planetary and Space Science, 130, 60–79, doi: 10.1016/j.pss.2016.05.007.

Sakai, S.-T., S. Watanabe, M. W. Morooka, M. K. G. Holmberg, J.-E. Wahlund, D. A. Gurnett, W. S. Kurth, (2013), Dust-plasma interaction through magnetosphere-ionosphere coupling in Saturn's plasma disk, Planetary and Space Science, 75, 11–16, doi: 10.1016/j.pss.2012.11.003.

Sanchez-Lavega, A., G. Fischer, L. N. Fletcher, E. Garcia-Melendo, B. Hesman, S. Perez-Hoyos, K. M. Sayanagi, L. A. Sromovsky, (2018), The great Saturn storm of 2010–2011, Chapter 13, In Saturn in the 21st Century, (eds.) K. Baines, M. Flasar, N. Krupp, T. Stallard, Cambridge University Press, Cambridge, pp. 377–416, doi: 10.1017/9781316227220.

Sanchez-Lavega, A., F. Colas, J. Lecacheux, P. Laques, D. Parker, I. Miyazaki, (1991), The great white spot and disturbances in Saturn’s equatorial atmosphere during 1990, Nature, 353, 397–401.

Santolik, O., D. A. Gurnett, G. H. Jones, P. Schippers, F. J. Crary, J. S. Leisner, G. B. Hospodarsky, W. S. Kurth, C. T. Russell, M. K. Dougherty, (2011), Intense plasma wave emissions associated with Saturn's moon Rhea, Geophysical Research Letters, 38, L19204, doi: 10.1029/GL049219.

Saur, J., F. M. Neubauer, J. E. P. Connerney, M. G. Kivelson, P. Zarka, (2004), Plasma interaction of Io with its plasma torus, Chapter 22, In Jupiter: The Planet, Satellites and Magnetosphere 1, (eds.) F. Bagenal, W. McKinnon, T. Dowling, Cambridge University Press, Cambridge, pp. 537–560.

Sayanagi, K. M., U. A. Dyudina, S. P. Ewald, G. Fischer, A. P. Ingersoll, W. S. Kurth, G. D. Muro, C. C. Porco, R. A. West, (2013), Dynamics of Saturn's great storm of 2010–2011 from Cassini ISS and RPWS, Icarus, 223, Issue 1, 460–478, doi: 10.1016/j.icarus.2012.12.013.

Schippers, P., N. Meyer-Vernet, A. Lecacheux, S. Belheouane, M. Moncuquet, W. S. Kurth, I. Mann, D. G. Mitchell, N. Andre, (2015), Nanodust detection between 1 and 5 AU using Cassini wave measurements, The Astrophysical Journal, 806, 77, doi: 10.1088/0004-637X/806/1/77.

Schippers, P., N. Meyer-Vernet, A. Lecacheux, W. S. Kurth, D. G. Mitchell, N. Andre, (2014), Nanodust detection near 1 AU from spectral analysis of Cassini/RPWS radio data, Geophysical Research Letters, 41, 5382-5388, doi: 10.1002/2014GL060566.

Schippers, P., M. Moncuquet, N. Meyer-Vernet, A. Lecacheux, (2013), Core electron temperature and density in the innermost Saturn magnetosphere from HF power spectra analysis on Cassini, Journal of Geophysical Research, 118, 7170–7180, doi: 10.1002/2013JA019199.

Schippers, P., N. Andre, D. A. Gurnett, G. R. Lewis, A. M. Persoon, A. J. Coates, (2012), Identification of electron Field-aligned current systems in Saturn's magnetosphere, Journal of Geophysical Research, 117, A05204, doi: 10.1029/2011JA017352.

Schippers, P., C. Arridge, J. D. Menietti, D. Gurnett, L. Lamy, B. Cecconi, D. Mitchell, N. Andre, W. Kurth, S. Grimald, M. Dougherty, A. Coates, D. Young, (2011), Auroral electron distributions within and close to the Saturn kilometric radiation source region, Journal of Geophysical Research, 116, A05203, doi: 10.1029/2011JA016461.

Schippers, P., M. Blanc, N. Andre, I. Dandouras, G. R. Lewis, L. K. Gilbert, A. M. Persoon, N. Krupp, D. A Gurnett, A. Coates, S. M. Krimigis, D. Young, M. K. Dougherty, (2008), Multi-instrument analysis of electron populations in Saturn's magnetosphere, Journal of Geophysical Research, 113, A07208, doi: 10.1029/2008JA013098.

Seki, K., A. Nagy, C. Jackman, F. Crary, D. Fontaine, P. Zarka, P. Wurz, A. Milillo, J. A. Slavin, D. C. Delcourt, M. Wiltberger, R. Ilie, X. Jia, S. A. Ledvina, M. W. Liemohn, R. W. Schunk, (2015), A review of general processes related to plasma sources and losses for solar system magnetospheres, Space Sciences Reviews, 192, 27–89.

Shafiq, M., J.-E. Wahlund, M. W. Morooka, W. S. Kurth, W. M. Farrell, (2011), Characteristics of the dust-plasma interaction near Enceladus' south pole, Planetary and Space Science, 59, Issue 1, 17–25, doi: 10.1016/j.pss.2010.10.006.

Shebanits, O., E. Vigren, J.-E. Wahlund, M. K. G. Holmberg, M. Morooka, N. J. T. Edberg, K. E. Mandt, J. H. Waite Jr., (2017), Titan's ionosphere: A survey of solar EUV influences, Journal of Geophysical Research, 122, 7491–7503, doi: 10.1002/2017JA023987.

Shebanits, O., J.-E. Wahlund, N. J. T. Edberg, F. J. Crary, A. Wellbrock, D. J. Andrews, E. Vigren, R. T. Desai, A. J. Coates, K. E. Mandt, J. H. Waite Jr., (2016), Ion and aerosol precursor densities in Titan's ionosphere: A multi-instrument case study, Journal of Geophysical Research, 121, 10, 10075–10090, doi: 10.1002/2016JA022980.

Shebanits, O., J.-E. Wahlund, K. Mandt, K. Ågren, N. J. T. Edberg, J. H. Waite, (2013), Negative ion densities in the ionosphere of Titan-Cassini RPWS/LP results, Planetary and Space Science, 84, 154–162, doi: 10.1016/j.pss.2013.05.021.

Shprits, Y. Y., J. D. Menietti, X. Gu, K. C. Kim, R. B. Horne, (2012), Gyroresonant interactions between the radiation belt electrons and whistler mode chorus waves in the radiation environments of Earth, Jupiter, and Saturn: A comparative study, Journal of Geophysical Research, 117, A11216, doi: 10.1029/2012JA018031.

Sillanpaa, I., D. T. Young, F. Crary, M. Thomsen, D. Reisenfeld, J.-E. Wahlund, C. Bertucci, E. Kallio, R. Jarvinen, P. Janhunen, (2011), Cassini plasma spectrometer and hybrid model study on Titan's interaction: Effect of oxygen ions, Journal of Geophysical Research, 116, A07223, doi: 10.1029/2011JA016443.

Sittler Jr., E. C., R. E. Hartle, R. E. Johnson, J. F. Cooper, A. S. Lipatov, C. Bertucci, A. J. Coates, K. Szego, M. Shappiro, D. G. Simpson, J.-E. Wahlund, (2010), Saturn's magnetospheric interaction with Titan as defined by Cassini encounters T9 and T18: New results, Planetary and Space Science, 58, 327–350, doi: 10.1016/j.pss.2009.09.017.

Sittler Jr., E. C., N. Andre, M. Blanc, M. Burger, R. E. Johnson, A. Coates, A. Rymer, D. Reisenfeld, M. F. Thomsen, A. Persoon, M. Dougherty, H. T. Smith, R. A. Baragiola, R. E. Hartle, D. Chornay, M. D. Shappirio, D. J. McComas, D. T. Young, (2008), Ion and Neutral Sources and Sinks within Saturn's Inner Magnetosphere: Cassini Results, Planetary and Space Science, 56, 3–18, doi: 10.1016/j.pss.2007.06.006.

Smith, A. W., C. M. Jackman, M. F. Thomsen, L. Lamy, N. Sergis, (2018), Multi-instrument investigation of the location of Saturn's magnetotail x-Line, Journal of Geophysical Research, 123, 5494–5505, doi: 10.1029/2018025532.

Snowden, D., R. V. Yelle, J. Cui, J.-E. Wahlund, K. Ågren, N. J. T. Edberg, (2013), The thermal structure of Titan's upper atmosphere, I: Temperature profiles from Cassini INMS observations, Icarus, 226, Issue 1, 552–582, doi: 10.1016/j.icarus.2013.06.006.

Southwood, D. J. and M. G. Kivelson, (2001), A new perspective concerning the influence of the solar wind on the Jovian magnetosphere, Journal of Geophysical Research, 106, 6123–6130.

Spahn, F., J. Schmidt, N. Albers, M. Hörning, M. Makuch, M. Seiß, S. Kempf, et al., (2006a), Cassini dust measurements at Enceladus and implications for the origin of the E ring, Science, 311, 1416–1418, doi: 10.1126/science.1121375.

Srama, R., S. Kempf, G. Moragas-Klostermeyer, S. Helfert, T. J. Ahrens, N. Altobelli, S. Auer, et al., (2006), In situ dust measurements in the inner Saturnian system, Planetary and Space Science, 54, 967–987, doi: 10.1016/j.pss.2006.05.021.

Srama, R., T. J. Ahrens, N. Altobelli, et al., (2004), The Cassini Cosmic Dust Analyzer, Space Science Reviews, 114, 465–518, doi: 10.1007/s11214-004-1435-z.

Sromovsky, L. A., K. H. Baines, P. M. Fry, (2013), Saturn's great storm of 2010–2011: Evidence for ammonia and water ices from analysis of VIMS spectra, Icarus, 226, 402–418.

Sulaiman, A. H., W. M. Farrell, S.-Y. Ye, W. S. Kurth, D. A. Gurnett, G. B. Hospodarsky, J. D. Menietti, D. Píša, G. J. Hunt, O. Agiwal, M. K. Dougherty, (2019), A persistent, large-scale, and ordered electrodynamic connection between Saturn and its main rings, Geophysical Research Letters, In press, June 16, 2019, doi:10.1029/2019GL083541.

Sulaiman, A. H., W. S. Kurth, G. B. Hospodarsky, T. F. Averkamp, S.-Y. Ye, J. D. Menietti, W. M. Farrell, D. A. Gurnett, M. K. Dougherty, G. J. Hunt, (2018a), Enceladus auroral hiss emissions during Cassini's Grand Finale, Geophysical Research Letters, 45, 7347–7353, doi: 10.1029/2018GL078130.

Sulaiman, A. H., W. S. Kurth, G. B. Hospodarsky, T. F. Averkamp, A. M. Persoon, J. D. Menietti, S.-Y. Ye, D. A. Gurnett, D. Píša, W. M. Farrell, M. K. Dougherty, (2018b), Auroral hiss emissions during Cassini's Grand Finale: Diverse electrodynamic interactions between Saturn and its rings, Geophysical Research Letters, 45, 6782–6789, doi:10.1029/2018GL077875.

Sulaiman, A. H., D. A. Gurnett, J. S. Halekas, J. N. Yates, W. S. Kurth, M. K. Dougherty, (2017a), Whistler-mode waves upstream of Saturn, Journal of Geophysical Research, 122, 227–234, doi: 10.1002/2016GL070405.

Sulaiman, A., X. Jia, N. Achilleos, N. Sergis, D. A. Gurnett, W. S. Kurth, (2017b), Large-scale solar wind flow around Saturn's nonaxisymmetric magnetosphere, Journal of Geophysical Research, 122, 9198–9206, doi: 10.1002/2017JA024595.

Sulaiman, A. H., W. S. Kurth, A. M. Persoon, J. D. Menietti, W. M. Farrell, S.-Y. Ye, G. B. Hospodarsky, D. A. Gurnett, L. Z. Hadid, (2017c), Intense harmonic emissions observed in Saturn's ionosphere, Geophysical Research Letters, 44, 12049–12056, doi: 10.1002/2017GL076184.

Sulaiman, A. H., A. Masters, M. K. Dougherty, D. Burgess, M. Fujimoto, G. B. Hospodarsky, (2015), Quasiperpendicular high mach number shocks, Physical Review Letters, 115, 125001, doi: 10.1103/PhysRevLett.115.125001.

Sundberg, T., D. Burgess, M. Scholer, A. Masters, A. H. Sulaiman, (2017), The dynamics of very high Alfvén Mach number shocks in space plasmas, Astrophysical Journal Letters, 836, 1, L4, doi: 10.3847/2041-8213/836/1/L4.

Szego, K., Achilleos, N., Arridge, C., Badman, S. V., Delamere, P., Grodent, D., Kivelson, M. G., Louarn, P., (2015), Giant planet magnetodiscs and aurorae – An introduction, Space Science Reviews, 187, 1, 1–3, doi: 10.1007/s11214-014-0131-x.

Szego, K., D. T. Young, T. Bagdonat, B. Barraclough, J.-J. Berthelier, A. J. Coates, F. J. Crary, M. K. Dougherty, G. Erdos, D. A. Gurnett, W. S. Kurth, A. Opitz, A. Rymer, M. F. Thomsen, (2006), A pre-shock event at Jupiter on 30 January 2001, Planetary and Space Science, 54, 200–211, doi: 10.1016/j.pss.2005.10.011.

Szego, K., D. T. Young, B. Barraclough, J.-J. Berthelier, A. J. Coates, D. J. McComas, F. J. Crary, M. K. Dougherty, G. Erdos, D. A. Gurnett, W. S. Kurth, M. F. Thomsen, (2003), Cassini plasma spectrometer measurements of Jovian bow shock structure, Journal of Geophysical Research, 108, No. A7, 1287, doi: 10.1029/2002JA009517.

Tao, C., L. Lamy, and R. Prange, (2014), The brightness ratio of H Lyman-α/H_2 bands in FUV auroral emissions: A diagnosis for the energy of precipitating electrons and associated magnetospheric acceleration processes applied to Saturn, Geophysical Research Letters, 41, 6644–6651, doi: 10.1002/2014GL061329.

Tao, X., R. Thorne, R. B. Horne, S. Grimald, C. S. Arridge, G. B. Hospodarsky, D. A. Gurnett, A. J. Coates, F. J. Crary, (2010), Excitation of electron cyclotron harmonic waves in the inner Saturn magnetosphere within local plasma injections, Journal of Geophysical Research, 115, A12204, doi: 10.1029/2010JA015598.

Taubenschuss, U., J. S. Leisner, G. Fischer, D. A. Gurnett, F. Nemec, (2011), Saturnian low frequency drifting radio bursts: Statistical properties and polarization, In Planetary Radio Emissions VII, (eds.) H. O. Rucker, W. S. Kurth, P. Louarn, G. Fischer, Austrian Academy of Sciences, Vienna, Austria, pp. 115–124.

Taubenschuss, U., H. O. Rucker, W. S. Kurth, B. Cecconi, M. D. Desch, P. Zarka, M. K. Dougherty, J. T. Steinberg, (2006a), External control of Saturn kilometric radiation, In Planetary Radio Emissions VI, (eds.) H. O. Rucker, W. S. Kurth, G. Mann, Austrian Academy of Sciences Press, Vienna, Austria, pp. 51–60.

Taubenschuss, U., H. O. Rucker, W. S. Kurth, B. Cecconi, P. Zarka, M. K. Dougherty, J. T. Steinberg, (2006b), Linear prediction studies for the solar wind and Saturn kilometric radiation, Annales Geophysicae, 24, 3139–3150, doi: 10.5194/angeo-24-3139-2006.

Taubenschuss, U., (2005), The linear prediction theory applied to Cassini Data, M.S. Thesis, Karl Franzens University of Graz, Graz, Austria.

Taylor, S. A., A. J. Coates, G. H. Jones, A. Wellbrock, A. N. Fazakerley, R. T. Desai, R. Caro-Carretero, M. W. Morooka, P. Schippers, J. H. Waite, (2018), Modeling, analysis, and interpretation of photoelectron energy spectra at Enceladus observed by Cassini, Journal of Geophysical Research, 123, 287–296, doi: 10.1002/2017JA024536.

Teolis, B. D., G. H. Jones, P. F. Miles, R. L. Tokar, B. A. Magee, J. H. Waite, E. Roussos, et al., (2010), Cassini finds an oxygen-carbon dioxide atmosphere at Saturn’s icy moon Rhea, Science, 330, 1813, doi: 10.1126/science.1198366.

Thomsen, M. F., S. V. Badman, C. M. Jackman, X. Jia, M. G. Kivelson, W. S. Kurth, (2017), Energy-banded ions in Saturn's magnetosphere, Journal of Geophysical Research, 122, 5181–5202, doi: 10.1002/2017JA024147.

Thomsen, M. F., D. G. Mitchell, X. Jia, C. M. Jackman, G. B. Hospodarsky, A. J. Coates, (2015a), Plasmapause formation at Saturn, Journal of Geophysical Research, 120, 2571–2583, doi: 10.1002/2015JA021008.

Thomsen, M. F., C. M. Jackman, D. G. Mitchell, G. Hospodarsky, W. S. Kurth, K. C. Hansen, (2015b), Sustained lobe reconnection in Saturn's magnetotail, Journal of Geophysical Research, 120, 10257–10274, doi: 10.1002/2015JA021768.

Thomsen, M. F., D. B. Reisenfeld, R. J. Wilson, M. Andriopoulou, F. J. Crary, G. B. Hospodarsky, C. M. Jackman, X. Jia, K. K. Khurana, C. Paranicas, E. Roussos, N. Sergis, R. L. Tokar,

(2014), Ion composition in interchange injection events in Saturn's magnetosphere, Journal of Geophysical Research, 119, 9761–9772, doi: 10.1002/2014JA020489.

Thomsen, M. F., E. Roussos, M. Andriopoulou, P. Kollmann, C. S. Arridge, C. P. Paranicas, D. A. Gurnett, R. L. Powell, R. L. Tokar, D. T. Young, (2012), Saturn's inner magnetospheric convection pattern: Further evidence, Journal of Geophysical Research, 117, A09208, doi: 10.1029/2011JA017482.

Tokar, R. L., R. E. Johnson, T. W. Hill, D. H. Pontius, W. S. Kurth, F. J. Crary, D. T. Young, M. F. Thomsen, D. B. Reisenfeld, A. J. Coates, G. R. Lewis, E. C. Sittler, D. A. Gurnett, (2006), The interaction of the atmosphere of Enceladus with Saturn's plasma: Cassini observations, Science, 311, 1409–1412, doi: 10.1126/science.1121061.

Tokar, R. L., R. E. Johnson, M. F. Thomsen, D. M. Delapp, R. A. Baragiola, M. Francis, D. B. Reisenfeld, B. Fish, D. T. Young, F. J. Crary, A. J. Coates, D. A. Gurnett, W. S. Kurth, (2005), Cassini observations of the thermal plasma in the vicinity of Saturn's main rings and the F and G rings, Geophysical Research Letters, 32, L14S04, doi: 10.1029/2005GL022690.

Tokarev, Y., J.-L. Bougeret, B. Cecconi, A. Lecacheux, M. Kaiser, W. Kurth, (2006), SURA-WAVES experiments: Calibration of the Cassini/RPWS/HFR instrumentation, In Planetary Radio Emissions VI, (eds.) H. O. Rucker, W. S. Kurth, an G. Mann, Austrian Academy of Sciences Press, Vienna, Austria, pp. 531–541.

Tokarev, Yu. V., D. A. Gurnett, W. S. Kurth, M. L. Kaiser, R. Manning, G. N. Boiko, S. P. Terent'ev, (2001), Observations of low-frequency cosmic background at various distances from the Sun, All-proceedings of the Russian Astronomical Conference: 2001, August 6–12, 2001, St. Petersburg, Russia, p. 175.

Tseng, W.-L., R. E. Johnson, M. K. Elrond, (2013), Modeling the seasonal variability of the plasma environment in Saturn’s magnetosphere between main rings and Mimas, Planetary and Space Science, 77, 126–135.

Ulusen, D., J. G. Luhmann, Y. J. Ma, K. E. Mandt, J. H. Waite, M. K. Dougherty, J.-E. Wahlund, C. T. Russell, T. E. Cravens, N. J. T. Edberg, K. Ågren, (2012), Comparisons of Cassini flybys of the Titan magnetospheric interaction with an MHD Model: Evidence for organized behavior at high altitudes, Icarus, 217, Issue 1, 43–54, doi: 10.1016/j.icarus.2011.10.009.

Ulusen, D., J. G. Luhmann, Y. J. Ma, S. Ledvina, T. E. Cravens, K. Mandt, J. H. Waite, J.-E. Wahlund, (2010), Investigation of the force balance in the Titan ionosphere: Cassini T5 flyby model/data comparisons, Icarus, 210, 867–880, doi: 10.1016/j.icarus.2010.07.004.

Vigren, E., M. Galand, R. V. Yelle, A. Wellbrock, A. J. Coates, D. Snowden, J. Cui, P. Lavvas, N. J. T. Edberg, O. Shebanits, J.-E. Wahlund, V. Viutton, K. Mandt, (2015), Ionization balance in Titan's nightside ionosphere, Icarus, 248, 539–546, doi: 10.1016/j.icarus.2014.11.012.

Vigren, E., M. Galand, O. Shebanits, J.-E. Wahlund, W. D. Geppert, P. Lawas, V. Vuitton, R. V. Yelle, (2014), Increasing positive ion number densities below the peak of ion-electron pair production in Titan's ionosphere, The Astrophysical Journal, 786, 69–73, doi: 10.1088/0004-637X/786/1/69.

Vigren, E., M. Galand, R. V. Yelle, J. Cui, J.-E. Wahlund, K. Ågren, P. P. Lavvas, I. C. F. Mueller-Wodarg, D. F. Strobel, V. Vuitton, A. Bazin, (2013), On the thermal electron balance in Titan's sunlit upper atmosphere, Icarus, 223, Issue 1, 234–251, doi: 10.1016/j.icarus.2012.12.010.

Vogl, D. F., B. Cecconi, W. Macher, P. Zarka, H.-P. Ladreiter, P. Fedou, A. Lecacheux, T. Averkamp, G. Fischer, H. O. Rucker, D. A. Gurnett, W. S. Kurth, G. B. Hospodarsky, (2004), In-flight calibration of the Cassini-Radio and Plasma Wave Science (RPWS) antenna system for direction-finding and polarization measurements, Journal of Geophysical Research, 109, A09S17, doi: 10.1029/2003JA010261.

Vogl, D. F., H. P. Ladreiter, P. Zarka, H. O. Rucker, W. Macher, W. S. Kurth, D. A. Gurnett, G. Fischer, (2001), First results on the calibration of the Cassini RPWS antenna system, In Planetary Radio Emissions V, (eds.) H. O. Rucker, M. L. Kaiser, Y. Leblanc, Austrian Academy of Sciences Press, Vienna, Austria, pp. 357–365.

Vuitton, V., P. Lavvas, R. V. Yelle, M. Galand, A. Wellbrock, G. R. Lewis, A. J. Coates, J.-E. Wahlund, (2009), Negative ion chemistry in Titan's upper atmosphere, Planetary and Space Science, 57, 1558–1572, doi: 10.1016/j.pss.2009.04.004.

Wahlund, J.-E., M. W. Morooka, L. Z. Hadid, A. M. Persoon, W. M. Farrell, D. A. Gurnett, G. B. Hospodarsky, W. S. Kurth, S.-Y. Ye, D. J. Andrews, N. J. T. Edberg, A. I. Eriksson, E. Vigren, (2018), In situ measurements of Saturn's ionosphere show it is dynamic and interacts with the rings, Science, 359, Issue 6371, 66–68, doi: 10.1126/science.aao4134.

Wahlund, J.-E., R. Modolo, C. Bertucci, A. J. Coates, (2013), Titan's magnetospheric and plasma environment (Chapter 12), In Titan – Interior, Surface, Atmosphere and Space Environment, (eds.) I. C. F. Müller-Wodarg, C. A. Griffith, E. Lellouch, T. E. Cravens, Cambridge University Press, Cambridge.

Wahlund, J.-E., M. Andre, A. I. E. Eriksson, M. Lundberg, M. W. Morooka, M. Shafiq, T. F. Averkamp, D. A. Gurnett, G. B. Hospodarsky, W. S. Kurth, K. S. Jacobsen, A. Pedersen, W. Farrell, S. Ratynskaia, N. Piskunov, (2009a), Detection of dusty plasma near the E-ring of Saturn, Planetary and Space Science, 57, 1795–1806, doi: 10.1016/j.pss.2009.03.011.

Wahlund, J.-E., M. Galand, I. Mueller-Wodarg, J. Cui, R. V. Yelle, F. J. Crary, K. Mandt, B. Magee, J. H. Waite, Jr., D. T. Young, A. J. Coates, P. Garnier, K. Ågren, M. Andre, A. I. Ericksson, T. E. Cravens, V. Vuitton, D. A. Gurnett, W. S. Kurth, (2009b), On the amount of heavy molecular ions in Titan's ionosphere, Planetary and Space Science, 57, 1857–1865, doi: 10.1016/j.psss.2009.07.014.

Wahlund, J.-E., R. Bostrom, G. Gustafsson, D. A. Gurnett, W. S. Kurth, A. Pedersen, T. F. Averkamp, G. B. Hospodarsky, A. M. Persoon, P. Canu, F. M. Neubauer, M. K. Dougherty, A. I. Eriksson, M. W. Morooka, R. Gill, M. Andre, L. Eliasson, I. Muller-Wodarg, (2005a), Cassini measurements of cold plasma in the ionosphere of Titan, Science, 308, 986–989, doi: 10.1126/science.1109807.

Wahlund, J.-E., R. Bostrom, G. Gustafsson, D. A. Gurnett, W. S. Kurth, T. Averkamp, G. B. Hospodarsky, A. M. Persoon, P. Canu, A. Pedersen, M. D. Desch, A. I. Eriksson, R. Gill, M. W.

Morooka, M. Andre, (2005b), The inner magnetosphere of Saturn: Cassini RPWS cold plasma results from the first encounter, Geophysical Research Letters, 32, L20S09, doi: 10.1029/2005GL022699.

Waite, J. H., R. Perryman, M. Perry, K. Miller, J. Bell, T. E. Cravens, C. Glein, J. Grimes, H. Hedman, T. Brockwell, B. Teolis, L. Moore, D. Mitchell, A. Persoon, W. S. Kurth, J.-E. Wahlund, M. Morooka, L. Hadid, S. Chocron, A. Nagy, R. Yelle, S. Ledvina, R. Johnson, (2018), Chemical interactions between Saturn's atmosphere and rings, Science, 362, Issue 6410, eaat2382, doi:10/1126/science.aat2382.

Wang, Z., D. A. Gurnett, G. Fischer, S-Y. Ye, W. S. Kurth, D. G. Mitchell, J. S. Leisner, C. T. Russell, (2010), Cassini observations of narrowband radio emissions in Saturn's magnetosphere, Journal of Geophysical Research: Space Physics, vol. 115, Issue A6, doi: 10.1029/2009JA014847.

Wang, Z., D. A. Gurnett, T. F. Averkamp, A. M. Persoon, W. S. Kurth, (2006), Characteristics of dust particles detected near Saturn's ring plane with the Cassini Radio and Plasma Wave instrument, Planetary and Space Science, 54, 957-966, doi: 10.1016/j.pss.2006.05015.

Wang, Z., (2006), The characteristics of dust particles detected by Cassini near Saturn's ring plane, Ph.D. Thesis, University of Iowa, Iowa City, Iowa.

Wang, Z., D. A. Gurnett, G. Fischer, S.-Y. Ye, W. S. Kurth, D. G. Mitchell, J. S. Leisner, C. T. Russell, (2010), Cassini observations of narrowband radio emissions in Saturn's magnetosphere, Journal of Geophysical Research, 115, A06213, doi: 10.1029/2009JA014847.

Warwick, J. W., J. B. Pearce, D. R. Evans, T. D. Carr, J. J. Schauble, J. K. Alexander, M. L. Kaiser, M. D. Desch, M. Pedersen, A. Lecacheux, G. Daigne, A. Boischot, C. H. Barrow, (1981), Planetary radio astronomy observations from Voyager 1 near Saturn, Science, 212, 239–243.

Wei, H. Y., C. T. Russell, J.-E. Wahlund, M. K. Dougherty, C. Bertucci, R. Modolo, Y. J. Ma, F. M. Neubauer, (2007), Cold ionospheric plasma in Titan's magnetotail, Geophysical Research Letters, 34, L24S06, doi: 10.1029/2007GL030701.

Went, D. R., G. B. Hospodarsky, A. Masters, K. C. Hansen, M. K. Dougherty, (2011), A new semiempirical model of Saturn's bow shock based on propagated solar wind parameters, Journal of Geophysical Research, 116, A07202, doi: 10.1029/2010JA016349.

Westlake, J. H., J. H. Waite Jr., K. E. Mandt, N. Carrasco, J. M. Bell, B. A. Magee, J.-E. Wahlund, (2012a), Titan’s ionospheric composition and structure: Photochemical modelling of Cassini INMS data, Journal of Geophysical Research, 117, E01003, doi: 10.1029/2011JE003883.

Westlake, J. H., C. P. Paranicas, T. E. Cravens, J. G. Luhmann, K. E. Mandt, H. T. Smith, D. G. Mitchell, A. M. Rymer, M. E. Perry, J. H. Waite, J.-E. Wahlund, (2012b), The observed composition of ions outflowing from Titan, Geophysical Research Letters, 39, L19104, doi: 10.1029/2012GL053079.

Williams, G. A. and C. D. Murray, (2011), Stability of co-orbital ring material with applications to the Janus-Epimetheus system, Icarus, 212, 275–293, doi: 10.1016/j.icarus.2010.11.038.

Williams, J. D., L.-J. Chen, W. S. Kurth, D. A. Gurnett, M. K. Dougherty, (2006), Electrostatic solitary structures observed at Saturn, Geophysical Research Letters, 33, L06103, doi: 10.1029/2005GL024532.

Williams, J. D., L.-J. Chen, W. S. Kurth, D. A. Gurnett, M. K. Dougherty, A. M. Rymer, (2005), Electrostatic solitary structures associated with the November 10, 2003 interplanetary shock at 8.7 AU, Geophysical Research Letters, 32, L17103, doi: 10.1029/2005GL023079.

Willis, I. C., L. J. Woolliscroft, T. F. Averkamp, D. A. Gurnett, R. A. Johnson, D. L. Kirchner, W. S. Kurth, W. Robison, (1995), The implementation of data compression in the Cassini RPWS dedicated data compression processor, In Proceedings, Data Compression Conference (DCC), Space and Earth Science Data Compression Workshop, Snowbird, UT, March 28–30, 1995, doi: 10.1109/DCC.1995.515601.

Wilson, R., F. Bagenal, A. Persoon, (2017), Survey of thermal plasma ions in Saturn's magnetosphere utilizing a forward model, Journal of Geophysical Research, 122, 7256–7278, doi: 10.1002/2017JA024117.

Wilson, R. J., R. L. Tokar, W. S. Kurth, A. M. Persoon, (2010), Properties of the thermal ion plasma near Rhea as measured by the Cassini Plasma Spectrometer, Journal of Geophysical Research, A05201, doi: 10.1029/2009JA014679.

Wilson, G. R. and J. H. Waite Jr., (1989), Kinetic modeling of the Saturn ring-ionosphere plasma environment, Journal of Geophysical Research, 94, 17287–17298.

Woodfield, E. E., R. B. Horne, S. A. Glauert, J. D. Menietti, Y. Y. Shprits, W. S. Kurth, (2018), Formation of electron radiation belts at Saturn by Z-mode wave acceleration, Nature Communications, 9, article 5062, doi: 10.1038/s41467-018-07549-4.

Woolliscroft, L. J. C., W. M. Farrell, H. St. C. Alleyne, D. A. Gurnett, D. L. Kirchner, W. S. Kurth, J. A. Thompson, (1993), Cassini radio and plasma wave investigation: Data compression and scientific application, Journal of the British Interplanetary Society, 46, 115.

Xin, L., D. A. Gurnett, O. Santolik, W. S. Kurth G. B. Hospodarsky, (2006), Whistler-mode auroral hiss emissions observed near Saturn's B ring, Journal of Geophysical Research, 111, A06214, doi: 10.1029/2005JA011432.

Xin, L., (2005), A study of whistler-mode resonance-cone emissions, Ph.D. Thesis, University of Iowa, Iowa City, Iowa.

Yair, Y., G. Fischer, F. Simoes, N. Renno, P. Zarka, (2008), Updated review of planetary atmospheric electricity, Space Science Reviews, 137, 29–49, doi: 10.1007/s11214-008-9349-9.

Yamauchi, M. and J.-E. Wahlund, (2007), Role of the ionosphere for the atmospheric evolution of planets, Astrobiology, 7, 783–800, doi: 10.1089/ast.2007.0140.

Yao, Z. H., A. Radioti, D. Grodent, L. C. Ray, B. Palmaerts, N. Sergis, K. Dialynas, A. C. Coates, C. S. Arridge, R. Roussos, S. V. Badman, S.-Y. Ye, J.-C. Gerard, P. A. Delamere, R. L. Guo, Z. Y. Pu, J. H. Waite, N. Krupp, D. G. Mitchell, M. K. Dougherty, (2018), Recurrent magnetic

dipolarization at Saturn: Revealed by Cassini, Journal of Geophysical Research, 123, 8502–8517, doi: 10.1029/2018JA025837.

Yaroshenko, V. V., S. Ratynskaia, J. Olson, N. Brenning, J.-E. Wahlund, M. Morooka, W. S. Kurth, D. A. Gurnett, G. E. Morfill, (2009), Characteristics of charged dust inferred from the Cassini RPWS measurements in the vicinity of Enceladus, Planetary and Space Science, 57, 1807–1812, doi: 10.1016/j.pss.2009.03.002.

Yates, J. N., D. J. Southwood, M. K. Dougherty, A. H. Sulaiman, A. Masters, S. W. H. Cowley, M. G. Kivelson, C. H. K. Chen, G. Provan, D. G. Mitchell, G. B. Hospodarsky, N. Achilleos, A. M. Sorba, A. J. Coates, (2016), Saturn's quasi-periodic magnetohydrodynamic waves, Geophysical Research Letters, 43, 11102–11111, doi: 10.1002/2016GL071069.

Ye, S.-Y., W. S. Kurth, G. B. Hospodarsky, A. M. Persoon, D. A. Gurnett, M. Morooka, J.-E. Wahlund, H.-W. Hsu, M. Seiss, R. Srama, (2018a), Cassini RPWS dust observation near Janus and Epimetheus orbits, Journal of Geophysical Research, doi: 10.1002/2017JA025112.

Ye, S.-Y., W. S. Kurth, G. B. Hospodarsky, A. M. Persoon, A. H. Sulaiman, D. A. Gurnett, M. Morooka, J.-E. Wahlund, H.-W. Hsu, Z. Sternovsky, X. Wang, M. Horanyi, M. Seiss, S. Srama, (2018b), Dust observations by the Radio and Plasma Wave Science Instrument during Cassini's Grand Finale, Geophysical Research Letters, 45, 10101–10109, doi: 10.1029/2018GL078059.

Ye, S.-Y., G. Fischer, W. S. Kurth, J. D. Menietti, D. A. Gurnett, (2018c), An SLS5 longitude system based on the rotational modulation of Saturn radio emissions, Geophysical Research Letters, 45, 7297–7305, doi: 10.1029/2018GL077976.

Ye, S.-Y., G. Fischer, W. S. Kurth, J. D. Menietti, D. A. Gurnett, (2017), Rotational modulation of Saturn kilometric radiation, narrowband emission, and auroral hiss, In Planetary Radio Emissions VIII, (eds.) G. Fischer, G. Mann, M. Panchenko, P. Zarka, Austrian Academy of Sciences Press, Vienna, Austria, pp. 191–204.

Ye, S.-Y., D. A. Gurnett, W. S. Kurth, (2016a), In-situ measurements of Saturn's dusty rings based on dust impact signals captured by Cassini RPWS, Icarus, 279, 51–61, doi: 10.1016/j.icarus.2016.05.006.

Ye, S.-Y., G. Fischer, W. S. Kurth, J. D. Menietti, D. A. Gurnett, (2016b), Rotational modulation of Saturn's radio emissions after equinox, Journal of Geophysical Research, 121(12), 11714–11728, doi: 10.1002/2016JA023281.

Ye, S.-Y., D. A. Gurnett, W. S. Kurth, T. F. Averkamp, M. Morooka, S. Sakai, J.-E. Wahlund, (2014a), Electron density inside Enceladus plume inferred from plasma oscillations excited by dust impacts, Journal of Geophysical Research, 119, Issue 5, 3373–3380, doi: 10.1002/2014JA019861.

Ye, S.-Y., D. A. Gurnett, W. S. Kurth, T. F. Averkamp, S. Kempf, H.-W. Hsu, R. Srama, E. Gruen, (2014b), Properties of dust particles near Saturn inferred from voltage pulses induced by dust impacts on Cassini spacecraft, Journal of Geophysical Research, 119, 6294–6312, doi: 10.1002/2014JA020024.

Ye, S.-Y., D. A. Gurnett, J. D. Menietti, W. S. Kurth, G. Fischer, (2012), Cassini observation of Jovian anomalous continuum radiation, Journal of Geophysical Research, 117, A04211, doi: 10.1029/2011JA017135.

Ye, S.-Y., G. Fischer, J. D. Menietti, Z. Wang, D. A. Gurnett, W. S. Kurth, (2011), An overview of Saturn narrowband radio emissions observed by Cassini RPWS (invited), In Planetary Radio Emissions VII, (eds.) H. O. Rucker, W. S. Kurth, P. Louarn, G. Fischer, Austrian Academy of Sciences, Vienna, Austria, pp. 99–114.

Ye, S.-Y., J. D. Menietti, G. Fischer, Z. Wang, B. Cecconi, D. A. Gurnett, W. S. Kurth, (2010a), Z-mode waves as the source of Saturn narrowband radio emissions, Journal of Geophysical Research, 115, A08228, doi: 10.1029/2009JA015167.

Ye, S.-Y., D. A. Gurnett, J. B. Groene, Z. Wang, W. S. Kurth, (2010b), Dual periodicities in the rotational modulation of Saturn narrowband emissions, Journal of Geophysical Research, 115, A12258, doi: 10.1029/2010JA015780.

Ye, S.-Y., D. A. Gurnett, G. Fischer, B. Cecconi, J. D. Menietti, W. S. Kurth, Z. Wang, G. B. Hospodarsky, P. Zarka, A. Lecacheux, (2009), Source locations of narrowband radio emissions detected at Saturn, Journal of Geophysical Research, 114, A06219, doi: 10.1029/2008JA013855.

Zaitsev, V. V., V. E. Shaposhnikov, M. L. Khodachenko, H. O. Rucker, M. Panchenko, (2010), Acceleration of electrons in Titan's ionosphere, Journal of Geophysical Research, 115, A03212, doi: 10.1029/2008JA013958.

Zakharenko, V., C. Mylostna, A. Konovalenko, P. Zarka, G. Fischer, J.-M. Griessmeier, G. Litvinenko, H. Rucker, M. Sidorchuk, B. Ryabov, D. Vavriv, V. Ryabov, B. Cecconi, A. Coffre, L. Denis, C. Fabrice, L. Pallier, J. Schneider, R. Kozhyn, V. Vinogradov, D. Mukha, R. Weber, V. Shevchenko, V. Nikolaenko, (2012), Ground-based and spacecraft observations of lightning activity on Saturn, Planetary and Space Science, 61, Issue 1, 53-59, doi: 10.1016/j.pss.2011.07.021.

Zarka, P., W. M. Farrell, G. Fischer, A. A. Konovalenko, (2008), Ground-based and space-based radio observations of planetary lightning, Space Science Reviews, 137, 257–269, doi: 10.1007/s11214-008-9366-8.

Zarka, P., L. Lamy, B. Cecconi, R. Prange, H. Rucker, (2007), Modulation of Saturn's radio clock by solar wind speed, Nature, 450, 265–267, doi: 10.1038/nature06237.

Zarka, P., B. Cecconi, L. Denis, W. M. Farrell, G. Fischer, G. B. Hospodarsky, M. L. Kaiser, W. S. Kurth, (2006), Physical properties and detection of Saturn's lightning radio bursts, In Planetary Radio Emissions VI, (eds.) H. O. Rucker, W. S. Kurth, G. Mann, Austrian Academy of Sciences Press, Vienna, Austria, pp. 111–122.

Zarka, P. and W. S. Kurth, (2005), Radio wave emission from the outer planets before Cassini, Space Science Reviews, 116, 371–397, doi: 10.1007/s11214-005-1962-2.

Zarka, P., B. Cecconi, W. S. Kurth, (2004a), Jupiter's low-frequency radio spectrum from Cassini/Radio and Plasma Wave (RPWS) absolute flux density measurements, Journal of Geophysical Research, 109, A09S15, doi: 10.1029/2003JA010260.

Zarka, P., W. M. Farrell, M. L. Kaiser, E. Blanc, W. S. Kurth, (2004b), Study of solar system planetary lightning with LOFAR, Planetary and Space Science, 52, 1435–1447, doi: 10.1016/j.pss.2004.09.011.

Zarka, P., (2004), Radio and plasma waves at the outer planets, Advances in Space Research, 33, 2045–2060, doi: 10.1016/j.asr.2003.07.055.

Zarka, P., J. Queinnec, F. J. Crary, (2001a), Low-frequency limit of Jovian radio emissions and implications on source locations and Io plasma wake, Planetary and Space Science, 49, 1137–1149, doi: 10.1016/S0032-0633(01)00021-6.

Zarka, P., R. A. Treumann, B. P. Ryabov, V. B. Ryabov, (2001b), Magnetically-driven planetary radio emissions and applications to extrasolar planets, Astrophysics and Space Science, 277, 293–300, doi: 10.1023/A:1012221527425.

Zarka, P., (2000), Radio emissions from the planets and their moons, In Radio Astronomy at Long Wavelengths, (eds.) R. G. Stone, K. W. Weiler, M. L. Goldstein, J.-L. Bougeret, American Geophysical Union Geophysical Monograph Series, vol. 119, pp. 167–178, doi: 10.1029/GM119p0167.

Zarka, P. and B. M. Pedersen, (1983), Statistical study of Saturn electrostatic discharges, Journal of Geophysical Research, 88, 9007–9018.

Zieger, B. and K. C. Hansen, (2008), Statistical validation of a solar wind propagation model from 1 to 10 AU, Journal of Geophysical Research, 113, A8, doi: 10.1029/2008JA013046.

Zlotnik, E. Ya., V. E. Shaposhnikov, V. V. Zaitsev, (2016), Interpretation of the zebra pattern in the Jovian kilometric radiation, Journal of Geophysical Research, 121, 5307–5318, doi: 10.1002/2016JA022655.